# REPORT DOCUMENTATION PAGE

Form Approved OMB No. 0704-0188



| 1. REPORT DATE *(DD-MM-YYYY)* | 2. REPORT TYPE | 3. DATES COVERED *(From – To)* |
|---|---|---|
| 20-08-2007 | Final Report | 1 Jul 07 - 02-Feb-10 |

**4. TITLE AND SUBTITLE**

Exploiting Formation Flying for Fuel Saving Supersonic Oblique Wing Aircraft

**5a. CONTRACT NUMBER**
FA8655-07-1-3024

**5b. GRANT NUMBER**

**5c. PROGRAM ELEMENT NUMBER**

**6. AUTHOR(S)**

Dr. Rajendar K Nangia

**5d. PROJECT NUMBER**

**5d. TASK NUMBER**

**5e. WORK UNIT NUMBER**

**7. PERFORMING ORGANIZATION NAME(S) AND ADDRESS(ES)**

Nangia Aero Research Associates
West Point, 78-Queens Road
Bristol BS8 1QX
United Kingdom

**8. PERFORMING ORGANIZATION REPORT NUMBER**

N/A

**9. SPONSORING/MONITORING AGENCY NAME(S) AND ADDRESS(ES)**

EOARD
Unit 4515 BOX 14
APO AE 09421

**10. SPONSOR/MONITOR'S ACRONYM(S)**

**11. SPONSOR/MONITOR'S REPORT NUMBER(S)**
Grant 07-3024

**12. DISTRIBUTION/AVAILABILITY STATEMENT**

Approved for public release; distribution is unlimited.

**13. SUPPLEMENTARY NOTES**

**14. ABSTRACT**

This report results from a contract tasking Nangia Aero Research Associates as follows: As per the formal proposal document (Nangia, USTP15.pdf, 3 phase work programme is envisaged.

Phase I-
Assuming a basic aircraft, we do a preliminary assessment of range increase as a function of the number of aircraft in formation.
Phase II-
A refined estimate of range increase as function of the number of aircraft in formation, with assumptions made in the Phase I relaxed
Phase III-
To Build up on work done in previous phases, Different Mach numbers, Apply to Extended Geometry and Flight parameters, Propulsion Issues, Size Issues, Aero-elastic effects

**15. SUBJECT TERMS**
EOARD, Control System, Aerodynamics

| 16. SECURITY CLASSIFICATION OF: | | | 17. LIMITATION OF ABSTRACT | 18, NUMBER OF PAGES | 19a. NAME OF RESPONSIBLE PERSON |
|---|---|---|---|---|---|
| a. REPORT | b. ABSTRACT | c. THIS PAGE | | | SURYA SURAMPUDI |
| UNCLAS | UNCLAS | UNCLAS | UL | 69 | 19b. TELEPHONE NUMBER *(Include area code)* +44 (0)1895 616021 |

**RKN / AERO / REPORT / 2007-10**
**Issue 1, July 2007**

# Exploiting Formation Flying for Fuel Saving – Supersonic Oblique Wing Aircraft

## Dr. R. K. Nangia

### SUMMARY

Currently there is a great emphasis on fuel-efficient flight and this may be reflected in planned budgets and constraints for future. The idea of Close Formation Flying (CFF) to reduce drag and hence fuel usage, has been appreciated. A fair deal of theoretical and experimental work in subsonic flight is available.

Many geometries need to be studied in CFF of large and small aircraft. Each aircraft in a formation is likely to produce off-design forces and moments. It will be a pre-requisite to ensure that these off-design forces and moments can be adequately and efficiently modelled and controlled. For example a large rolling moment is produced on a trailing aircraft. Simply using aileron may tackle the induced roll but, as a result, drag may increase and compromise any advantages.

Recently NASA has conducted tests on a formation of two F/A-18 aircraft. The performance benefits occur at certain geometry relationships in the formation (e.g. the trail aircraft overlaps the wake of the lead aircraft by 10-15% semi-span).

Amongst many projects at AFRL, importance is being attached to the Oblique Wing aircraft. A research programme “Switchblade” is being conducted under DARPA sponsorship. With varying sweep, Switchblade can achieve a wide and efficient subsonic-supersonic flight envelope capability. An unmanned flying demonstrator is being developed by Northrop-Grumman. The programme remains challenging in view of balancing the asymmetry, stability levels and aero-elastic implications.

This report summarises theoretical analysis on a generic OFW planform in CFF at Mach 1.4. The analysis begins with an assessment of the planar (uncambered) OFW. Typical flight envelope parameters and design targets are established. Several design options are presented. The performance of the OFW, both planar and designed, in CFF is established and benefits, in terms of increased L/D throughout a range of formation geometries are determined.

Results (trimmed for lift only at this stage) show up to 50% reduction in lift-induced drag of the trail aircraft. This implies 30– 35% increases in lift-drag ratio and hence similar increases in range. Multiple aircraft formations reflect the benefits on all trailing aircraft. In view of the encouragement, further detailed work has been proposed in several areas.

**EOARD Grant No.07-3024**

**Consulting Engineers**
**Nangia Aero Research Associates**
**WestPoint, 78 Queens Road, Clifton**
**Bristol BS8 1QX, UK**

The Investigation which is the subject of this report was initiated by USAF - EOARD, 223/231 Old Marylebone Road, London, NW1 5TH, UK and was carried out under the terms of Grant No 07 - 3024

## INITIAL DISTRIBUTION LIST

| | | |
|---|---|---|
| 1 | Dr. Surya Surampudi | USAF-EOARD, London NW1 5TH, UK |
| 1 | Mr. Dieter Multhopp | AFRL/VAAA Bldg 45<br>2130 8th Street, WPAFB, Ohio, USA 45433-7542 |
| 2 | Dr. Carl P. Tilmann | AFRL/VAAA Bldg 45<br>2130 8th Street, WPAFB, Ohio, USA 45433-7542 |
| 2 | Mr. William Blake | AFRL/VACA Bldg 146<br>2130 8th Street, WPAFB, Ohio, USA 45433-7542 |
| 2 | Dr. Keith Numbers | AFRL/VAAA, Long Range Strike Integrating Concept Office |
| 2 | Dr. R.K. Nangia | Nangia Aero Research Associates<br>WestPoint, 78-Queens Road, Clifton<br>BRISTOL BS8 1QX, UK. |

## CONTRACTUAL DECLARATIONS

"The Contractor, Dr. R. K. Nangia**,,** hereby delcares that, to the best of its knowledge and belief, the technical data delivered herewith under Grant No.07-3024 is complete, accurate, and complies with all requirements of the grant."

**DATE: July 2007 Name and Title of Authorized Official: Dr R K Nangia**

"I certify that there were no subject inventions to declare as defined in FAR 52.227-13, during the performance of this contract."

**DATE: July 2007 Name and Title of Authorized Official: Dr R K Nangia**

## CONTENTS

# 1. INTRODUCTION, BACKGROUND AND WORK PROGRAMME

## 1.1. Background

Currently there is emphasis on fuel-efficient flight and this may be reflected in planned budget constraints in the future. The idea of aircraft in Close Formation Flying (CFF) to reduce fuel usage has been appreciated for some time. Recently NASA has conducted tests on a formation of two F/A-18 aircraft to establish possible benefits (Refs.1-4 & **Fig.1.1**). It was shown that benefits occur at certain geometry relationships in the formation, for example when the trail aircraft overlaps the wake of the lead aircraft by 10-15% semi-span. **Fig.1.2** shows T-38 aircraft in formation.

**Fig.1.3** shows examples of CFF Wind Tunnel work carried out in support of flight tests on the F/A-18. **Fig.1.4** refers to CFF work on "ICE" models. Note the possibility of trimming out the interference roll effects by using tip controls. These particular cases refer to aircraft with wings of relatively low Aspect Ratio (AR).

For high AR transonic aircraft Jenkinson, in 1995 (Ref.5), proposed a CFF of large aircraft as being more efficient, in comparison with flying very large aircraft alone. He indicated that individual aircraft could start from different airports and then fly in formation over large distances before peeling away ready for landing at the required destinations.

There are many results available using idealized approaches e.g. vortex lattice formulations (Ref.6). Ref.6 also contains a sizable bibliography. There is scope for many geometries to be investigated. Aircraft formations can comprise large and small aircraft. Each aircraft in a formation is likely to produce off-design forces and moments. It will be a pre-requisite to ensure that these off-design forces and moments can be adequately and efficiently modelled and controlled. For example a large rolling moment is produced on a trailing aircraft in CFF. Simply using aileron may tackle the induced roll but, as a result, drag may increase and compromise any advantages arising due to formation flying.

### Oblique Flying Wings (OFW) & "Switchblade" Programme

**Fig.1.5** shows an OFW concept of the 1990's, designed for Mach 1.4 – 1.6 cruise, Ref.7. Realisation of such a project appeared difficult in view of the large size (weight 1.5 million pounds for up to 1000 passengers), cabin width, passenger ride quality and other reasons.

Amongst many projects at AFRL, importance is currently being attached to the Oblique Wing aircraft, **Fig.1.6**. A research programme, "Switchblade" (Ref.8), is being conducted under DARPA sponsorship. With varying sweep, Switchblade can achieve a wide and efficient subsonic-supersonic flight envelope capability. An unmanned flying demonstrator is being built by Northrop-Grumman. The programme remains challenging in view of balancing the asymmetry, stability levels and aero-elastic implications (e.g. Refs.11-12). After successful demonstrations, the idea will be to exploit the OFW towards other categories of aircraft for civil and military applications.

The work relates to the, perhaps unique, idea of the prediction of benefits, in terms of L/D and Range increments, that may be gained by using the OFW concept in CFF at supersonic speeds.

## 1.2. Introduction to the Present work and Methods

### Our Recent Design Techniques & Flying in Formation

We have recently developed wing design methods that drive wing designs towards pre-defined spanwise load distributions, coupling these to camber surface definition. The target distributions can be tuned for particular requirements, e.g. minimum drag (elliptic loading),

roll, yaw or pitch control, control of interference effects, etc. The method is particularly useful in defining control surface deflection over a range of flight conditions. The methods have been used and developed during recent wing / winglet / morphing design programmes (Refs.13-14).

By exploiting this method, we have assessed the aerodynamics of subsonic-transonic wings in formation and then re-designed them to eliminate the induced roll / pitch effects. A number of flight formations with aircraft of varying size and spacing have been studied (Refs.15-17). Predictions show benefits of 30%, or more, in lift-induced drag. This is encouraging.

It is considered that the benefits from CFF will extend to supersonic flight, making for even greater efficiency. It is widely believed that this area of work has not been attempted. Therefore a need has arisen to evaluate the Mach number effects on formation flight and the possible advantages and disadvantages. The drag benefits will vary as Mach number changes. For Mach number close to 0.8, the wing sweep is about 30 deg. For Mach 1.6 cruise, the sweep will be near 60 deg. or more.

Compared with conventional symmetric aircraft flying in formation, the asymmetric OFW aircraft present appreciably different and “handed” geometric relationships. Further formation options arise when we include future Long Range Supersonic Strike (LRS) aircraft (AFRL). All this has the makings of a very interesting, phased research programme.

### 1.3. Content and Layout of this Report

The remainder of this report is contained in **Sections 2 to 13,** supported by **Appendix A1**.

**Section 2** discusses the scope of OFW and CFF, showing the wide range of possibilities. The phased programme of work is outlined.

**Section 3** gives an understanding of Wakes albeit on conventional high Aspect ratio transonic aircraft

**Section 4** gives an idea of formation effects in subsonic and transonic flows.

**Section 5** discusses previous work on OFW.

**Section 6** discusses the basic OFW considerations in the present study. Typical flight envelope and design parameters are defined leading to the planform derivation. The theoretical methods used are discussed.

**Section 7** presents results for the uncambered, planar wing, without and with TE devices. A Drag analysis for the particular OFW is presented.

**Section 8** discusses the designed OFW. Two designs are presented.

**Section 9** is on CFF using planar OFW

**Section 10** is on CFF using designed OFW

**Section 11** presents various comparisons of OFW and CFF.

**Section 12** further work.

**Section 13** mentions concluding remarks.

**Appendix A1** is devoted to preliminary work on Wave drag aspects of OFW in CFF.

We begin with visualising the scope of the work programme before more detail.

## 2. SETTING UP THE SCOPE OF THE PRESENT PROGRAMME

An extremely wide range of considerations were taken into account when establishing the scope of the work setting up the work programme. The wide range of possibilities that arise

from the OFW and CFF are discussed in Section 2.1. After consultation with AFRL/VA these have been formalized into a phased work programme discussed in Section 2.2.

## 2.1. Wide Range of Possibilities

Initially we consider the basic design requirements and the overall flight envelope. A wide range of possibilities arises. A design reference needs to be established.

**Oblique Wing Design Reference Selection**

We need to assume representative parameters and design appropriate generic geometry in consultations with the technical monitors at AFRL.

**Oblique Wing Formations**

**Fig.2.1** refers to a few possibilities of OFW formations. **Fig.2.2** shows a selection of "handed" Core formations. Typical size / spacing parameters need to be considered for oblique wings flying at various sweep angles.

Geometry Parameters / Combinations
- Formation Positioning Changes (chordwise, lateral and vertical sense)
- Relative Size Effects
- Handed Formations with other aircraft

Flow parameters Combinations
- Transonic Cruise
- Supersonic Cruise
- Sideslip Effects – implying position changes

Controls
- Control of Forces & Moments
- Varying Camber and twist with TE Flap or vari-cam or other systems, flow-control
- LE / TE Controls both

Performance Aspects
- Induced-Drag Reductions relative to total drag
- Performance Figures - Effect on Range

Aero-elastic Implications
- Bending, Twist and 'g' flight
- Many other factors need to be addressed

All of the above reflects the many parametric combinations that can be investigated. We need to make a judicious choice of parameters to be studied in concert with the technical monitors.

The proposed work is interesting. It can be "tailored" to suit sponsors requirements, time-scales, phases and budget guidelines.

Although we have several working methods and computer programmes, ranging from linearized theory, panel codes, Euler, some of these have needed limited development, particularly with regard to geometry handling and interfacing of the codes.

**Project Designer's Viewpoint**

We take the viewpoint of a Project designer towards demonstrating a new (radical) concept to fulfil performance and mission criteria throughout the flight envelope. A series of design trade studies will give an idea of how a design fulfils the demands of mission requirements (range, payload, duration against weight, cost etc.). Further, exchange rates are needed to understand the balance between the various criteria likely to be imposed.

The work programmes are aimed at giving baseline and comparative metrics. Technologies introduction can be assessed. This will pave the way towards longer-term system integration.

## 2.2. Phased Programme Envisaged After Consultations with AFRL/VA

Scientists Consulted: Mr. William Blake, Mr. Dieter Multhopp and Dr. Carl Tilmann.

Baseline Vehicle

The study should consider a generic vehicle with the following characteristics as a baseline:

- Wing aspect ratio in the unslewed (minimum sweep) state: 12
- Unswept leading and trailing edge in the unslewed state (Phase I only)
- Tip geometry as needed (streamwise in the cruise condition is acceptable)
- Wing thickness to chord ratio in the unslewed state: 0.15
- Typical Aerofoil
- Decide on TE flap / control (segmented/continuous, say 10-15% chord – full span)
- Wing loading at the mid-cruise point: 40 lb/sq ft
- Payload, OEW, MTOW etc. to be decided
- Assume a reasonably designed Reference Configuration (camber – Twist)
- Stability levels to be decided

Flight Conditions and Propulsion

- Cruise Mach: 1.4
- Maximum cruise altitude: 65,000 ft
- Typical SFC to be assumed

Phase I study

- The primary focus of the Phase I effort is a preliminary assessment of range increase as a function of the number of aircraft in formation. This implies L/D assessments.
- A maximum formation size of four aircraft is desired.
- The primary study variables arethe longitudinal, lateral and vertical spacings.
- Once promising formations have been identified, secondary aspects such as roll trim and adjustment of incidence of trail vehicles such that all aircraft operate at approximately the same lift coefficient should be considered.
- Formations should consist of the study vehicle only with no mixed aircraft formations and only be analysed at the supersonic cruise condition.
- Details to be studied in subsequent Phases

Phase II studies

- The primary focus of the Phase II effort should be a refined estimate of range increase as a function of the number of aircraft in formation, with assumptions made in Phase I relaxed.
- The primary assumption to be relaxed is the wing planform. Variations in wing sweep and taper ratio should be studied.
- This Phase should also conduct a more thorough trim analysis in pitch and yaw.
- A preliminary assessment of propulsion integration issues.
- Decide on Phase III Content

Phase III studies

- Build up on work done in previous phases
- Different Mach numbers
- Apply to Extended Geometry and Flight parameters, Propulsion Issues, Size Issues
- Aero-elastic effects

Deliverable items:

The results from the study should include, as a minimum, the following parameters for each formation examined:

Freestream Mach number and altitude
Six DoF coefficients ($C_L$, $C_D$, $C_m$, $C_l$, $C_n$, $C_Y$) for each vehicle in the formation.
Relative incidence angle of each vehicle in the formation.
Relative spacing ($\Delta x$, $\Delta y$, $\Delta z$) of each vehicle in the formation.

## 3. UNDERSTANDING WAKE FLOWS

Interesting explanatory diagrams have been offered by Schanzer in Ref.18. Although based on Transonic aircraft, these should be indicative and applicable to supersonic regimes after allowing for Mach lines and Mach wave effects.

The magnitude of energy stored in the wing trailing wake of a large transport is indicated in **Fig.3.1** via the contrails generated by the engines. We are also able to determine the spanwise extent of the fully developed and rolled up tip vortices. The trailing wake regions are illustrated and described in **Figs.3.2&3**.

For the supersonic OFW, we consider cases with the wing LE swept behind the Mach cone of the leading tip. In general, the Trail aircraft in CFF will lie within the region bounded by Mach lines emanating from the Lead aircraft.

## 4. PREVIOUS WORK ON CLOSE FORMATION FLYING (CFF) IN SUBSONIC / TRANSONIC FLOW (SYMMETRIC AIRCRAFT)

The cruise drag of an aircraft comprises several components (Section 6.2). The major components are: friction, lift-induced and propulsion installation. The lift-induced $C_{Di}$ part can be 35% to 50% of the total drag depending on $C_L$. In CFF, the $C_{Di}$ can be favourably influenced. Using a simple horse-shoe vortex model, **Fig.4.1**, Blake and Multhopp (Ref.11) have published an interesting graph on lift-induced drag variation as a function of the relative (lateral) positions between a Lead and a Trail aircraft wing, **Fig.4.2**. Both wings are unswept and are of the same size. Although subject to chordwise location effects, it is shown that the "sweet spot" for a drag reduction of 50% occurs at about 20% semi-span overlap with the wings at the same altitude. The ability to fly accurately to maintain lateral position is crucial. Half of the drag benefit is lost if the lateral/vertical position cannot be maintained to better than 10% of wing semi-span.

It is also interesting to note that in symmetric formation (0% lateral spacing), a drag penalty appears depending strongly upon vertical separation (50% semi-span vertical spacing, penalty near 25%. For 25% semi-span vertical spacing, the penalty rises to near 50%). This symmetric formation is frequently used in Air-to-Air Refuelling (AAR). The 0% drag penalty line corresponds to about 40% semi-span overlap of wings (at vertical spacing equal to 0% semi-span and more). We confirm that some locations will be more desirable.

The changes in drag are accompanied by interference effects e.g. in pitch, roll and yaw. **Fig.4.3** shows the variation of Cl/Cn (rolling and yawing moment sensitivity factor) with relative position for two equi-sized wings in formation. The Cl/Cn factor varies rapidly over a relatively small spanwise region, $1.0 > Cl/Cn > -1.0$ for $20\% < y/s < 30\%$.

In our recent work, we have analysed such formation aspects, with more detailed flow models, on representative swept-back wings and have included OFW and aircraft size differences (Refs.15 - 17). Such considerations will be important in practical operations.

## 5. PREVIOUS WORK ON OBLIQUE FLYING WINGS (OFW)

In previous work, Ref.9, we have studied the effects of sweep on an OFW with constant chord, **Fig.5.1**. The effects of incidence ($1.25^o$, $1.50^o$ & $1.75^o$) on the $C_P$ distributions for the planar and designed wings are noted in **Fig.5.2**. For the planar case, the Cp distributions are extremely "peaky" towards the trailing tip region, indicating likely flow separation. These distributions are much improved and tolerable for the designed case. This work and associated development ideas have provided a significant impetus to our current work.

## 6. BASIC OFW CONSIDERATIONS, PRESENT STUDY

Two primary specifications exist for the Switchblade project. A Reconnaissance capability of 15hrs subsonic loiter carrying a payload of 40 000 lb and a Strike capability of Mach 1.6 cruise (Mach 2.0 dash) carrying a 150 000 lb payload. The aircraft is to have a radius of operation of 2875 nm (5750 nm range).

### 6.1. Flight Envelope, Mach and Reynolds Number Variation

There are several aspects to be considered in design of aircraft configurations, e.g.

- Type of spanwise loadings and design of wing camber and twist.
- Trimmed flight at low speeds with different $C_L$ levels. The TE geometry can be varied.
- High-speed design of thick wings (fuel volume), tolerant to large $C_L$ variation. TE flaps.
- Integration of intakes / fuselages.
- "Reasonable" off-design performance – tolerance to cross-winds at landing and take-off.
- Roll, Pitch and Yaw Stability levels, Control laws.

For the current project, the selected parameters are: cruise Mach number of 1.4 at 65 000 ft, Dynamic pressure q = 163.2 lb / $ft^2$. A wing loading of 40 lb/$ft^2$ leads to a $C_L$ of 0.245. The $C_L$ – Mach number relationship is shown in **Fig.6.1.1**. Maintaining the cruise $C_L$ of 0.245 at lower altitudes would require Mach numbers of 0.72 at 37,000 ft, 0.41 at 10 000 ft and 0.34 at sea level. An increased $C_L$ will be required for Take-Off and Landing at a more appropriate Mach number. The Altitude – Mach number relationships for constant $C_L$ values is also shown in **Fig.6.1.1**. Typical Reynolds number values per linear foot are also shown. Mach 1.4 cruise at an altitude of 65,000 ft results in a Reynolds number of 0.64 x $10^6$ / ft. At Sea Level, Take-off at Mach 0.2 results in a Reynolds number of 1.42 x $10^6$ / ft.

It is interesting to note that for conventional aircraft, the cruise $C_L$ values are near 0.5 and at Take-Off and Landing near 0.8 to 1.2. The low speed and high speed demands on the OFW configurations obviously "conflict" and this leads to a challenging work programme.

### 6.2. Broad Drag Considerations

Drag breakdown for Subsonic and Transonic flow was briefly discussed in Section 4. Here we discuss drag breakdown in supersonic flow. The Total Drag of an aircraft may be broken down into various components. For simplicity we consider four main groups: Friction drag, Form drag, Lift Induced drag and Wave drag.

A conventional aircraft has wings, fuselage, tailplane, vertical fin, power-plant and other external excrescences. All surfaces contribute to Friction drag. The lifting surfaces (wing and tailplane) naturally generate Lift Induced drag and broadly speaking are the main contributors to Wave drag. Form drag arises from the overall shape and volume of the aircraft and includes interference terms (wing / fuselage, nacelle / wing, etc.). The OFW geometries considered here do not feature fuselage components thus reducing interference drag.

When determining the benefits of CFF, changes in Lift Induced Drag ($C_{Di}$ in coefficient terms) are the most significant contributor. The Trail aircraft in formation is "riding" on the trailing wake of the Lead aircraft and, where the upwash effects are favourable, the Trail

aircraft receives a beneficial lift contribution. There may also be a change to the primary Lift Induced drag. However, the major benefits arise when the Trail aircraft reduces incidence to eliminate the excess Lift induced by formation flying. This naturally reduces the Lift Induced drag term. The other drag terms are not significantly altered.

We consider the fundamental Drag coefficient breakdown as

$C_D = C_{Do} + C_{Di}$ where

$C_{Do}$ is a zero Lift Drag term that arises from viscosity effects (skin friction and boundary layer), thickness Drag, and Mach number dependent Wave Drag on an equivalent planar wing, i.e.
$C_{Do} = C_{Do}$ (Viscosity) + $C_{Do}$ (thickness) + $C_{Do}$ (Wave due to Volume).
The term $C_{Do}$ (Wave due to Volume) = $C_{Dw0}$ will alter in formations.
The estimation of $C_{DWo}$ is discussed in Appendix A1 for a specimen Oblique Wing from first principles using Harris Wave Drag, Supersonic Area Rule programme.

$C_{Di}$ is the Lift Induced Drag coefficient that includes a contribution to Drag at Zero overall Lift in the case of a twisted wing. It will also contain Wave drag.

A general, variation of Lift Induced Drag factor (k) with Mach number for a wide range of sweep angles is shown in **Fig.6.2.1** for attained suction levels. We note

$k = (C_{Di} \pi AR) / C_L^2$

We may further subdivide the Drag into component parts as follows:

$C_D = C_{Do} + C_{DT} + C_{DW}$ where

$C_{Do}$ is the zero Lift Drag term defined above

$C_{DT}$ is a Trefftz plane analysis estimate of the Drag coefficient which is Lift dependent but independent of Mach number and

$C_{DW}$ is a Wave Drag component dependent upon both Lift and Mach number.

We define two Lift Induced Drag factor components $k_T$ and $k_W$ such that

$C_{DT} = k_T C_L^2 / (\pi AR)$, $k_T$ varies with spanwise loading shape ($k_T = 1$ for elliptic loading)
$C_{DW} = k_W C_L^2 / (\pi AR)$, $k_W$ is of the order of 0.6.

The Lift part of Wave Drag has been set up as a term dependent on the wing sweep angle.

Comparing an OFW with a conventional wing of equal volume we arrive at the following approximate wave drag component ratios

| | **OFW** | **Conventional** |
|---|---|---|
| **Linear dimensions:** | | |
| Span | 1 | 1 |
| Wing Length | 2 | 1 |
| **Wave Drag components:** | | |
| Area Rule, ( ~ Volume$^2$ / length$^4$) | 1/16 | 1 |
| Lift Distribution, ( ~ Lift$^2$ / length$^2$) | 1/4 | 1 |
| Wing Sweep at root, ( ~ cosine (sweep angle)) | 0.866 | 1 |
| Wing Twist, (Tip to Centre to Tip) | +1.5 +1.0 –0.5 | -5.0 +4.0 –5.0 |
| Total Twist and Factor | 2.0 and 1/9 | 18.0 and 1 |

For a pair of identical OFW in CFF (left tip adjacent to right tip) the total Lift, length, span and volume all double giving rise to the following approximation

| | Formation OFW | OFW |
|---|---|---|
| **Linear dimensions:** | | |
| Span | 2 | 1 |
| Wing Length | 2 | 1 |
| **Wave Drag components:** | | |
| Area Rule, ( ~ Volume$^2$ / length$^4$) | 1/4 | 1 |
| Lift Distribution, ( ~ Lift$^2$ / length$^2$) | 1 | 1 |
| Wing Sweep at root, ( ~ cosine (sweep angle)) | 1 | 1 |
| Wing Twist, (Tip to Centre to Tip) | +1.5 +1.0 –0.5 | +1.5 +1.0 –0.5 |
| Total Twist and Factor | 4.0 and 2 | 2.0 and 1 |

Drag analysis for the current OFW configuration is discussed in Section 7.2.

### 6.3. Wing Planform Derivation (Sweep, AR, t/c, etc.)

The derivation of a suitable planform is illustrated in **Fig.6.3.1**. The unswept case ($\Lambda_{LE} = 0^o$) has an Aspect Ratio (AR) of 12.0 with typical t/c = 15.0%. At $\Lambda_{LE} = 30^o$, typically Mach 0.8 conditions, AR = 8.11 with effective streamwise t/c = 13.0%. For Mach 1.4, $\Lambda_{LE} = 60^o$,AR = 3.31 and t/c = 7.5%. To simplify the geometry generation, ensuring that the LE apex and TE apex lay at y = 0.1 and 0.9 respectively, the chord length was modified whilst maintaining $\Lambda_{LE}$ and $\Lambda_{TE} = 60^o$. AR for the resulting planform, **Fig.6.3.1**, was 3.21. For span b = 1.0, the reference area (Sref) and reference length ($c_{ref}$) both equal 0.311769. For the planar case at Mach 1.4, the Centre of Pressure (CP) location is shown in **Fig.6.3.1**. The CP or Neutral Point lies at 0.884896 b aft of the LE Apex and 0.056285 b to the right of centreline. The choice of Centre of Gravity (cg) location will define the degree of stability.

The effects of Trailing Edge (TE) controls on the $\Lambda_{LE} = 60^o$ case at Mach 1.4 have been assessed. The TE of the wing ($0.0<y<0.9$) was subdivided into eight, approximately equi-span, flap segments. Each TE flap has chord of 20% local wing chord. The theoretical panelled geometry was deflected to represent, as closely as possible, the nominal flap geometry. From left to right, viewed from rear, the TE flaps are labelled A to H, **Fig.6.3.1**.

The TEF control powers were evaluated and are discussed in Section 7.3. A simple TEF scheduling sequence was derived to trim the Trail aircraft (3-DoF) in an arbitrarily chosen CFF configuration, Section 9.1.

### 6.4. Theoretical and Analytical Methods Available

Several theoretical methods were available for assessment, design and evaluation of the configuration. Each method offers its own particular attributes and a judicious choice is required during the overall design and evaluation process. Rapid planform assessments have been be made using a Supersonic Panel Method (Panair). Several camber surface designs were derived using the usual modal Linear Theory techniques under various constraints (Mach, design $C_L$, stability levels). The designed OFW was evaluated using Supersonic Panel and Euler methods. By using the results from the various methods appropriately, an overall drag breakdown has been achieved (Section 7.2).

The effects on Lead and Trail aircraft in various Formation configurations were assessed, mainly on the Planar OFW, using the Supersonic Panel Method. Beneficial formation locations, indicated by increased $C_L$ and reduced $C_{Di}$, were identified, initially from a broad range of lateral and vertical displacements at three streamwise displacements. Favourable locations in the y-z plane were then more closely scrutinised. For selected cases, the additional $C_L$ induced on the Trail OFW was trimmed out (1-DoF) by reducing incidence. The resulting additional reduction in $C_{Di}$ was evaluated. Specific formation geometries were assessed using Euler methods.

We note here that Trail aircraft in CFF may be trimmed (6-DoF) in a variety of ways. Changes in sideslip angle could achieve the required reduction in $C_L$ (effected here with reduction in AoA) but with greater Drag reductions and possible beneficial moment control. The deflection of control surfaces to maintain trim conditions may result in Drag increments.

## 7. UNCAMBERED OBLIQUE FLYING WING

The performance of the selected planform, $\Lambda_{LE} = 60^o$, AR = 3.21, t/c = 7.5%, was assessed at Mach 1.4. Initially the basic, "clean" wing was evaluated. With a view to assessing typical TE control surface powers, a second configuration with deflected TE was also evaluated.

### 7.1. Wing (No TE Devices)

A typical panel distribution for the $\Lambda_{LE} = 60^o$, AR = 3.21 planform (t/c = 7.5%) is shown in **Fig.7.1.1**. The spanwise distribution (equally spaced) of the 21 constant 7.5% t/c aerofoil sections is also shown. The tip stations (left and right) have zero chord and appear as single points. Spanwise distributions of $C_{LL}$, $C_{DL}$, $C_{mL}$ with and without $c/c_{ref}$ factor applied are shown in **Fig.7.1.2** at $\alpha = 1.0^o$, $3.83^o$, $4.83^o$ and $5.83^o$. High loadings are noted in the tip areas, effective Taper Ratio = 0.0. At this stage, the tip planform areas and t/c distributions are not representative of any final configuration and will therefore not be designed in any great detail. The chordwise pressure distributions ($C_P$-x) are shown in **Fig.7.1.3** for $\alpha = 3.83^o$, $4.83^o$ and $5.83^o$. The very high suctions in the trailing tip area are noted.

**Fig.7.1.4** shows spanwise loadings for the planar OFW geometry defined with 41 aerofoil sections equally distributed across the span. The results show little difference from those obtained with 21 stations ($\delta C_L$ near +/-0.001 at identical AoA). The corresponding chordwise pressure distributions ($C_P$-x) are shown in **Fig.7.1.5**.

Total loads and moments variations ($C_L$ - $\alpha$, $C_m$ - $C_L$ and $C_l$ - $\alpha$) at M = 1.4 are shown in **Fig.7.1.6**. The solid lines are results from Linear Theory. Supersonic Panel Method results are shown with symbols. An Incidence of $4.83^o$ is required for $C_L = 0.245$. Results for 21 or 41 spanwise stations are very consistent (less than 0.1% difference in $C_L$ and $C_{Di}$). The majority of the subsequent work will be conducted with 21 stations. The $C_m$ - $C_L$ curve suggests the planform is unstable. Neutral stability would be achieved by Moving the moment reference centre (MRC) forward by 0.2% $c_{ref}$ .

Euler method (Ref.30) results were obtained for the planar OFW geometry at Mach 1.4 at three AoA. $C_P$ and surface Mach contours are shown in **Fig.7.1.7**. These confirm the results obtained from the Supersonic Panel Method. The high suction regions with corresponding high surface velocities are evident at higher AoA on the trailing tip.

### 7.2. OFW Drag Assessment

A primary aim of the current work is to gain an understanding of the possible advantages of CFF for OFW. Detailed design analysis of a definitive planform is not the aim and a fairly brief drag analysis is undertaken. We are mainly concerned with assessing improvements in L/D afforded by CFF rather than a highly accurate evaluation of L/D values. From the various theoretical methods available (Linear Theory, Supersonic Panel Methods, Euler Methods, etc.) we are able to establish a satisfactory assessment of the Drag breakdown.

We consider initially the isolated wing ($\Lambda_{LE} = 60^o$, AR = 3.21, $C_L = 0.245$). **Fig.7.2.1** shows the variation of $C_{Di}$ with $C_L$ at Mach 1.4 from Supersonic Panel Method results. The dashed line shows the theoretical values for k = 1.5. The lower solid line shows results from Trefftz plane analysis using wing geometry with 41 spanwise stations. The k value at $C_L = 0.245$ is

1.113. Using input geometry with 21 spanwise stations, k = 1.085. The upper solid line represents the zero suction values ($C_{LDi} = C_L \tan(\alpha)$).

From Linear Theory results, **Fig.7.2.2** shows the variation of k values with Mach number for varying degrees of attained suction. The 0% suction line represents k values achieved on thin wings with sharp LE with fully separated flow. Using input geometry with representative thickness and LE radii, Linear Theory predicts "best achievable" attained suction levels. The resulting k values are shown in **Fig.7.2.2**. Also shown is the k = 1 line and k values resulting from Trefftz plane analysis.

We can estimate a k value of about 1.6 at at Mach 1.4. This also relates to **Fig.6.2.1** for wing sweep $60^o$. For $C_L = 0.245$, AR = 3.21, k = 1.6 gives $C_{Di}$ of approximately 100 counts. For peak L/D ($C_{Do} = C_{Di}$) these relationships lead to L/D = 12.25. This implies that $C_{Do}$ contains the Wave drag due to volume ($C_{ow0}$ ).

Trefftz plane analysis for the planar (uncambered) OFW at Mach 1.4 gives $k_T = 1.085$ at $C_L = 0.245$, see Section 6.2. A wave drag k factor ($k_W$) contribution of 0.592 results in an overall k value of 1.677. Introducing $C_{Do} = 0.0100$ gives L/D = 12.25.

This method of Drag breakdown allows easy analysis for the CFF assessment. In CFF, if we assume that the Lead OFW is unaffected by the Trail wing and aerodynamic performance matches that of an isolated OFW. We then need only assess the drag reduction ($\Delta C_{Di}$) on the Trail wing in CFF at each formation geometry from Trefftz plane analysis. The resulting increase in L/D can then be evaluated.

### 7.3. Wing with TE Devices

Each of the TE flaps (A to H) described in Section 6.3 was deflected, TE up / down, by –1.0 / +1.0 deg. The resulting increments, per $^o$TEF, in $C_L$ are shown in bar-chart form in **Fig.7.3.1**. Increments in $C_l$, $C_m$ and $C_n$ for each flap are shown in **Fig.7.3.2**. Results for positive TEF (TE down) are shown as solid lines, negative TEF results are shown as dashed lines. The desired flap segmentation does not necessarily lie on panel geometry lines and hence the flaps have varying planform area. At this stage, the TEF powers have not been non-dimensionalised by local flap area. In general, opposing TEF deflections gave equal but opposite increments in each of the four components. These results have indicated that suitable combinations of TEF deflections may be deployed to control the induced effects of CFF. A simple TEF scheduling sequence, using flaps A and H only, has been evaluated for one, arbitrarily chosen, CFF configuration, Section 9.1. We have shown that one CFF formation can be trimmed in $C_L$, $C_l$ and $C_m$ (3-DoF). Further work would be required to evaluate other CFF cases and to include $C_n$. This can be undertaken at a later stage when a more definitive geometry is available. It may prove more effective to use changes in camber design to eliminate induced Lift and control roll, rather than discrete TE flaps.

## 8. DESIGNED OBLIQUE FLYING WING

The design requirements for the $\Lambda_{LE} = 60^o$, AR = 3.21 planform were $C_L = 0.245$ at Mach 1.4. A constant thickness distribution across the span (t/c = 7.5%) was chosen. On novel layouts such as the OFW it is often the experience that the complexities defy the use of automated hands-off design processes. We have therefore been more prudent and have chosen a process that allows a significant understanding to be gained with reasonable control over the design process (Refs.20 – 29).

A Modal Linear Theory technique has been used to define the camber surface required for design $C_L$ and $C_m$ constraints at the design Mach number. A simple calibration was required to match the Linear Theory method with the Supersonic Panel Method. A Linear Theory

method design $C_L$ of 0.22 with $C_m$ constraint of –0.1 gave $C_L$ = 0.246 at $\alpha = 5.09^o$ with the Supersonic Panel Method.

### 8.1. Designed Wing without Spanwise Loading Constraint (ycg at yac), Wing-1

The spanwise distribution of the cambered, 7.5% t/c, aerofoil sections (21 across the span) is in **Fig.8.1.1**. Note that the right, trailing tip has more camber / twist than the left, leading tip.

Spanwise distributions of $C_{LL}$, $C_{DL}$, $C_{mL}$ with and without $c/c_{ref}$ factor applied are shown in **Fig.8.1.2** at $\alpha = 1.26^o$, $4.09^o$, $5.09^o$ and $6.09^o$. The chordwise pressure distributions ($C_P$-x) are in **Fig.8.1.3** for $\alpha = 4.09^o$, $5.09^o$ and $6.09^o$. The Cp distributions for the designed wing are well behaved. The high suctions evident at corresponding $C_L$ in **Fig.7.1.4** are ameliorated.

In **Fig.8.1.4** we compare directly the $C_P$ – x distributions for the planar, uncambered wing with those for the designed wing case, each with 21 spanwise stations. The significant improvement in chordwise pressure distributions for the designed case can be observed.

Total loads and moments variations ($C_L$ - $\alpha$, $C_m$ - $C_L$ and $C_l$ - $\alpha$) from the Supersonic Panel Method at M = 1.4 are shown in **Fig.8.1.5**, together with results for the planar, uncambered wing (Supersonic Panel Method). For the design case an incidence of $5.09^o$ is required for $C_L$ = 0.245. The $C_m$ - $C_L$ curve suggests the planform is marginally stable. Neutral stability would be achieved by Moving the moment reference centre (MRC) rearward by 0.3% $c_{ref}$ . Stability issues will require further analysis once a representative geometry is defined.

### 8.2. Designed Wing with Spanwise Loading Constraint (ycg at 0.5b), Wing-2

The spanwise distribution of the cambered, 7.5% t/c, aerofoil sections for this design case (21 spanwise stations) is shown in **Fig.8.2.1**. The design requirement for zero roll at the design $C_L$ has resulted in an almost symmetrical spanwise load distribution, **Fig.8.2.2**. Off-design, the distributions become less symmetric indicating a variation in rolling moment ($C_l$) as $C_L$ changes. The chordwise pressure distributions ($C_P$ - x) are shown in **Fig.8.2.3** for $\alpha = 3.83^o$, $4.83^o$ and $5.83^o$. The pressure distributions for the designed wing are well behaved. The high suctions evident in the planar wing case have been ameliorated.

The design process was repeated using 41 spanwise stations. The resulting geometry, spanwise loadings and chordwise distributions (AoA = $5.43^o$) are shown in **Fig.8.2.4**. There are no discernable differences in the geometries. The spanwise loads are shown for AoA = $4.43^o$, $5.43^o$ and $6.43^o$. At AoA = $5.43^o$, $C_L$ = 0.247 and 0.245 for the 21 and 41 spanwise station cases respectively. Chordwise distributions for the Planar and designed Wing-2 cases, each with 41 spanwise stations are shown for $C_L$ = 0.24 in **Fig.8.2.5**. Again, the improved distributions for the design case are evident. There is little perceivable difference between results for 21 and 41 spanwise stations and consequently, geometries with 21 stations have been used for the major part of the remaining CFF comparisons.

Total loads and moments variations ($C_L$ - $\alpha$, $C_m$ - $C_L$ and $C_l$ - $\alpha$) from the Supersonic Panel Method at M = 1.4 are shown in **Fig.8.2.6**, together with results for the planar, uncambered wing. For the design case an incidence of $5.43^o$ is required for $C_L$ = 0.245. Using 41 strips made very little difference in total loads.

The $C_m$ - $C_L$ curve suggests that the planform is unstable. Neutral stability would be achieved by moving the moment reference centre (MRC) forward by 1.0% $c_{ref}$. The $C_l$ - $\alpha$ curve indicates a slight positive $C_l$ at the design point. The dashed line in **Fig.8.2.6** is for results with the MRC moved 1% b to the right of centreline. Stability issues will require further analysis once a representative geometry is defined.

## 9. FORMATIONS OF BASIC UNCAMBERED OBLIQUE FLYING WINGS

The $\Lambda_{LE}$ = 60$^o$, AR = 3.21 uncambered (planar) wing geometry described in Section 6.3 is used for initial estimates of the induced effects due to Close Formation Flying (CFF). The asymmetry of the OFW will have a significant effect on the relevant attributes of formation layouts. For a two aircraft formation (Lead and Trail), the effects at various lateral and vertical displacements at three streamwise separations are determined. We also briefly look at three and four aircraft formations.

For a two aircraft formation, provided the Trail aircraft lies within the Mach cone of the Lead aircraft and the Mach cone of the Trail aircraft does not interfere with the Lead aircraft, the Lift and Drag of the Lead aircraft in formation remain unaffected and are therefore identical to the isolated aircraft values. For certain formation geometries, the Trail aircraft experiences an increase in Lift and a reduction in Lift Induced Drag. The additional lift can be reduced to a value equal to that of the isolated aircraft by a reduction in Trail aircraft incidence (trimmed, 1-DoF). Future work could include the re-design of the Trail aircraft geometry to eliminate additional Lift, Pitch and Roll effects (3-DoF) induced by CFF.

In certain CFF situations, the Mach cone of the Trail aircraft interferes with the Lead aircraft. Interference effects result. In these cases we need to trim both aircraft to the same target $C_L$ (0.245) before estimating the CFF benefits in terms of reduced Drag and improved L/D.

**Drag estimation for aircraft in CFF**

We define three methods for estimating the Lift Induced Drag ($C_{Di}$) term for OFW in CFF. Both OFW are trimmed to the same $C_L$ (0.245) by adjusting each OFW incidence as required. The change in incidence ($d\theta$) on the Trail OFW is used for the change in $C_{Di}$ as follows:

$$\Delta C_{Di} = d\theta \,.\, C_L \qquad \text{[Blake]}$$

Using the Supersonic Panel Method on the trimmed CFF configuration, surface pressure integration will give an indication of $C_{Di}$ on each OFW in the configuration. We consider results on the OFW in CFF and isolated:

$$\Delta C_{Di} = (C_{Di})_{CFF} - (C_{Di})_{ISO} \qquad \text{[Integration method]}$$

Trefftz plane analysis for a CFF configuration will yield the total $C_L$ and $C_{Di}$ for the configuration. In general we assume that the Lead OFW acts as an isolated OFW and interference effects are minimal. Using the Trefftz plane values:

$$\Delta C_{Di} = (C_{Di})_{Trefftz} - 2*(C_{Di})_{ISO} \qquad \text{[k method]}$$

We look at results for a few specific formation geometries before considering the overall trends in terms of $C_L$ and L/D gain on the Trail aircraft.

## 9.1. Core 1 type formation, dx = -2.0

**Two aircraft formation**

Typical Core 1 type formations, Section 2.1, are shown in **Fig.9.1.1**. The leading, left tip of the Trail aircraft is generally aligned with the trailing, right tip of the Lead aircraft. **Fig.9.1.1** shows the relative displacements in the x-y plane.

As a result of the way in which the geometries are generated for theoretical analysis, a particular x, y, z sign convention has evolved. All displacements (dx, dy and dz) refer to the Lead wing offset with respect to the Trail wing location and are measured between identical points on each (e.g. wing apex). Streamwise displacement, dx, by definition of “Lead” and “Trail”, is negative. Lateral displacement, dy, is negative for Core 1 CFF, Lead wing to the left of the Trail wing. Vertical displacement, dz, is negative for Lead below Trail, **Fig.9.1.1**.

A key formation geometry, from the theoretical point of view, occurs when the Lead aircraft right tip is co-incident with the Trail aircraft left tip. The wings then act as a continuous, very

high AR configuration. In **Fig.9.1.1** this condition is defined by dx = -1.5588, dy = -0.9, dz = 0.0. Note that interference effects occur at this CFF situation. The total $C_{DW0}$ remains the same as that for the lead wing in isolation, i.e. the Trail wing does not cause any extra wave drag penalty, see Appendix A1.

The spanwise loadings for the Trail aircraft in formation (dx = -2.0, dy = -1.0, dz = -0.03) are compared with those for the isolated case in **Fig.9.1.2**. The increase in $C_L$ is clearly seen. It is noted that the increase is biased towards the left tip of the Trail aircraft, inducing a negative $\Delta C_l$. An increase in $C_{Di}$ and also in $C_m$ is noted for this untrimmed case ($d\theta = 0.0$). Values of $C_L$, $C_l$ and $C_m$ are noted in the following table.

| | dθ | Dy | dz | $C_L$ | $C_l$ | $C_m$ |
|---|---|---|---|---|---|---|
| Lead | | -1.0 | -0.03 | 0.245 | -0.0001 | +0.0004 |
| Trail | +0.00 | 0.0 | 0.00 | 0.305 | -0.0081 | +0.0445 |

Reducing the AoA on the Trail aircraft ($d\theta = -1.177^o$) so that both aircraft are at the same $C_L$ results in the spanwise loads distribution shown in **Fig.9.1.3**. The drag reduction on the Trail aircraft is evident. The modified $C_L$ distribution, now less "triangular" in shape, will still result in a negative $C_l$ increment as shown in the following table.

| | dθ | dy | dz | $C_L$ | $C_l$ | $C_m$ |
|---|---|---|---|---|---|---|
| Lead | | -1.0 | -0.03 | 0.245 | -0.0001 | +0.0004 |
| Trail | -1.177 | 0.0 | 0.00 | 0.245 | -0.0080 | +0.0449 |

The modified $C_P$-x distributions resulting from the reduced AoA on the Trail aircraft are compared with those for the uncorrected case in **Fig.9.1.4**. The reduced $C_P$ levels arising from the lower AoA are evident.

The following table gives a comparison of Drag reductions resulting from the three methods, at dx = -2.0 at selected dy and dz displacements.

| Dy | dz | $C_P$ integration $\Delta C_{Di}$ = | k method $\Delta C_{Di}$ = | dθ | dθ (rad).$C_L$ $\Delta C_{Di}$ = |
|---|---|---|---|---|---|
| -1.0 | -0.05 | -0.0036 | -0.0036 | -1.0529 | -0.0045 |
| -1.0 | -0.03 | -0.0039 | -0.0040 | -1.1741 | -0.0050 |
| -1.0 | +0.01 | -0.0044 | -0.0047 | -1.2958 | -0.0055 |
| -0.90 | -0.01 | -0.0051 | -0.0053 | -1.3378 | -0.0057 |

For the particular CFF case (dy = -1.0, dz = -0.01) the Trail wing L/D = 16.0, an increase of 31%. We shall compare these benefits to those obtained using designed wing geometry in Section 10. Drag reductions and L/D improvements for the Planar OFW in Core 1 CFF, over the range of dx, dy and dz explored, are given in graphical form and discussed in Section 11.

**Using TEF deflections to correct for $C_l$ and $C_m$ in CFF**

A series of TEF were defined on the OFW, Section 6.3 and their effectiveness (control power) evaluated in Section.7.3. We have arbitrarily chosen a Core 1 CFF configuration (dx = -2.0, dy = -0.9, dz = -0.05) and determined the changes in lift, drag and moments (pitch, roll and yaw) on the Trail aircraft due to CFF. Results for the isolated OFW, the OFW in CFF and the increments due to CFF are shown in the table below.

To establish the principles and feasibility we have determined TEF deflection angles for TEF A and H only ($\varepsilon_A$ and $\varepsilon_H$) and the change in AoA required to correct, to a first order, for pitch, roll and lift (3-DoF) in the CFF case chosen. The values are $\varepsilon_A = -0.73$, $\varepsilon_H = 4.82$ and $\Delta\alpha = -1.118^o$. The CFF induced $C_l$ has been reduced by two-thirds and induced $C_m$ by three-

quarters. The desired $C_L$ has been achieved with a notable reduction in $C_{Di}$. However, the isolated configuration has not been trimmed in Yaw. Deflection of TEF A and H only to correct for $C_L$, $C_m$ and $C_l$ (3-Dof) has had a favourable effect in reducing $C_n$.

| | $C_L$ | $C_{Di}$ | $C_l$ | $C_m$ | $C_n$ |
|---|---|---|---|---|---|
| Isolated wing | 0.245 | 0.0065 | -0.0001 | 0.0004 | 0.0078 |
| Trail in CFF | 0.298 | 0.0050 | -0.0032 | 0.0212 | 0.0073 |
| CFF induced increments | 0.053 | -0.0015 | -0.0031 | 0.0208 | -0.0005 |
| Trail in CFF after trimming | 0.243 | 0.0037 | 0.0010 | -0.0044 | 0.0051 |
| Trail trimmed increments | -0.002 | -0.0028 | +0.0011 | -0.0048 | -0.0027 |

We note that this preliminary solution has been obtained by means of simultaneous equations in three unknowns using only two of the eight available TEF. A full optimisation procedure using Lagrange multipliers will be needed to trim the OFW in CFF whilst minimising drag.

**Three Aircraft Formation**

Adding a second Trail aircraft to a two aircraft Core 1 type formation leads to a three aircraft "echelon" formation. As we move from the Lead to the second to the third aircraft, x increases by 2.0 span units, z increases by 0.03 span units and y increases by 1.0 span units, i.e. aircraft in the formation are above and to the right of the preceding aircraft.

The spanwise loadings on all three aircraft in formation are shown in **Fig.9.1.5**. The increase in $C_L$ gained by the second aircraft is comparable to that for the Trail aircraft in a two aircraft formation. The third aircraft in this three aircraft Core 1 type formation has marginally more additional lift than the second. In general, the load distributions on the second and third aircraft are very similar. As noted for the two aircraft CFF, the increase is biased towards the left tip of the trailing aircraft, inducing negative $\Delta C_l$. An increase in $C_{Di}$ and also in $C_m$ is noted for this untrimmed case ($d\theta = 0.0$). $C_L$, $C_l$ and $C_m$ values are noted as follows.

| | $d\theta$ | dx | dy | dz | $C_L$ | $C_l$ | $C_m$ |
|---|---|---|---|---|---|---|---|
| Lead | +0.00 | -4.0 | -2.0 | -0.06 | 0.245 | -0.0001 | +0.0004 |
| Second | +0.00 | -2.0 | -1.0 | -0.03 | 0.305 | -0.0081 | +0.0445 |
| Trail | +0.00 | 0.0 | 0.0 | 0.00 | 0.320 | -0.0094 | +0.0518 |

Reducing the AoA on the second aircraft ($d\theta = -1.177^o$) to achieve CL = 0.245, but leaving the Trail aircraft untrimmed, results in $C_L$, $C_l$ and $C_m$ values shown in the following table.

| | $d\theta$ | dx | dy | dz | $C_L$ | $C_l$ | $C_m$ |
|---|---|---|---|---|---|---|---|
| Lead | +0.00 | -4.0 | -2.0 | -0.06 | 0.245 | -0.0001 | +0.0004 |
| Second | -1.767 | -2.0 | -1.0 | -0.03 | 0.245 | -0.0080 | +0.0449 |
| Trail | +0.00 | 0.0 | 0.0 | 0.00 | 0.305 | -0.0075 | +0.0414 |

To achieve $C_L = 0.245$ on the Trail wing requires a reduction in AoA of $1.186^o$. All three aircraft in this Core 1 CFF are now trimmed to the same CL value (1-DoF). The resulting $C_l$ and $C_m$ values shown in the following table. The spanwise loadings are shown in **Fig.9.1.6**.

| | $d\theta$ | dx | dy | dz | $C_L$ | $C_l$ | $C_m$ |
|---|---|---|---|---|---|---|---|
| Lead | +0.00 | -4.0 | -2.0 | -0.06 | 0.245 | -0.0001 | +0.0004 |
| Second | -1.767 | -2.0 | -1.0 | -0.03 | 0.245 | -0.0080 | +0.0449 |
| Trail | -1.186 | 0.0 | 0.0 | 0.00 | 0.245 | -0.0074 | +0.0418 |

The following table summarises the drag reductions on the Second and Third (Trail) wings in a three aircraft Core 1 type formation. Drag reductions with the three methods are shown.

| | dz | $C_P$ integration $\Delta C_{Di}$ = | k method $\Delta C_{Di}$ = | dθ | dθ (rad).$C_L$ $\Delta C_{Di}$ = |
|---|---|---|---|---|---|
| Second | -0.03 | -0.0040 | -0.0041 | -1.1767 | -0.0050 |
| Trail | 0.00 | -0.0042 | -0.0041 | -1.1858 | -0.0051 |

In this "regularly" displaced CFF configuration, the drag reductions (compared to the isolated case) for the second and third aircraft are almost identical. Appreciable L/D gains for the total formation result. Assuming the Lead aircraft remains unaffected, it maintains its L/D = 12.25. L/D for the second and third aircraft increases to 15.4 (25% increase for each).

**Four or more aircraft formation**

It is anticipated that adding more Trail aircraft in a "regular" pattern in the formation will give similar drag reductions for all Trail aircraft. Theoretically, there is no limit. Obviously, the effects of viscosity, etc. will have a bearing on the total benefits and these will need to be considered in further analysis.

## 9.2. Core 2 type formation, dx = -2.0

**Two Aircraft Formation**

Typical Core 2 type formations, Section 2.1, are shown in **Fig.9.2.1**. The trailing, right tip of the Trail aircraft is generally aligned with the leading, left tip of the Lead aircraft. **Fig.9.2.1** shows the relative displacements in the x-y plane. The sign conventions used are discussed in Section 9.1. The spanwise loadings for the Trail aircraft in formation (dx = -2.0, dy = +1.0, dz = -0.03) are compared with those for the isolated case in **Fig.9.2.2**. The Lift increments are not as significant as those for the equivalent Core 1 case but are biased towards the right tip of the Trail wing, accentuating the "triangular" nature of the distribution, inducing a positive $\Delta C_l$. An increase in $C_{Di}$ and a negative $C_m$ are noted for this untrimmed case (dθ = 0.0). $C_L$, $C_l$ and $C_m$ values are noted in the following table.

| | dθ | dy | dz | $C_L$ | $C_l$ | $C_m$ |
|---|---|---|---|---|---|---|
| Lead | | +1.0 | -0.03 | 0.245 | -0.0001 | +0.0004 |
| Trail | +0.00 | 0.0 | 0.00 | 0.274 | +0.0033 | -0.0185 |

Reducing the AoA on the Trail wing (dθ = -0.571$^o$) so that both aircraft are at the same $C_L$ results in the spanwise loads distribution shown in **Fig.9.2.3**. These are now very similar. The drag reduction on the Trail aircraft is evident. The modified $C_L$ distribution, will still result in a positive $C_l$ increment as shown in the following table.

| | dθ | dy | dz | $C_L$ | $C_l$ | $C_m$ |
|---|---|---|---|---|---|---|
| Lead | | +1.0 | -0.03 | 0.245 | -0.0001 | +0.0004 |
| Trail | -0.571 | 0.0 | 0.00 | 0.245 | +0.0034 | -0.0182 |

The $C_P$ – x distributions are shown in **Fig.9.2.4**.

The following table summarises the drag reduction on the Trail wing in a Core 2 type formation. The Lead wing is displaced dx = -2.0, dy = 1.0, dz = -0.01 and -0.03 with respect to the Trail wing (i.e. Trail is to the left and above the Lead wing). Drag reductions with the three methods are shown.

| dy | dz | $C_P$ integration $\Delta C_{Di}$ = | k method $\Delta C_{Di}$ = | dθ | dθ (rad).$C_L$ $\Delta C_{Di}$ = |
|---|---|---|---|---|---|
| +1.0 | -0.01 | -0.0030 | -0.0031 | -0.5955 | -0.0025 |
| +1.0 | -0.03 | -0.0029 | -0.0021 | -0.5694 | -0.0024 |

The resulting L/D increments are of the order of 12% to 18%. Drag reductions and L/D improvements for the Planar OFW in Core 2 CFF, over the full range of dx, dy and dz explored, are given in graphical form and discussed in detail in Section 11.

**Three Aircraft or More in a Formation**

Adding a second Trail aircraft to a two aircraft Core 2 type formation leads to a three aircraft "echelon" formation. As we move from the Lead to the second to the third aircraft, z increases by 0.03 span units and y decreases by 1.0 span units, i.e. aircraft in the formation are above and to the left of the preceding aircraft. The spanwise load distributions on all three aircraft in formation are shown in **Fig.9.2.5**. The load distributions for the second and Trail aircraft are very similar. The increases in $C_L$ gained by the second and third aircraft are proportional to those for the Core 1 three aircraft formation. As noted for the two aircraft CFF, the increase is biased towards the right tip of the trailing aircraft, inducing positive $\Delta C_l$. An increase in $C_{Di}$ and a negative $C_m$ are noted for this untrimmed case (dθ = 0.0). $C_L$, $C_l$ and $C_m$ values are noted in the following table.

| | dθ | dx | dy | dz | $C_L$ | $C_l$ | $C_m$ |
|---|---|---|---|---|---|---|---|
| Lead | | -4.0 | +2.0 | -0.06 | 0.245 | -0.0001 | +0.0004 |
| Second | +0.00 | -2.0 | +1.0 | -0.03 | 0.274 | +0.0033 | -0.0185 |
| Trail | +0.00 | 0.0 | 0.0 | 0.00 | 0.281 | +0.0038 | -0.0212 |

Trimming the second aircraft to $C_L$ = 0.245 by reducing AoA (1-DoF, dθ = -0.571$^o$) but leaving the Trail aircraft untrimmed, results in $C_L$, $C_l$ and $C_m$ values shown as follows:.

| | dθ | dx | dy | dz | $C_L$ | $C_l$ | $C_m$ |
|---|---|---|---|---|---|---|---|
| Lead | +0.00 | -4.0 | +2.0 | -0.06 | 0.245 | -0.0001 | +0.0004 |
| Second | -0.571 | -2.0 | +1.0 | -0.03 | 0.245 | +0.0034 | -0.0182 |
| Trail | +0.00 | 0.0 | 0.0 | 0.00 | 0.278 | +0.0034 | -0.0190 |

Trimming the second and third aircraft to $C_L$ = 0.245 (1-DoF) results in the spanwise load distributions shown in **Fig.9.2.6** and the $C_L$, $C_l$ and $C_m$ values shown in the following table.

| | dθ | dx | dy | dz | $C_L$ | $C_l$ | $C_m$ |
|---|---|---|---|---|---|---|---|
| Lead | +0.00 | -4.0 | +2.0 | -0.06 | 0.245 | -0.0001 | +0.0004 |
| Second | -0.571 | -2.0 | +1.0 | -0.03 | 0.245 | +0.0034 | -0.0182 |
| Trail | -0.649 | 0.0 | 0.0 | 0.00 | 0.245 | +0.0035 | -0.0190 |

The following table summarises the drag reductions on the Second and Third wings in a Core 2 type formation. Drag reductions resulting from the three methods are shown.

| | dz (Lead 0.19) | $C_P$ integration $\Delta C_{Di}$ = | k method $\Delta C_{Di}$ = | dθ | dθ (rad).$C_L$ $\Delta C_{Di}$ = |
|---|---|---|---|---|---|
| Second | +0.03 | -0.0029 | -0.0028 | -0.5706 | -0.0024 |
| Third | +0.06 | -0.0033 | -0.0034 | -0.6494 | -0.0028 |

At these displacements, the L/D gains for the second and third aircraft (+16%) are not as significant as those for the Core 1 type formation.

**Four or more aircraft formation**

Similar conclusions may be drawn for Core 2 multiple aircraft CFF configurations as were drawn for the Core 1 case.

## 10. FORMATIONS OF DESIGNED OBLIQUE FLYING WINGS

In this section we assess the CFF effects using $\Lambda_{LE}$ = 60°, AR = 3.21 designed wing geometry, Section 8, for both Lead and Trail aircraft. Two design cases were chosen, one without spanwise loading constraint (ycg at yac), Wing-1 and one with spanwise loading constraint (ycg at 0.5b), Wing-2. Selected points and lateral scans at dx = 2.0 were assessed using the designed geometries.

### 10.1. Core 1 type formation

**Two aircraft formation**

Typical Core 1 type formations for the designed wing are similar to those of Section 2.1 (**Fig.9.1.1)**. The leading, left tip of the Trail aircraft is generally aligned with the trailing, right tip of the Lead aircraft. **Fig.9.1.1** shows the relative displacements in the x-y plane.

**Core 1 type formation, dx = -2.0, Wing-1**

The spanwise loadings for the Trail wing in a formation of designed wings (dx = -2.0, dy = -1.1, dz = +0.01) are compared with those for the isolated case in **Fig.10.1.1**. The increase in $C_L$ for the untrimmed case is clearly seen. It is noted that the increase is biased towards the left tip of the Trail aircraft, inducing a negative $\Delta C_l$. An increase in $C_{Di}$ and also in $C_m$ is noted for this untrimmed case.

Reducing the AoA on the Trail aircraft so that both aircraft in formation are at the same $C_L$ results in modified spanwise loads distributions. These are also shown in **Fig.10.1.1**. The drag reduction on the Trail aircraft is evident. The modified $C_L$ distribution will still result in a positive $C_l$ increment. $C_m$ is now much closer to the isolated aircraft value.

The following table summarises the drag reduction on the Second wing in a Core 1 type formation of designed, Wing-1 OFW. The displacements are dx = -2.0, dy = -1.0, dz = +0.01 and -0.01 (i.e. Trail is to the right, above and below the Lead wing). Drag reductions resulting from the three methods are shown.

dx = -2.0 (between adjacent wings)

| dy | dz | $C_P$ integration $\Delta C_{Di}$ = | k method $\Delta C_{Di}$ = | dθ | dθ (rad).$C_L$ $\Delta C_{Di}$ = |
|---|---|---|---|---|---|
| -1.0 | +0.01 | -0.0046 | -0.0047 | -1.2960 | -0.0055 |
| -1.0 | -0.01 | -0.0045 | -0.0047 | -1.2950 | -0.0055 |

In both these cases, Trail wing L/D = 16.0, a 31% increase due to CFF. These are very similar to those obtained for the Planar wings at the same CFF configurations. Drag reductions and L/D improvements for the designed Wing-1 OFW in Core 1 CFF, over the full range of dx, dy and dz explored, are given in graphical form and discussed in detail in Section 11.

**Core 1 type formation, dx = -2.0, dy = -1.0, Wing-2**

The following table summarises the drag reduction on the Second wing in a Core 1 type formation of designed, Wing-2 OFW. The displacements are dx = -2.0, dy = -1.0, dz = +0.01 and -0.01 (i.e. Trail is to the right, above and below the Lead wing). Drag reductions resulting from the two of the three methods are shown.

dx = 2.0 (between adjacent wings)

| dy | dz | $C_P$ integration $\Delta C_{Di}$ = | k method $\Delta C_{Di}$ = | dθ | dθ (rad).$C_L$ $\Delta C_{Di}$ = |
|---|---|---|---|---|---|
| -1.0 | +0.01 | -0.0040 | -0.0039 | -1.1335 | -0.0049 |
| -1.0 | -0.01 | -0.0039 | -0.0039 | -1.1202 | -0.0048 |

Drag reductions and L/D improvements for the designed Wing-2 OFW in Core 1 CFF, over the full range of dx, dy and dz explored, are given in graphical form and discussed in detail in Section 11.

## 10.2. Core 2 type formation

**Two aircraft formation**

Designed Wing-1 was not assessed in Core 2 CFF.

**Core 2 type formation, dx = -2.0, dy = 1.0, Wing-2**

The following table summarises the drag reduction on the Second wing in a Core 2 type formation of designed, Wing-2 OFW. The displacements are dx = -2.0, dy = 1.0, dz = -0.01, +0.01 and +0.05 (i.e. Trail is to the left, below and above the Lead wing). Drag reductions resulting from the three methods are shown.

dx = -2.0 (between adjacent wings)

| Dy | dz | $C_P$ integration $\Delta C_{Di}$ = | k method $\Delta C_{Di}$ = | dθ | dθ (rad).$C_L$ $\Delta C_{Di}$ = |
|---|---|---|---|---|---|
| 1.0 | -0.01 | -0.0034 | -0.0035 | -0.6888 | -0.0030 |
| 1.0 | +0.01 | -0.0033 | -0.0035 | -0.6811 | -0.0029 |
| 1.0 | +0.05 | -0.0028 | -0.0032 | -0.5940 | -0.0025 |

Drag reductions and L/D improvements for the designed Wing-2 OFW in Core 2 CFF, over the full range of dx, dy and dz explored, are given in graphical form and discussed in detail in Section 11.

# 11. COMPARISONS

We compare three methods (Pressure integration, k method and Blake's method) of deriving the Lift Induced Drag ($C_{Di}$) component for the Trail wing in Close Flying Formation (CFF). The methods were described in Section 9. Comparisons are made for wings in CFF at the same $C_L$, i.e. in 1-DoF trimmed condition. At this stage we have not trimmed for induced moments.

Reductions in $C_{Di}$ for the Trail OFW in CFF derived using the k method, with $k_w = 0.59$, have been used to evaluate L/D and ΔL/D% increments with respect to the isolated OFW case.

For this initial investigation we have conducted a preliminary Drag analysis that leads to L/D = 12.25 for the planar OFW. For current comparative purposes these values have also been used for the design cases Wing-1 and Wing-2.

We begin with a brief discussion relating to the type of spanwise load distribution exhibited by each OFW geometry (Planar, Wing-1 design and Wing-2 design). It is noted that the type of spanwise loading has a significant bearing on the magnitude of L/D benefits gained in CFF with respect to Core 1 or Core 2 type arrangements. As a result of the current phase of work we are able to define CFF geometry relationships that are likely to be beneficial although, bearing in mind that the OFW geometry is not definitive, optimisation has not been persevered with.

**Planar OFW in CFF**

The Planar wing load distribution in isolation is "triangular". In Core 1 CFF (dy = -1.0, Lead to left of Trail) this becomes more elliptical and produces comparatively large $C_{Di}$ reductions but coupled with a large induced rolling moment ($\Delta C_l$ = -0.00970). After trimming the Trail wing incidence (-1.2958$^o$) to give the same $C_L$ (0.245) as the Lead wing, the induced $\Delta C_l$ remains unaffected. The resulting increase in L/D is of the order of 30%.

In Core 2 CFF (dy = 1.0, Lead to right of Trail) the "triangular" nature of the wing loading is maintained, producing comparatively small $C_{Di}$ reductions, coupled with a smaller magnitude induced rolling moment ($\Delta C_l$ = +0.0040). After trimming the Trail wing incidence (-0.5955$^o$) for $C_L$, the induced $\Delta C_l$ remains unaffected. The increase in L/D for this case is of the order of 18%.

The use of TE devices to trim out the induced roll will give rise to additional drag. Further work is required to assess the magnitude of reduction in CFF benefits arising from the trimming of the Trail wing.

**Wing-1 Design OFW in CFF**

The spanwise loading distribution of Wing-1 in isolation is "triangular", similar to the planar wing distribution. In Core 1 CFF this becomes more elliptical and produces comparatively large $C_{Di}$ reductions but coupled with a large induced rolling moment.

Again, the use of TE devices to trim out the induced roll will give rise to additional drag and further work is required to assess the effects.

**Wing-2 Design OFW in CFF**

The spanwise load distribution of Wing-2 in isolation is of elliptical form. When trimmed (1-DoF, both aircraft at same $C_L$) in Core 1 CFF the distribution maintains its shape producing less significant but more representative $C_{Di}$ reductions. The induced rolling moment is proportionally less and therefore requires smaller deflection of TE devices for trim incurring lower additional drag penalties. Further work is required to quantify the magnitude of these effects.

**Drag Breakdown and L/D increments**

Drag evaluated using each of the methods (to estimate the Lift Induced Drag ($C_{Di}$) component) is denoted in the figures using the corresponding letter, Pressure integration (P), k method (K) and Blake's method (B).

## 11.1. Core 1 type CFF

Planar OFW

The drag breakdown for the Trail wing in CFF (Planar geometry) as relative vertical displacement between Lead and Trail varies, is shown in **Fig.11.1.1**. Two Core 1 lateral displacements are considered, dy = -1.1 b in **Fig.11.1.1(a)** and dy = -1.0 b in **Fig.11.1.1(b)**. A displacement of dy = -1.1 implies a 10% b Gap laterally between the OFW tips (dy = -1.0 ~ tips in line, dy = -0.9 ~ 10% b Lap). At dy = -1.1, method K gives approximately 25 drag

count reduction in $C_{Di}$ throughout the vertical displacement range shown. Method B gives approximately 30 drag count reduction.

With the Lead and Trail OFW tips in line (dy = -1.0), **Fig.11.1.1 (b)**, the $C_{Di}$ reductions are greater, reaching a maximum when the wings are almost at the same altitude.

The $C_{Di}$ reductions (k method) give L/D improvements shown in **Fig.11.1.2**. At dy = -1.1, L/D increments of about 15% are shown over the vertical displacement range considered. As the lateral and vertical displacements decrease, L/D improvements of up to 35% are evident.

The effect of longitudinal displacement is also shown in **Fig.11.1.2**. Although further work is required on this aspect it can be seen that the benefits in L/D increase as the longitudinal displacement decreases.

Where the Lead wing laterally overlaps the Trail wing (e.g. dy = -0.9 ~ 10% b Lap), additional L/D improvements are indicated. We have noted, however, that increased panel density may be required for accurate integration of the spanwise loads. For expediency, the majority of the work has been carried out with input geometry having 21 spanwise stations. This appears adequate where overlap does not occur. Where necessary additional computations with 41 spanwise stations have been carried out to establish the L/D trends. Further work, in relevant areas, needs to be done on this aspect.

Designed Wing-2 OFW

We use the design Wing-2 geometry for both the Lead and Trail OFW in CFF. The drag breakdown for the Trail wing, as relative vertical displacement varies, is shown in **Fig.11.1.3** for lateral displacement dy = -1.0. For the designed wing there appears to be a more noticeable effect due to vertical displacement. Methods K and P give similar results and method B is slightly more optimistic.

The $C_{Di}$ reductions (k method) result in the L/D improvements shown in **Fig.11.1.4**. Results for the planar wing at dy = -1.0 are also shown. We note, from the earlier comments regarding the types of spanwise load distributions, that the L/D increments for the Planar wing in Core 1 CFF are likely to be greater than those for a suitably designed wing. Further work is required to establish CFF configurations that may give even greater L/D improvements for the designed wing.

## 11.2. Core 2 type CFF

Planar OFW

The drag breakdown for the Trail wing in Core 2 CFF (Planar geometry), as relative vertical displacement varies, is shown in **Fig.11.2.1**. Two Core 2 lateral displacements are considered, dy = +0.9 b in **Fig.11.2.1(a)** and dy = +1.0 b in **Fig.11.2.1(b)**. Where the Lead wing laterally overlaps the Trail wing (dy = +0.9 ~ 10% b Lap), greater Drag reductions are indicated than when the tips are in line (dy = +1.0). However, as noted above, further work needs to be carried out to assess the implications of panel density for particular cases.

Comparing **Fig.11.1.1(b)** Core 1 and **Fig.11.2.1(b)** Core 2, both 0% Gap, significantly greater drag reductions are evident for Core 1 than for Core 2. In Core 1, the highly loaded right tip of the Lead wing has a beneficial effect in improving the lift distribution on the Trail wing left tip. In Core 2, the lightly loaded left tip of the Lead wing has little effect on the relatively poor spanwise distribution of the Trail wing.

We note that for Core 1, the method of Blake yields slightly greater $C_{Di}$ reductions that the other two methods. In Core 2 this trend is reversed. Using designed Wing-2 geometries these trends are maintained for Core 1 and Core 2. Blake's method assumes that the spanwise load

distribution is maintained on the Trail wing in CFF. As noted, this is not the case for Planar or design Wing-1 OFW in Core 1 CFF.

These $C_{Di}$ reductions (k method) result in the L/D improvements shown in **Fig.11.2.2** for dy = +1.0 (0% Gap) and +0.9 (10% b Lap). Comparing **Figs.11.1.2** and **11.2.2** the L/D gains in Core 2 for comparable Laps on the Trail wing are not as marked as fro Core 1. This is attributable to the nature of the spanwise load distribution.

Designed Wing-2 OFW

The drag breakdown for the Trail wing, as relative vertical displacement varies, is shown in **Fig.11.2.3** for lateral displacement dy = +1.0 using Wing-2 design for both Lead and Trail wings. Comparing **Figs.11.1.3(a)** and **11.2.3** (0% b Lap, Core 1 and 2 respectively) methods P and K give very similar magnitudes of $C_{Di}$ reduction. For design Wing-2, the spanwise loading is symmetrical. The influence of the Lead wing wake on the Trail wing will now be of the same order for Core 1 and Core 2 type CFF. Differences now may be attributed to the asymmetrical planform and relative streamwise displacements between Lead and Trail.

The $C_{Di}$ reductions (k method) result in the L/D improvements shown in **Fig.11.2.4**. Results for the planar wing at dy = +1.0 are also shown. In this case (Core 2), the designed wing gives greater L/D increments than the Planar wing case. However, comparing **Figs.11.1.4** and **11.2.4**, the L/D increments for wing-2 in Core 1 are of the same order as those in Core 2.

Further work is required to establish CFF configurations that may give even greater L/D improvements for the designed wing.

## 11.3. Core 1 to 4 type CFF with more than two aircraft

We have noted that the benefits of CFF appear to be constant for additional Trail aircraft in CFF. Similarly for a single Trail following two Lead aircraft the benefits are cumulative and for two Trail following a single Lead the benefits are shared. It will be interesting to derive Drag breakdowns for the Trail aircraft in Core 3 and 4 CFF and for multiple aircraft in CFF once a suitable designed OFW is established.

## 11.4. Y-Z plane contour plots of significant variables ($C_L$, L/D, $C_l/C_n$)

The scope of the planar wing formation geometries assessed (points in the y-z plane) at dx = 2.0 are shown in **Fig.11.4.1**. As the results at individual y-z locations are analysed some locations will be seen to be more beneficial than others. We are then able to "home-in" on areas of particular interest, namely high gains in L/D for the aircraft in formation. This is highlighted by the proliferation of points near $-1.1<y<-0.9$ and $-0.02<dz<0.02$ in **Fig.11.4.1**.

Provided there is adequate coverage in the y-z plane, contour plots of significant variables can be produced. We consider contour plots, in the y-z plane, of $C_L$ , L/D and $C_l/C_n$ arising on the Trail wing (untrimmed for $C_L$) in CFF (dx = 2.0) in **Fig.11.4.2**. From this type of plot the areas providing increases in $C_L$ can be seen, **Fig.11.4.2(a)**. An initial estimate of L/D is obtained using the untrimmed Trail wing $C_L$ and $C_D$. Immediately it can be seen that there are regions where L/D increments exceed 13% near y = +1.0 and –1.0, i.e. Core 1 and Core 2 formations, **Fig.11.4.2(b)**. Contour plots of $C_l/C_n$ will be useful during the design and CFF evaluation stages. Here we present $C_l/C_n$, **Fig.11.4.2(c)**, for the untrimmed case. These need to be assessed in conjunction with $C_l$ and $C_n$ variation.

**Fig.11.4.3** presents L/D contours with AOA correction to ensure that Trail and Lead aircraft are at the same $C_L$. In evaluating L/D, two values of delk ($k_W$, see Section 6.2) have been used (0.6 and 0.7). A 15% increase in delk gives rise to a 3% reduction in L/D. This indicates the importance of establishing accurate parameters for the isolated designed wing before fully analysing the benefits of CFF.

## 12. FURTHER WORK

So far, we have been concerned with Phase 1 studies. In this report we are limited to one Mach number and a single OFW planform. An in-depth assessment of possible benefits arising from CFF for this OFW has been made using planar, uncambered geometry. A limited amount of CFF assessment has been made using two designed OFW geometries. This brings us to the realms of the next phases of work.

Phase II studies

The primary focus of the Phase II is refined estimates of range increase as function of the number of aircraft in formation, with assumptions made in the Phase I relaxed e.g.

- The primary assumption to be relaxed is the wing planform. Variations in wing sweep and taper ratio should be studied. See **Fig.12.1**.

- This Phase should also conduct a more thorough trim analysis including pitching and yawing moments.
- A preliminary assessment of propulsion integration issues.
- Decide on Phase III Content

Phase III studies

This phase builds up on work done in previous phases

- Different Mach numbers
- Apply to Extended Geometry and Flight parameters, Propulsion Issues, Size Issues
- Aero-elastic effects

## 13. CONCLUDING REMARKS

Currently there is great emphasis on fuel-efficient flight and this may be reflected in planned budgets for future. The idea of Close Formation Flying (CFF) to reduce drag and hence fuel usage has been appreciated. A fair deal of theoretical and experimental work in subsonic flight is available.

Amongst many projects at AFRL, importance is being attached to the Oblique Wing aircraft. A research programme “Switchblade” is being conducted under DARPA sponsorship. With varying sweep, Switchblade can achieve a wide and efficient subsonic-supersonic flight envelope capability.

This report has summarised theoretical analysis on a generic OFW planform in CFF at Mach 1.4. The analysis began with an assessment of the planar (uncambered) OFW. Typical flight envelope parameters and design targets were established. Several design options have been described.

The performance of the OFW, both planar and designed, in CFF has been established. There are some interesting aspects e.g. the shape of spanwise loadings and control of such configurations. The nature of the spanwise load distribution has a significant effect on the choice of CFF geometry for maximum L/D benefits.

Benefits, in terms of increased L/D throughout a range of formation geometries have been determined.

Results (trimmed for lift only at this stage) show up to 50% reduction in lift-induced drag of the trail wing. This implies 30– 35% increases in lift-drag ratio and similar increases in range.

The possibility of utilising slideslip (change of sweep) to trim Trail aircraft in CFF has been noted. This would need to be used in conjunction with other control devices but may have significant advantages in Drag reduction.

A preliminary analysis of wave drag evaluation for OFW in CFF has been carried out. Benefits were noted but these occurred in “very tight” formations only. A further, in depth, analysis is required.

Multiple aircraft formations reflect the added benefits on all trailing aircraft.

The major benefits of CFF can be deduced using Planar wing geometry. Areas of interest can then be evaluated in greater detail using designed wing geometries. Stability issues will need to be addressed once suitable wing geometry has been defined.

In view of the encouragement, continued detailed work has been proposed in several areas. For comparative purposes and exchange rates. It is apparent that we are only at a starting post and a sizeable, interesting work programme remains!

## ACKNOWLEDGEMENTS

The author has pleasure in acknowledging helpful technical comments and discussions with Dr Surya Surampudi (USAF-EOARD), Mr. D. Multhopp, Dr. C. Tilmann and Mr. W Blake (US-AFRL). The technical help of Dr. M. E. Palmer is appreciated.

This material is based upon work supported by the European Office of Aerospace Research and Development, Air Force Office of Scientific Research, Air Force Research Laboratory, under Grant No. 07-3024 (EOARD).

Any opinions, findings and conclusions or recommendations expressed in this material are those of the author(s) and do not necessarily reflect the views of the European Office of Aerospace Research and Development, Air Force Office of Scientific Research, Air Force Research Laboratory.

## REFERENCES

1. HAGENAUER, B. "NASA Studies Wingtip Vortices." Aerospace Engineering Online: Technology Update, Jan/Feb 02, http://www.sae.org/aeromag/techupdate/02-2002/page5.htm.

2. IANNOTTA, B. "Vortex Draws Flight Research Forward." Aerospace America, Mar 02, 26-30.

3. RAY, R. J., et al. "Flight Test Techniques Used to Evaluate Performance Benefits During Formation Flight." AIAA paper 2002-4492, Monterey CA, Aug 02.

4. WAGNER, G., et al. "Flight Test Results of Close Formation Flight for Fuel Savings." AIAA paper 2002-4490, Monterey CA, Aug 02.

5. JENKINSON, L.R., CAVES, R.E & RHODES, D.R., “A Preliminary Investigation into the Application of Formation flying to civil operation, AIAA Paper –95-3898, 1995.

6. IGLESIAS, S., “Optimum Spanloads Incorporating Wing Structural Considerations & Formation Flying”, Virginia Polytechnic, 2000 Thesis.

7. HIRSCHBERG, M.J., HART, D.M. & BEUTNER, T.J., “A Summary of a Half Century of Oblique Wing Research”, AIAA 2007-150.

8. DARPA sponsored Oblique Wings, Referred in: Flight International Article, 13-19 September, 2005.

9. NANGIA, R.K. & GREENWELL, D.I., "Wing Design of Oblique Wing Combat Aircraft", ICAS 2000-1.6.1, 2000.

10. Van Der VELDEN, A, Multi-Disciplinary SST Design at Deutsche Aerospace”, EAC’94, Toulouse, October 1994.

11. BLAKE, W.B. & MULTHOPP, D., “Design, Performance and Modelling Considerations for Close Formation Flight”, AIAA Paper 98-4343, August 1998.

12. SOBIECZKY, H., “Manual Aerodynamic Optimisation of Oblique flying Wing, ICAS-98-1.1.3, 1998.

13. NANGIA, R.K., PALMER, M.E., “Morphing UCAV wings, Incorporating in-Plane & Fold-Tip Types – Aerodynamic Design Studies”, AIAA-2006-2835. 25th Applied Aero Conference, San Francisco, June 2006.

14. NANGIA, R.K., PALMER, M.E. & DOE, R.H., “ Aerodynamic Design Studies of Conventional & Unconventional Wings with winglets”, AIAA-2006-3460. 25th Applied Aero Conference, San Francisco, June 2006.

15. NANGIA, R.K., PALMER, M.E., “Formation Flying of Commercial Aircraft – Assessment using a New Approach - Wing Span Load & Camber Control”, Proposed Paper for AIAA, 2006-7.

16. NANGIA, R.K., PALMER, M.E., “Formation Flying of Commercial Aircraft – Assessment using a New Approach - Wing Span Load & Camber Control”, Proposed Paper for AIAA, 2006-7.

17. NANGIA, R.K., PALMER, M.E., “Formation Flying of Oblique Wing Aircraft, Assessment of Variations in Relative Size / Spacing – Induced Effects & Control”, Proposed Paper for AIAA, 2006-7.

18. SCHANZER, G., “Developments in Flight Control Guidance & Control”, Guggenheim Memorial Lecture, ICAS 2006.

19. NANGIA, R.K., “Towards Design of Long-Range Supersonic Military Aircraft”, RKN/AERO/REPORT/2004-10 – Part 6, Issue 1, 2004.

20. NANGIA, R.K., "The Design of "Manoeuvrable" Wings using Panel Methods, Attained Thrust & Euler Codes", ICAS-92.

21. NANGIA, R.K. & GREENWELL, D.I., "Wing Design of Oblique Wing Combat Aircraft", ICAS 2000-1.6.1, 2000.

22. NANGIA, "Design of Conventional & Unconventional Wings for UAV's", RTA-AVT Symposium, "UV for Aerial & Naval Military Operations", Ankara, Turkey, Oct. 2000.

23. NANGIA, R.K., PALMER, M.E. & DOE, R.H., "A Study of Supersonic Aircraft with Thin Wings of Low Sweep", AIAA-2002-0709, January 2002.

24. NANGIA, R.K. & MILLER, A.S. "Vortex Flow Dilemmas & Control on Wing Planforms for High Speeds", RTO AVT Symposium, Loen, Norway, May 01.

25. NANGIA, R.K., "Developing an Inverse Design Method using 3-D Membrane Analogy", Future Paper.

26. KUCHEMANN, D. "The Aerodynamic Design of Aircraft", Pergamon.

27. JUPP, J., Wing aerodynamics and the Science of Compromise", RAeS Lanchester Lecture, 2001.

28. JONES, R.T., "Wing Theory", Princeton.

29. McCORMICK, B.W. "Aerodynamics Aeronautics and Flight Mechanics", Wiley.

30. GUPTA, K.K. & MEEK, J.L., "Finite Element Multidisciplinary Analysis", AIAA, 2000.

## LIST OF SYMBOLS & ABBREVIATIONS

Only the general symbols are defined here. Other symbols are of local significance within the Section they arise in.

| | |
|---|---|
| AoA | Angle of Attack ($\alpha$), usually referred to the body axis |
| AR | Aspect Ratio |
| A | Axial Force along wing-plane x-axis (for definition of CA) |
| b | = 2 s, Wing span |
| BL | Boundary Layer |
| c | Local Wing Chord |
| $c_{aero}$ | = c, Aerodynamic Wing Chord |
| $c_{av}$ | = c = cref, Average Wing Chord |
| $C_A$ | = A/(q S), Axial Force Coefficient, measured in Wing plane |
| $C_{AL}$ | = Local Axial Force Coefficient |
| $C_D$ | = Drag Force /(q S), Drag Coefficient |
| $C_{D0}$ | Drag Coefficient at zero lift (see text) |
| $C_{Di}$ | Lift Induced Drag |
| CG | Centre of Gravity |
| $C_l$ | = l/(q S b), Rolling Moment Coefficient<br>Body Axis, positive right tip up, anti-clockwise viewed from behind |

| | |
|---|---|
| $C_L$ | = CL = L/(q S), Lift Coefficient |
| $C_{LL}$ | = Local Lift Coefficient |
| $C_{Lmax}$ | Maximum Lift Coefficient |
| $C_m$ | = m/(q S c), Pitching Moment Coefficient<br>Body Axis, positive nose up |
| $C_{mo}$ | Cm at zero Lift |
| $C_n$ | = n/(q S b), Yawing Moment Coefficient<br>Body Axis, positive right tip back, clockwise viewed from above |
| $C_N$ | = N/(q S), Normal Force Coefficient |
| CoP | Centre of Pressure |
| $C_P$ | Coefficient of Pressure |
| $c_{r,}\ c_t$ | Wing Root chord, Wing Tip chord |
| DoF | Degrees of Freedom |
| $d\theta$ | change in AoA required to trim (1-DoF) |
| k | $= \pi\ A\ C_{Di}/C_L^{\ 2}$, Lift Induced Drag Factor |
| l | Rolling moment (Body Axis, positive right tip up) |
| LE | Leading Edge |
| m | Pitching moment (Body Axis, positive nose up) |
| M | Mach Number |
| MRC | Moment Reference Centre |
| n | Yawing moment (Body Axis) |
| N | Normal Force |
| OFW | Oblique Flying Wing |
| q | $= 0.5\ \rho\ V^2$, Dynamic Pressure |
| r | Aerofoil radius |
| rn | Aerofoil radius normal to c |
| R | Reynolds Number, based on cav (unless otherwise stated) |
| s | Wing semi-span |
| S | Wing Area, taken here as (front-wing + tip-wing) area |
| t | Aerofoil thickness |
| TE | Trailing Edge |
| V | Airstream Velocity |
| x,y,z | Orthogonal Wing Co-ordinates, x along body axis |
| $x_{ac}$ | Location of Aerodynamic Centre along x-axis |
| $x_{cp}$ | Location of Centre of pressure along x-axis |
| $\alpha$ | Angle of Attack (AoA), usually referred to the body axis |
| $\lambda$ | Wing Taper Ratio |
| $\Lambda$ | LE Sweep Angle |
| $\rho$ | Air Density |
| $\eta$ | = y/s, Non-dimensional spanwise Distance |

## APPENDIX A1

### Estimation of Wave Drag in Close Formation Flying, Using Harris Wave Drag, Supersonic Area Rule Programme

For an initial estimation of wave drag ($C_{DW0}$) in CFF we have simplified the asymmetric OFW geometry as shown in **Fig.A1.1**. The wing is represented by constant aerofoil sections across the span, i.e. tip has finite thickness. This simplified planform, reflected in the x-z plane, represents a conventional swept wing. Offsetting the planform laterally (ydisp) splits the conventional swept wing into an OFW and its reflected image. The aim is to give an understanding using a range of Mach numbers from about 1.2 to 1.8. It is believed that this represents a unique exercise (to the best of our knowledge).

For Mach 1.4, **Fig.A1.1** shows the variation in $C_{DW0}$ as ydisp is increased from zero to five OFW span units (b). $C_{DW0}$ is based on the configuration planform area. The effect of aerofoil section thickness ratio (t/c) is also shown. The conventional swept wing case is represented at ydisp = 0. As ydisp increases, $C_{DW0}$ decreases rapidly until for ydisp > 0.5b constant levels are reached for each t/c value. For the current OFW work we have used ydisp = 3.0b.

For Mach 1.4, **Fig.A1.2** shows the effect of t/c variation on $C_{DW0}$ for the symmetric swept wing and the OFW. The effect of Mach number variation on $C_{DW0}$ for the symmetric swept wing is shown in **Fig.A1.3** for t/c = 7.5% and 10.0%.

In **Fig.A1.4**, typical OFW CFF configurations are sketched and possible Mach line interference regions noted. Typical sampling points, represented by the Trail wing LE apex, are also shown. We are assuming that the trail wing does not affect the lead wing. Interpolated results from these arrays are used to define the contour plots of $\Delta C_{DW0}$ reductions at Trail wing vertical displacements of 0.0b, 0.1b and 0.2b in **Fig.A1.5**.

We note that for the unique case in which the Lead and Trail wings join to form one continuous wing, the total $C_{DW0}$ remains the same as that for the OFW in isolation i.e. the Trail wing does not cause any extra wave drag penalty. This preliminary analysis of wave drag for OFW in CFF has shown that wave drag reduction benefits are limited to “very tight” formations. If the Trail wing LE apex lies within a small area close to the Lead wing trailing tip LE ($dy < 0.3b$, $-0.05 < dx < +0.05$) a wave drag reduction of about 10 counts will be achieved.

A Wave Drag contribution is included in the estimated $C_{Do}$ value of 100 counts. For most realistic CFF configurations the Wave Drag effect may not be too large. A 10 count reduction in $C_{Do}$ for the OFW would result in a 5% gain in L/D. A further, in depth, analysis of Wave Drag is required.

FIG. 1 .1 F/A-18 FORMATIONS, NASA

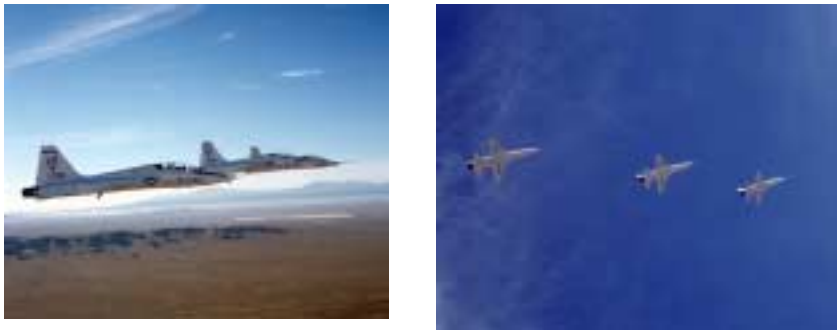

FIG. 1.2 T-38 FORMATIONS

Fig. 1.3 FA-18 FORMATION STUDIES IN WIND TUNNEL

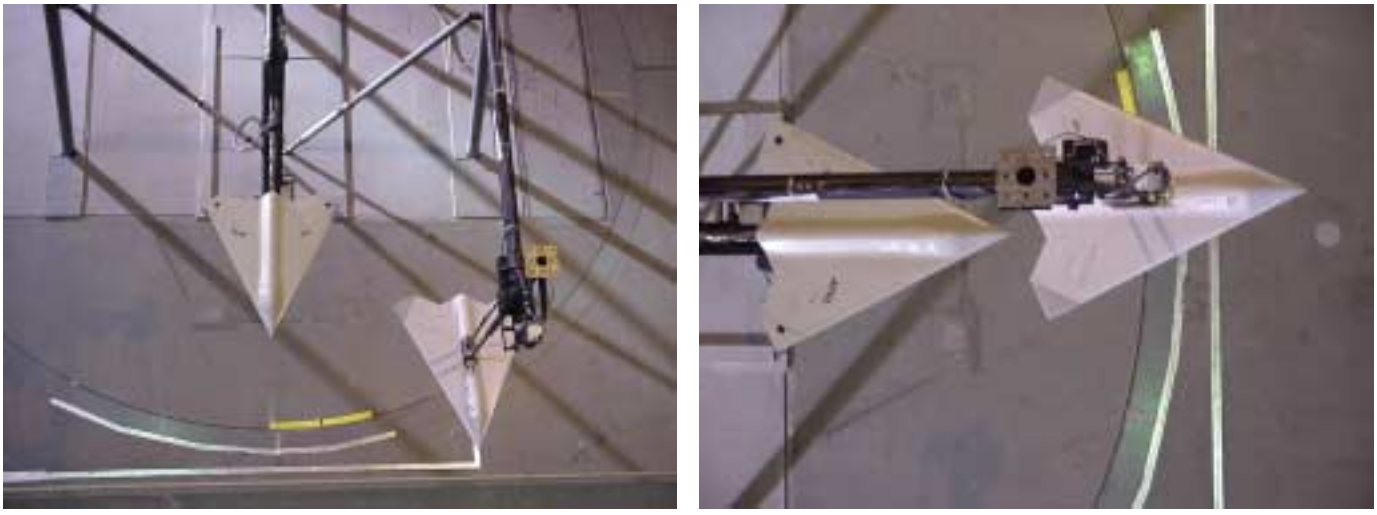

Fig. 1.4 ICE MODELS, FORMATION STUDIES IN WIND TUNNEL

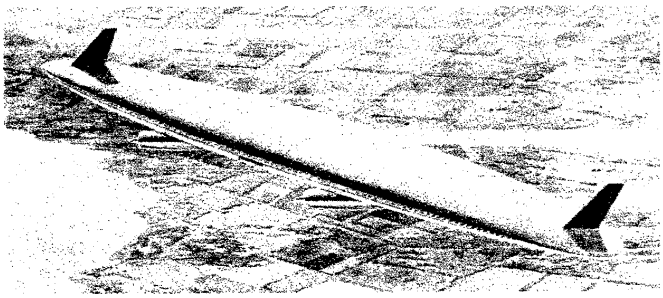

**Fig. 1.5 OBLIQUE FLYING WINGS (OFW)**
**Possible Commercial Application**

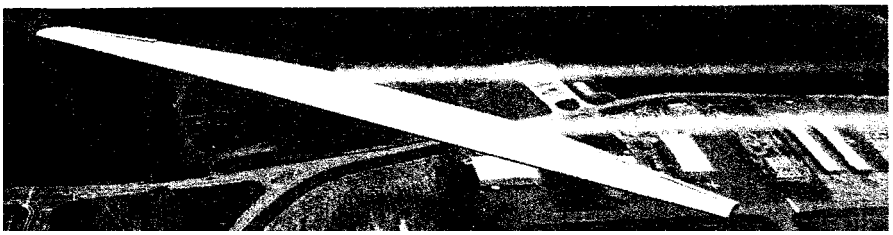

**Fig. 1.6 OBLIQUE FLYING WINGS, OFW (AFRL, DARPA)**

**Fig. 1.7 MULTIPLE AIRCRAFT FORMATION (INVERTED V-SENSE)**

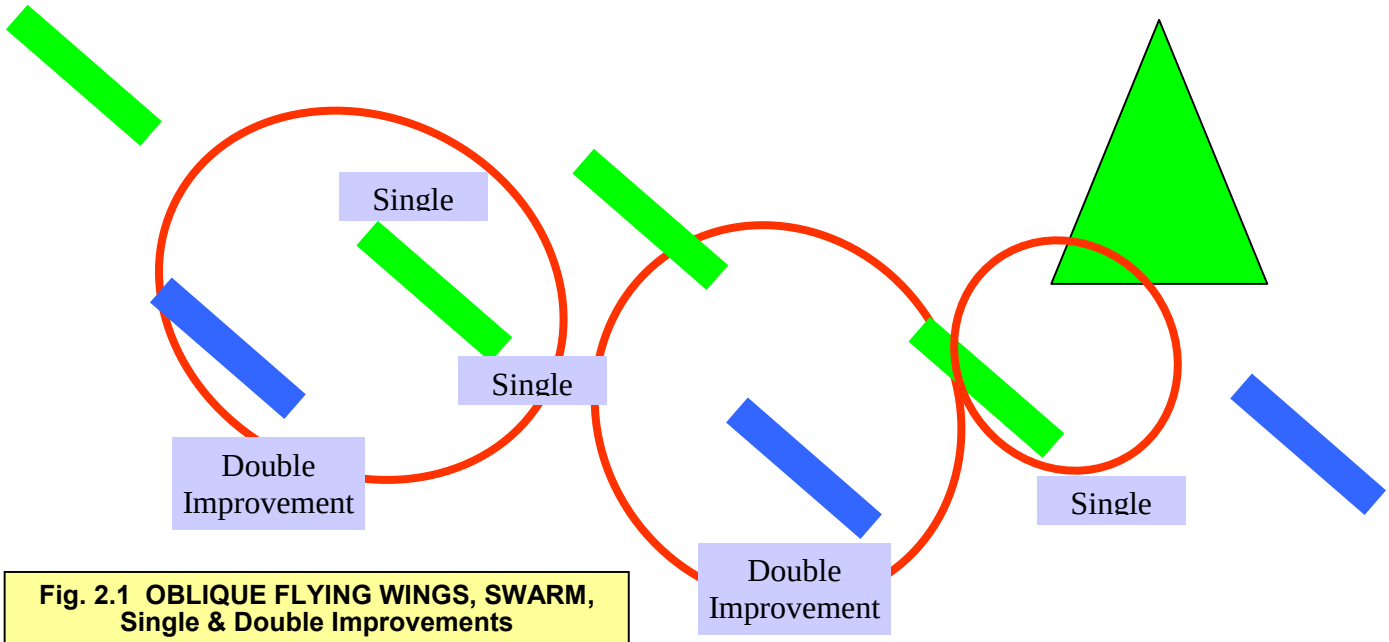


**Fig. 2.1 OBLIQUE FLYING WINGS, SWARM, Single & Double Improvements**

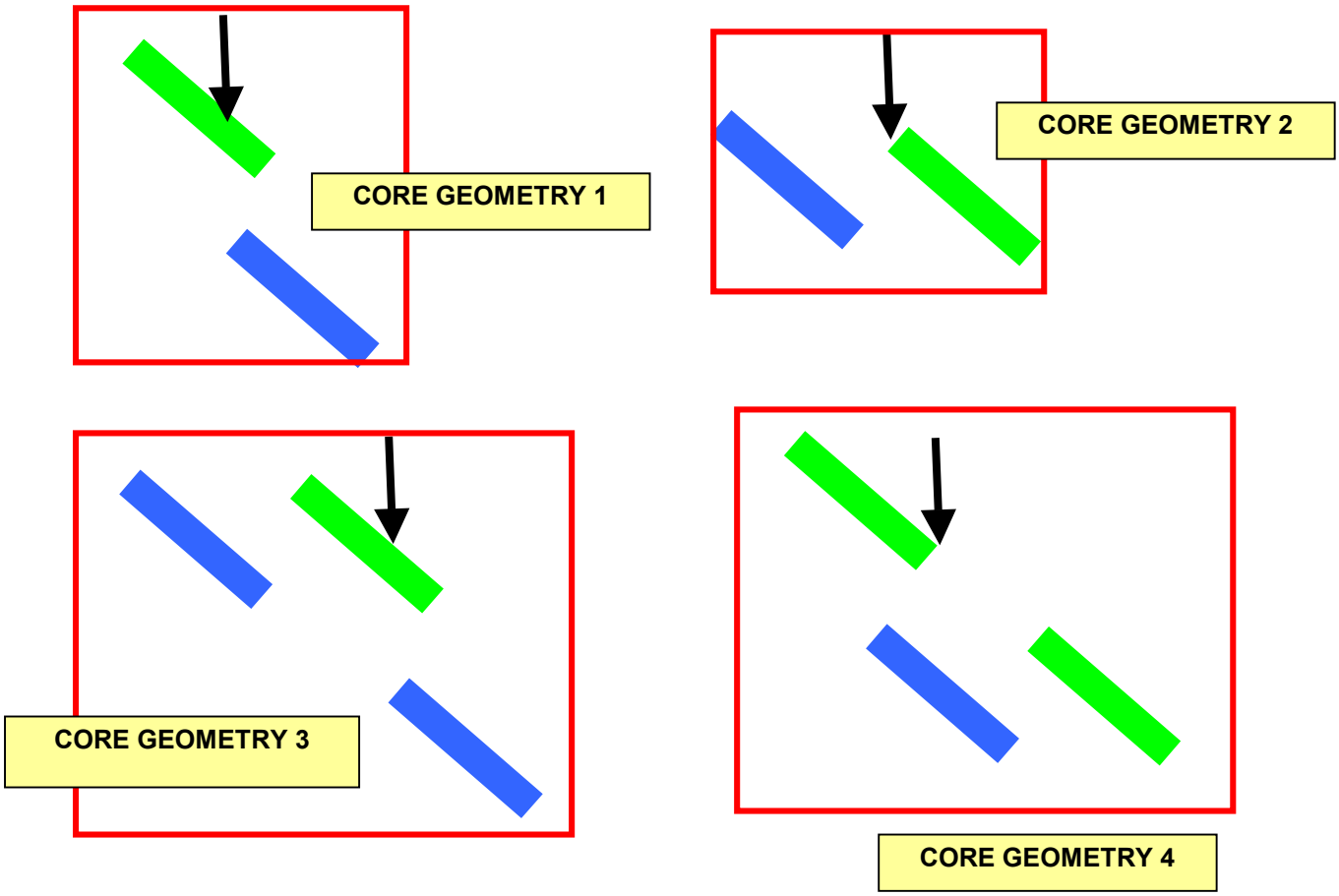


**Fig. 2.2 OBLIQUE FLYING WINGS, CORE GEOMETRY TYPES**

**Fig. 3.1 VORTEX WAKE IMPRESSION, Schanzer**

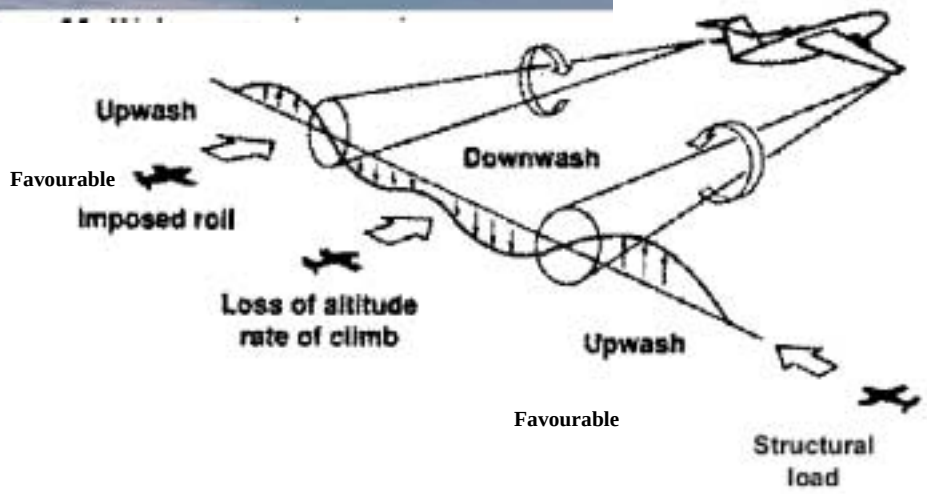


**Fig. 3.2 RESPONSE OF AIRCRAFT WHEN PASSING THROUGH A VORTEX WAKE, Schanzer**

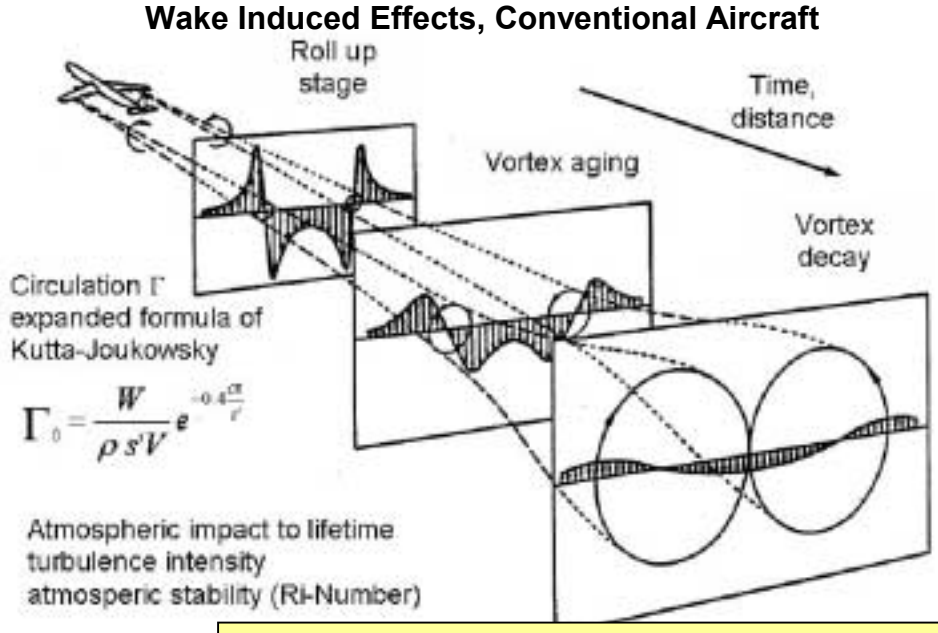


**Fig. 3.3 VORTEX WAKE DEVELOPMENT BEHIND A TRANSONIC AIRCRAFT, Schanzer**

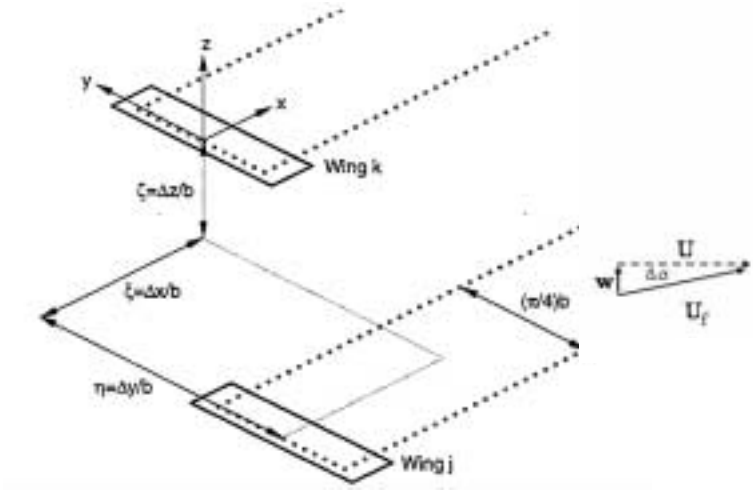


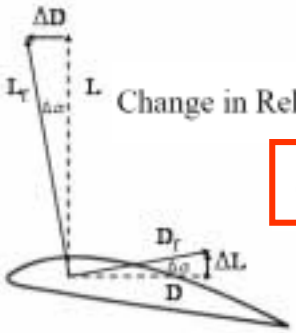


Change in Relative Angle of Attack

$$\Delta\alpha = \tan\left(\frac{w}{U}\right) \approx \frac{w}{U}$$

$$L = L_f\cos(\Delta\alpha) + D_f\sin(\Delta\alpha) \approx L_f + D_f\Delta\alpha \approx L_f + D_f\frac{w}{U} \approx L_f$$

$$D = D_f\cos(\Delta\alpha) - L_f\sin(\Delta\alpha) \approx D_f - L_f\Delta\alpha \approx D_f - L_f\frac{w}{U}$$

Or the difference in drag can be expressed as:

$$\Delta D \approx -L_f\frac{w}{U} \approx -L\frac{w}{U}$$

**FIG. 4.1 FORMATIONS, SIMPLE Horse-shoe Vortex Model & Lift, Drag EFFECTS (Blake & Multhopp)**

z/s, Vertical Spacing

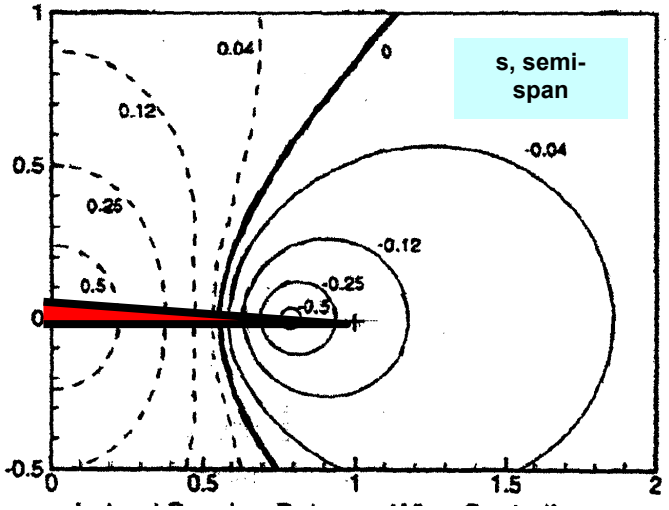


y/s, Lateral Spacing , Wings Centre-lines

**FIG. 4.2 Induced Drag as a Function of Relative Position, 2 Equal Sized Unswept Wings**

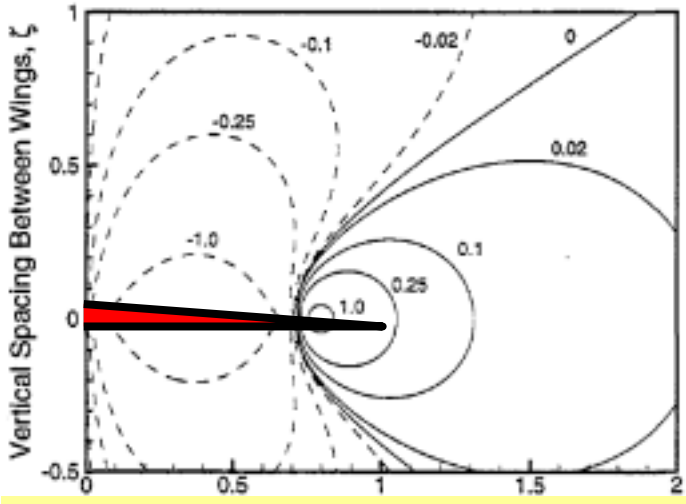


**FIG. 4.3 Variation in Cl/Cn factor as a Function of Relative Position, 2 Equal Sized Unswept Wings**

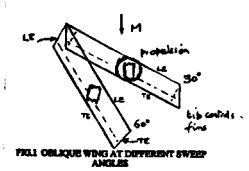

FIG. 1 OBLIQUE WING AT DIFFERENT SWEEP ANGLES

FIG. 2 POSSIBLE FLIGHT ENVELOPE

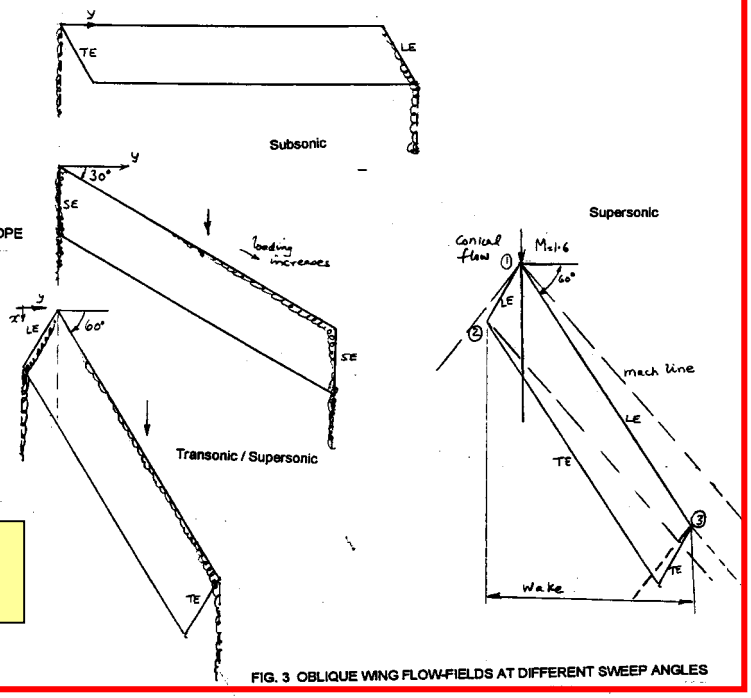


FIG. 3 OBLIQUE WING FLOW-FIELDS AT DIFFERENT SWEEP ANGLES

**Fig. 5.1 OBLIQUE FLYING WINGS, PREVIOUS WORK**

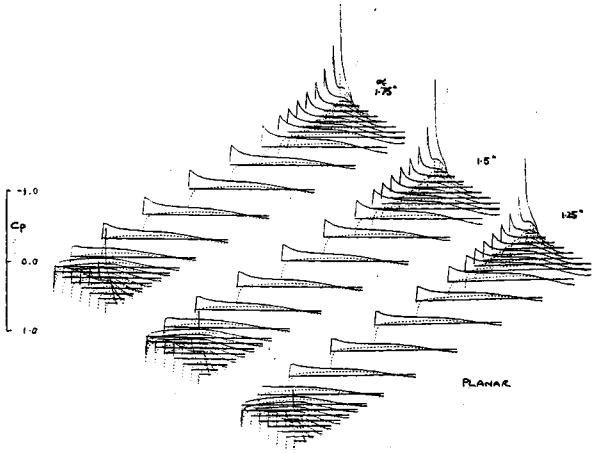


**Planar**

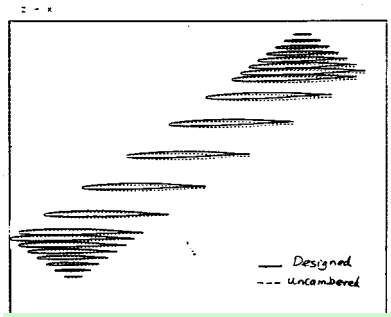


**Geometry**

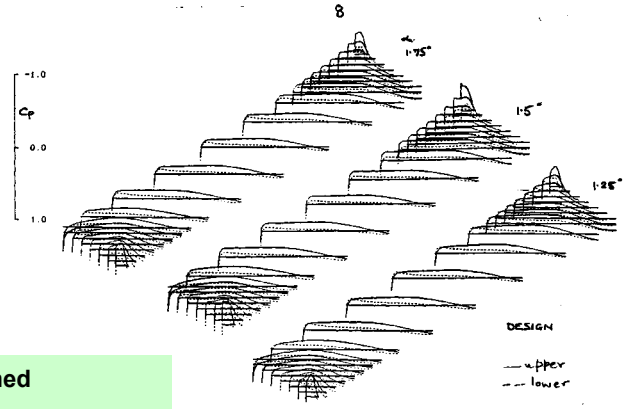


**Designed**

**FIG. 5.2 OBLIQUE FLYING WINGS, PREVIOUS WORK, Ref.8**

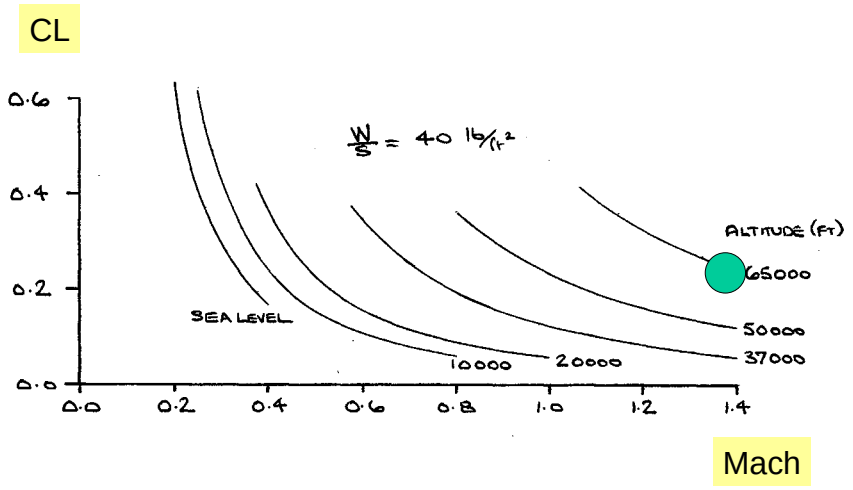


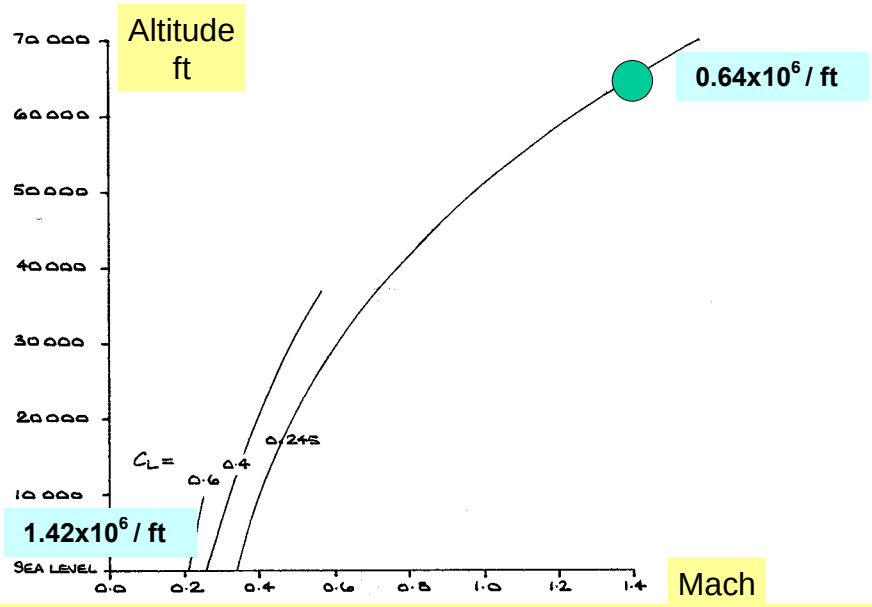


**FIG. 6.1.1 FLIGHT ENVELOPE , Mach, CL & ALTITUDE CONSIDERATIONS**

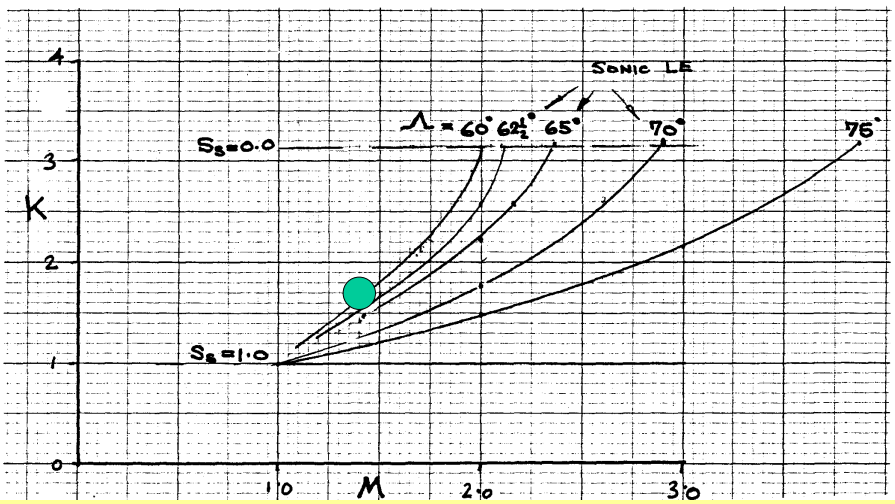


**FIG. 6.2.1 LIFT INDUCED DRAG FACTOR (k) VARIATION WITH MACH NUMBER, SUPERSONIC CONICAL FLOW ON DELTA WINGS, EFFECT OF SWEEP**

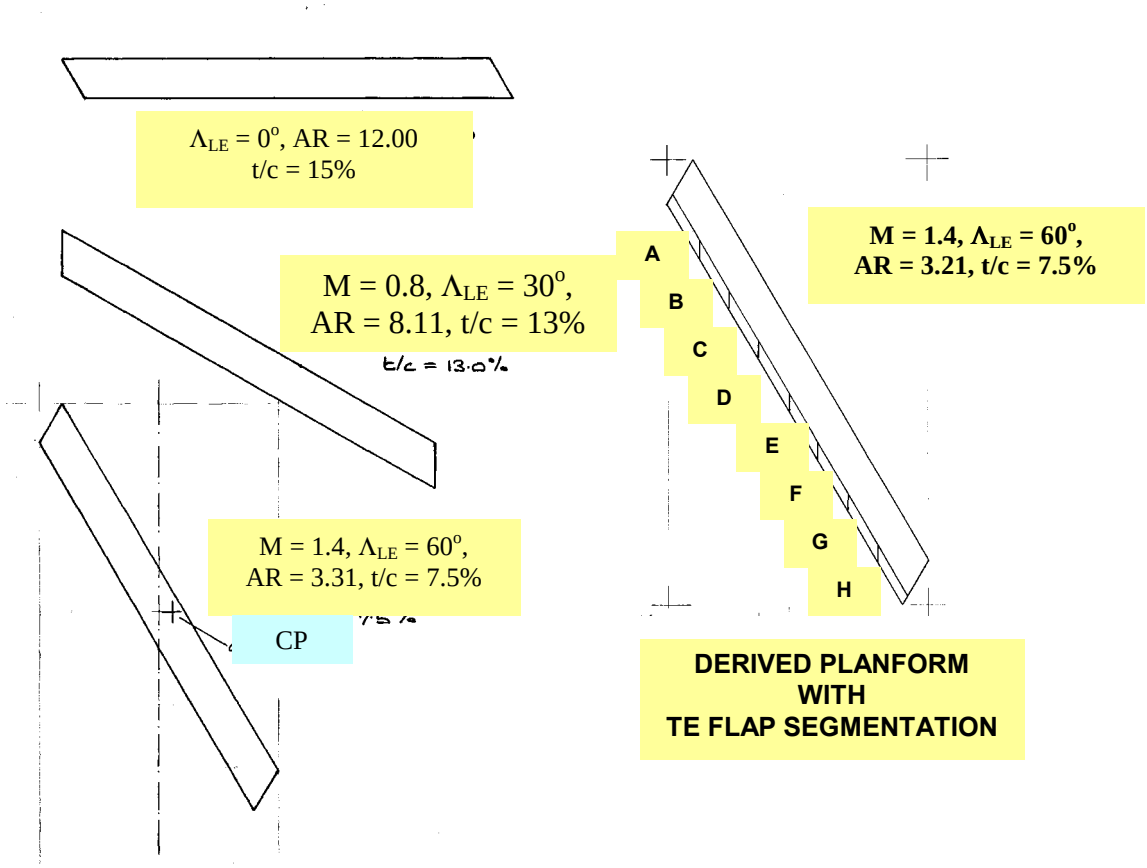


**FIG. 6.3.1 OFW PLANFORM DERIVATION, AR, t/c VARIATIONS. LOCATION OF TE FLAPS**

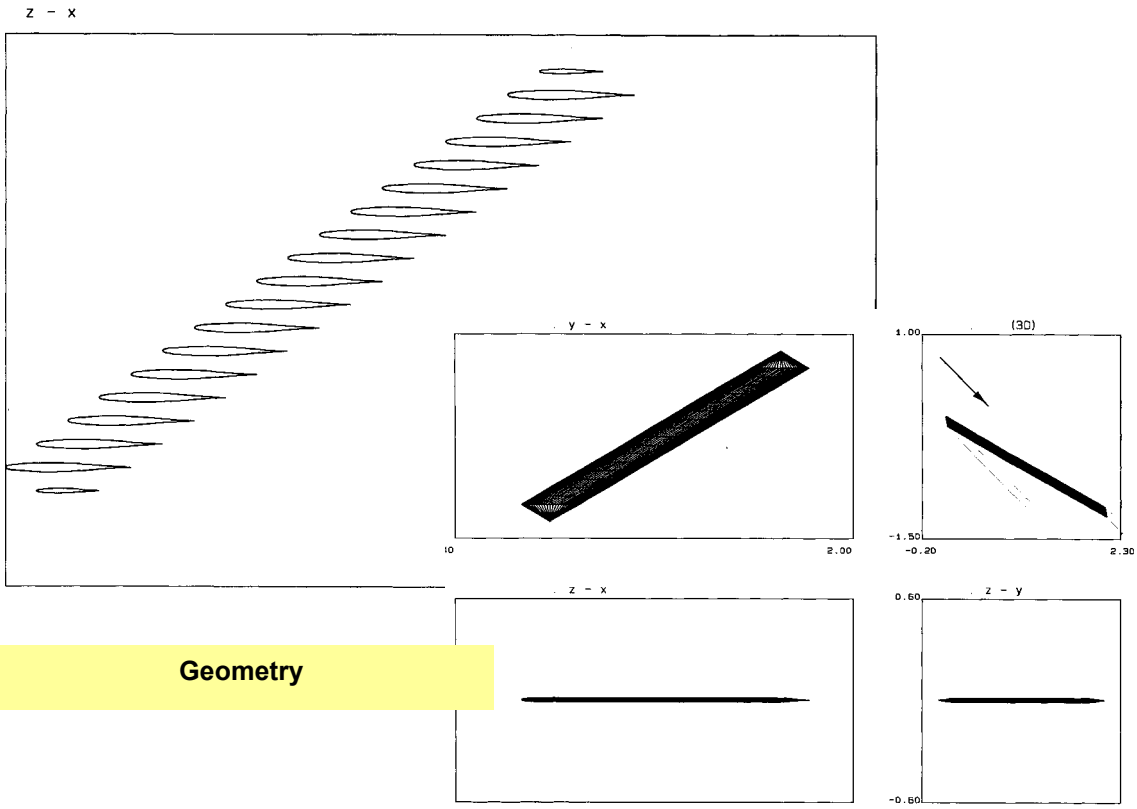


Geometry

FIG.7.1.1 PLANAR UNCAMBERED WING, 21 SPANWISE STATIONS

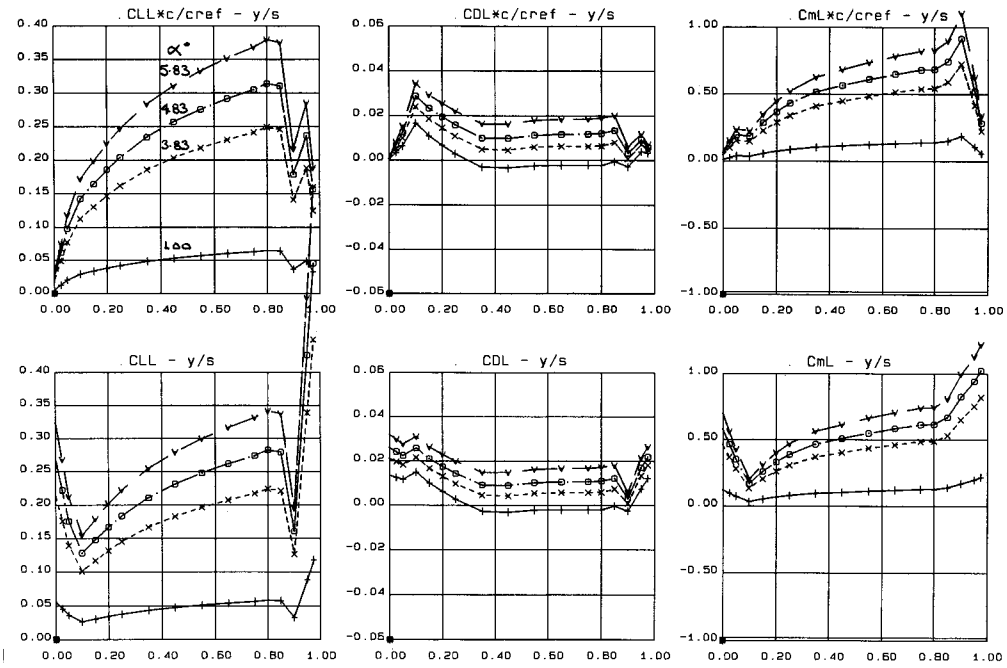


Spanwise Loadings

FIG.7.1.2 PLANAR UNCAMBERED WING, 21 SPANWISE STATIONS

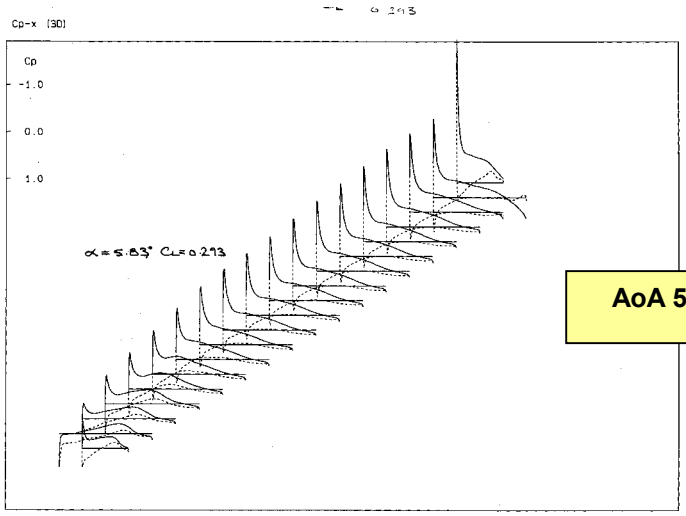


AoA 5.83, CL=0.293

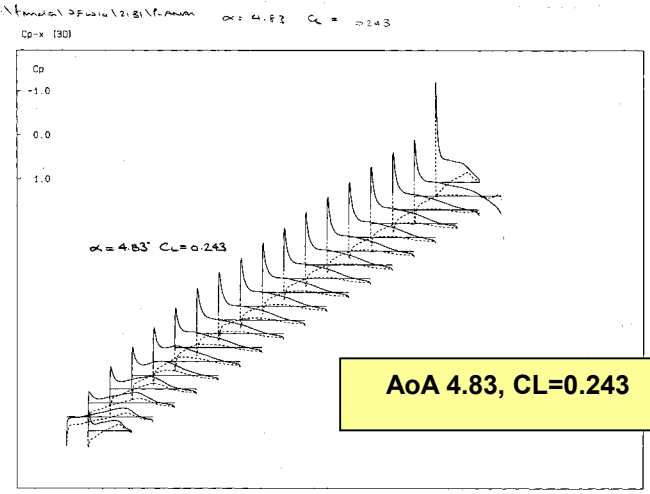


AoA 4.83, CL=0.243

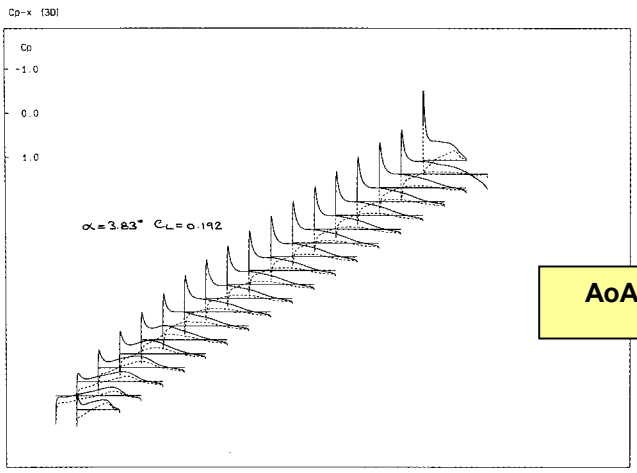


AoA 3.83, CL=0.192

**FIG.7.1.3 PLANAR UNCAMBERED WING, Cp DISTRIBUTIONS AT 3 AOA**

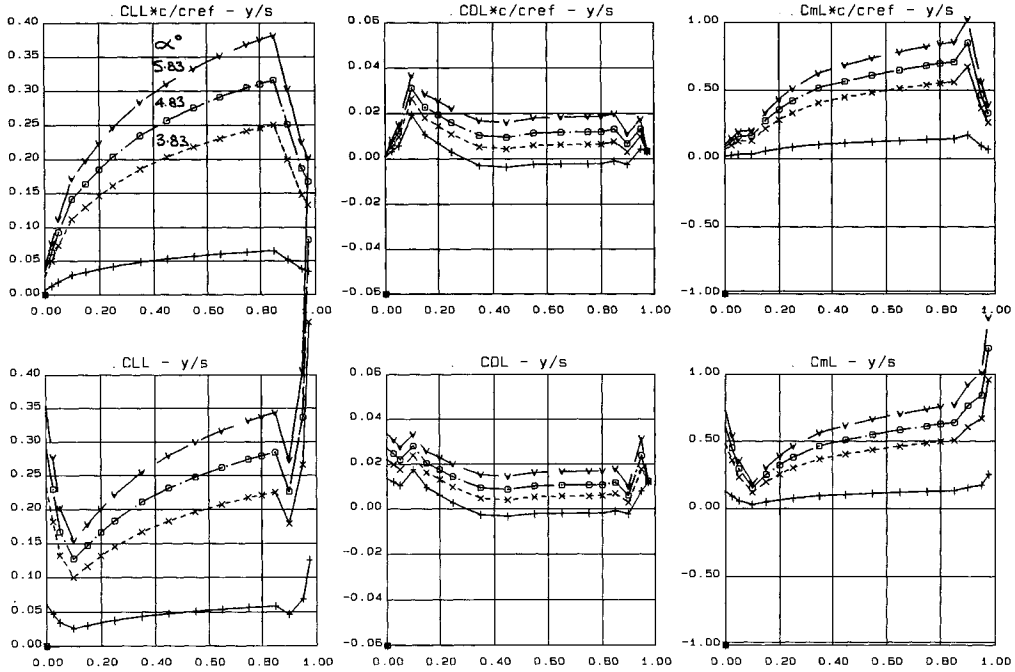


**FIG. 7.1.4 UNCAMBERED WING, SPANWISE LOADINGS, 41 Stns**

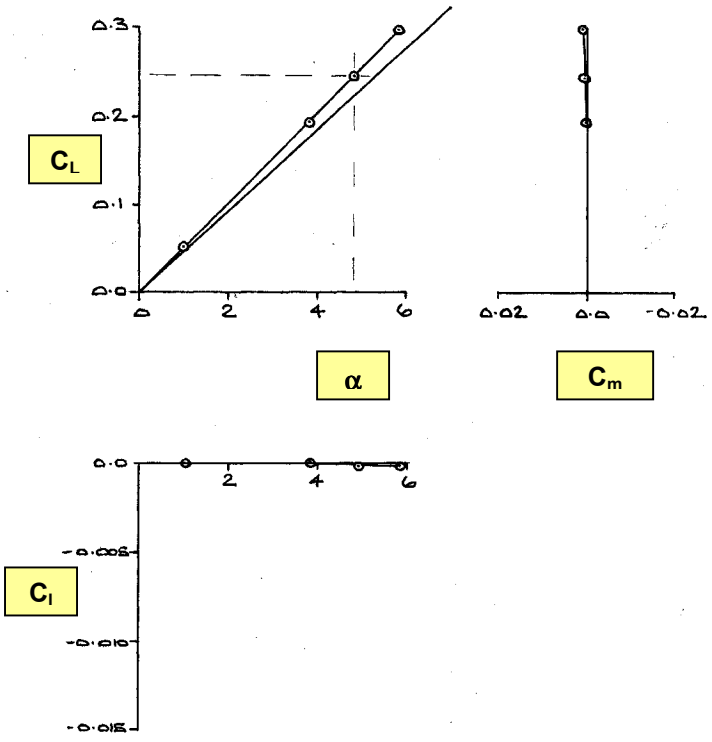


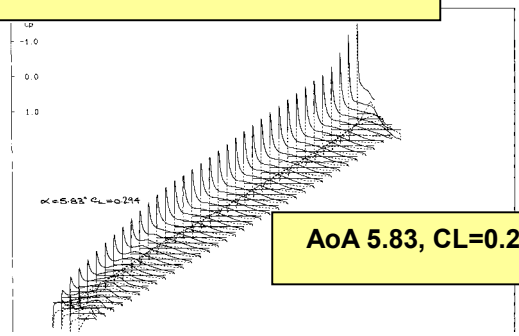

**AoA 5.83, CL=0.294**

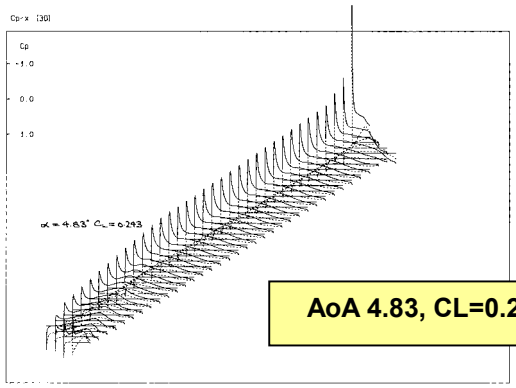

**AoA 4.83, CL=0.243**

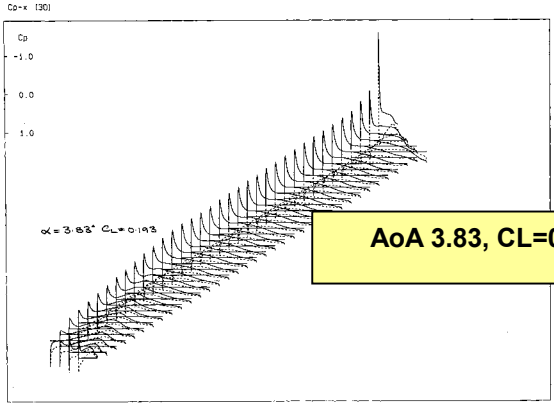

**AoA 3.83, CL=0.193**

**FIG. 7.1.6 UNCAMBERED WING, Total Loads ($C_L$ – α, $C_m$ – $C_L$, $C_l$ – α), Mach 1.4**

**FIG. 7.1.5 UNCAMBERED WING, $C_P$ DISTRIBUTIONS AT 3 AoA, 41 Stns**

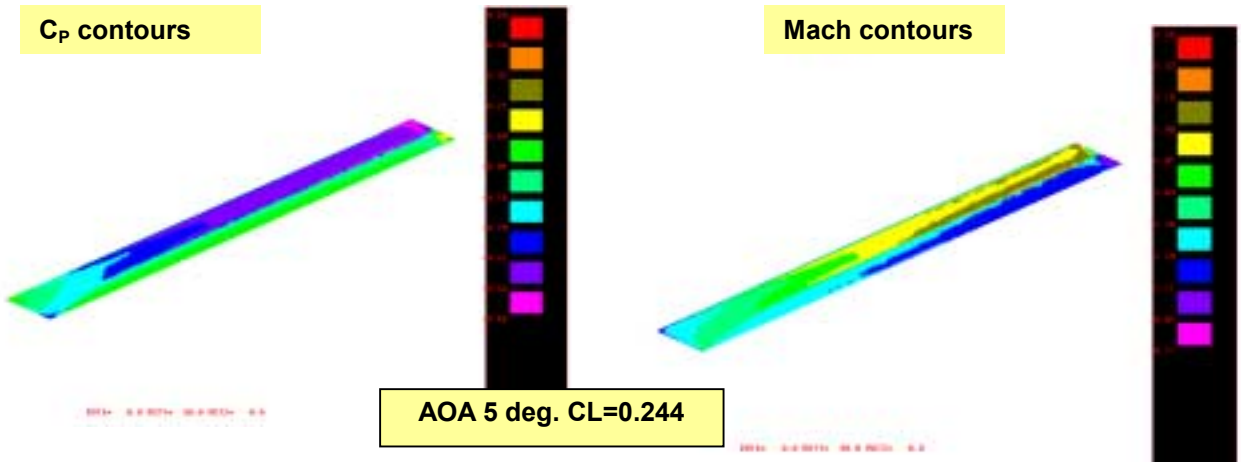


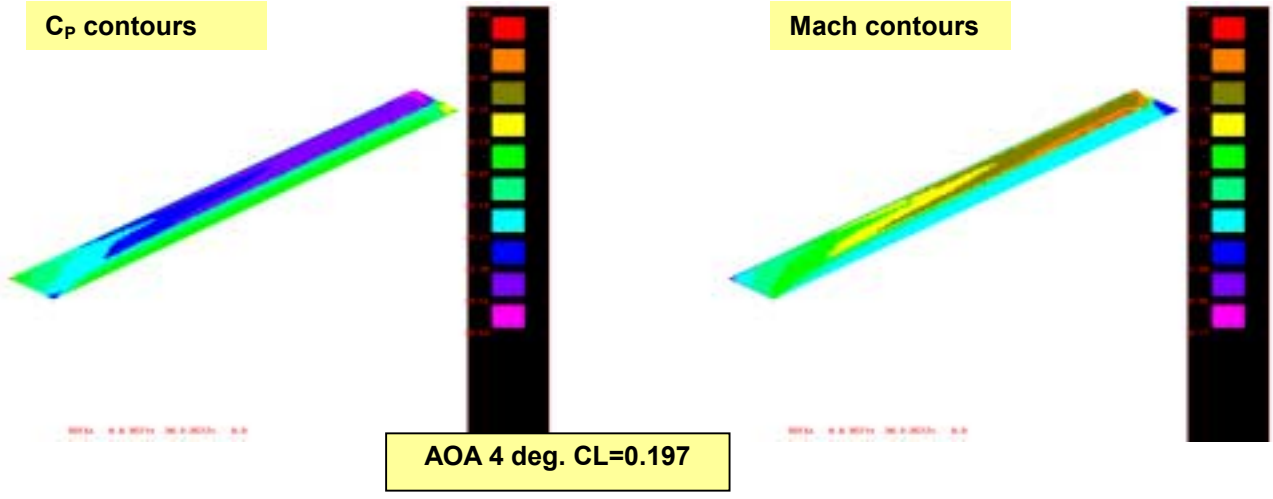


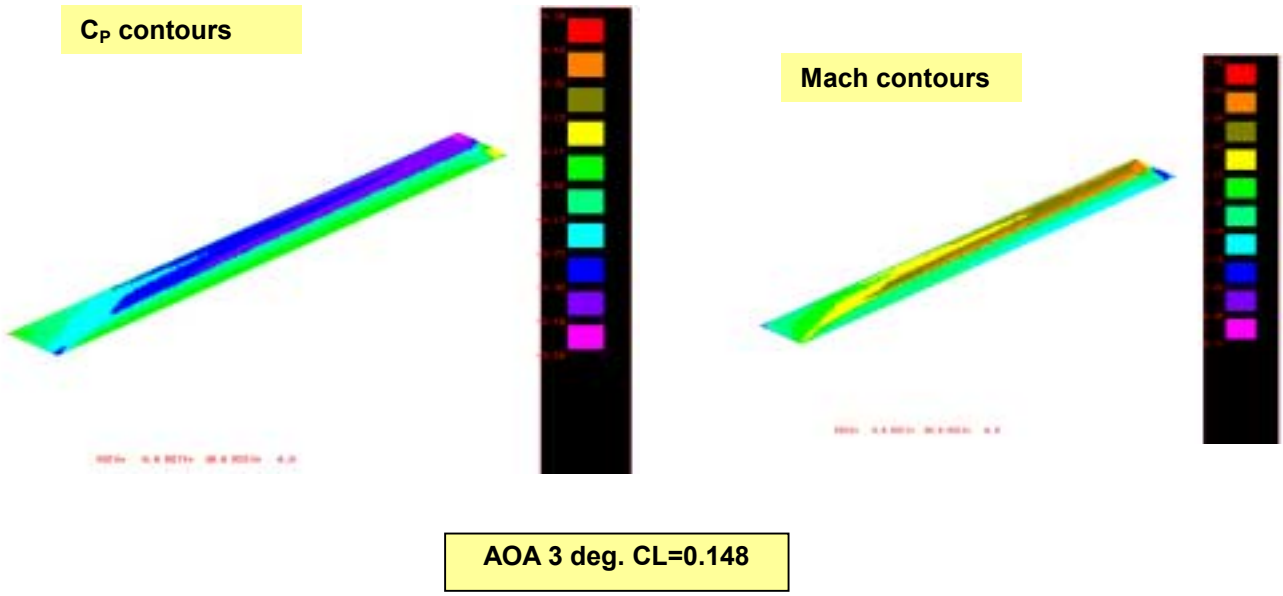


**FIG.7.1.7 PLANAR UNCAMBERED WING**

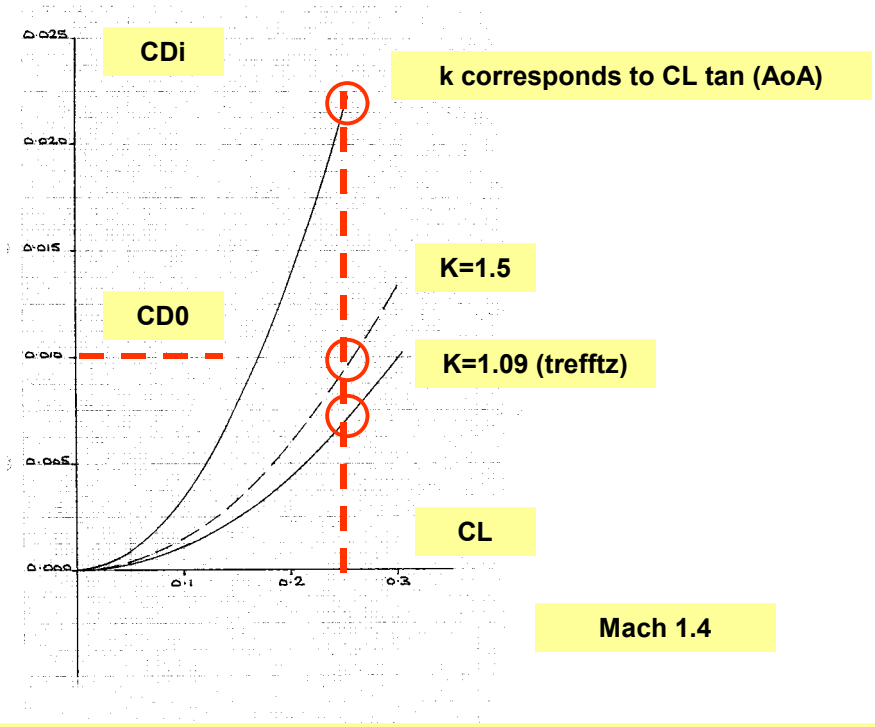


FIG. 7.2.1 DRAG CONSIDERATIONS

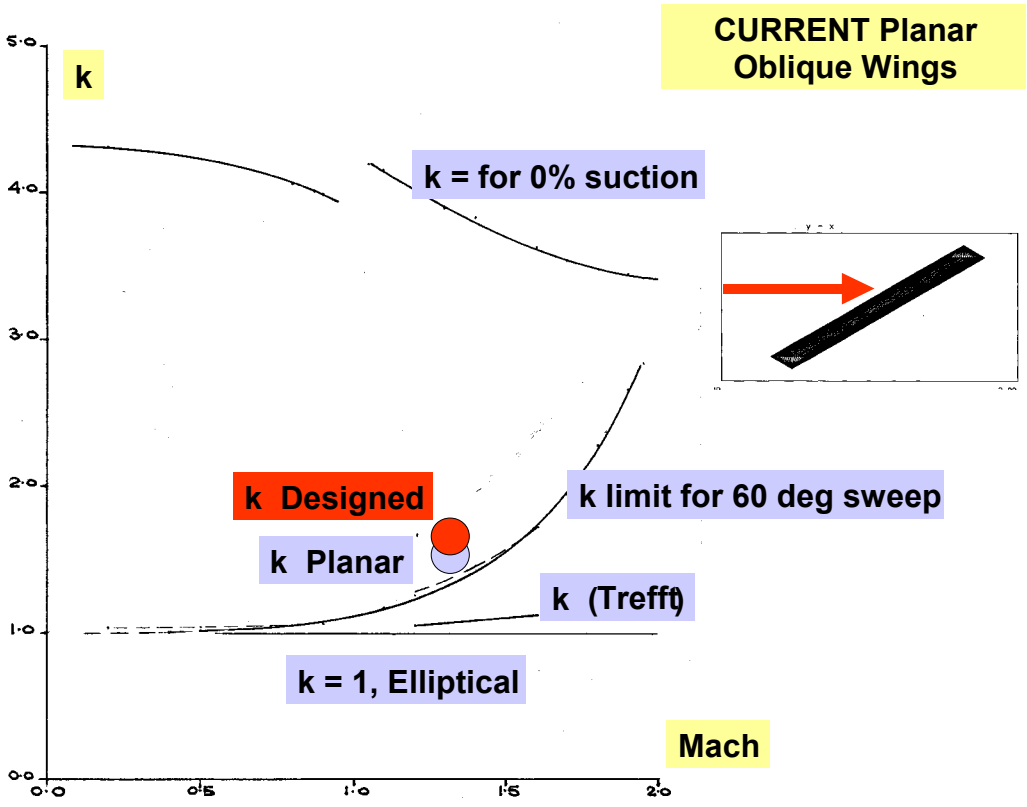


FIG. 7.2.2 DRAG CONSIDERATIONS, Low CL

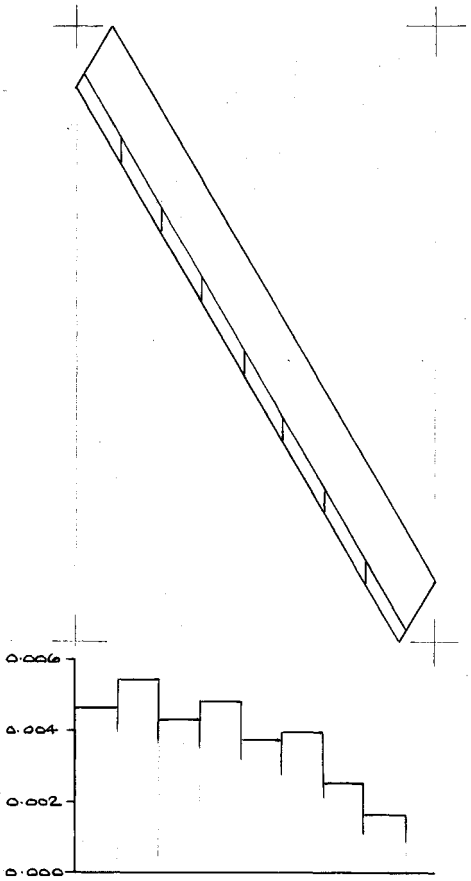


**FIG. 7.3.1 EFFECT OF TEF FLAP DEFLECTION ON $C_L$**

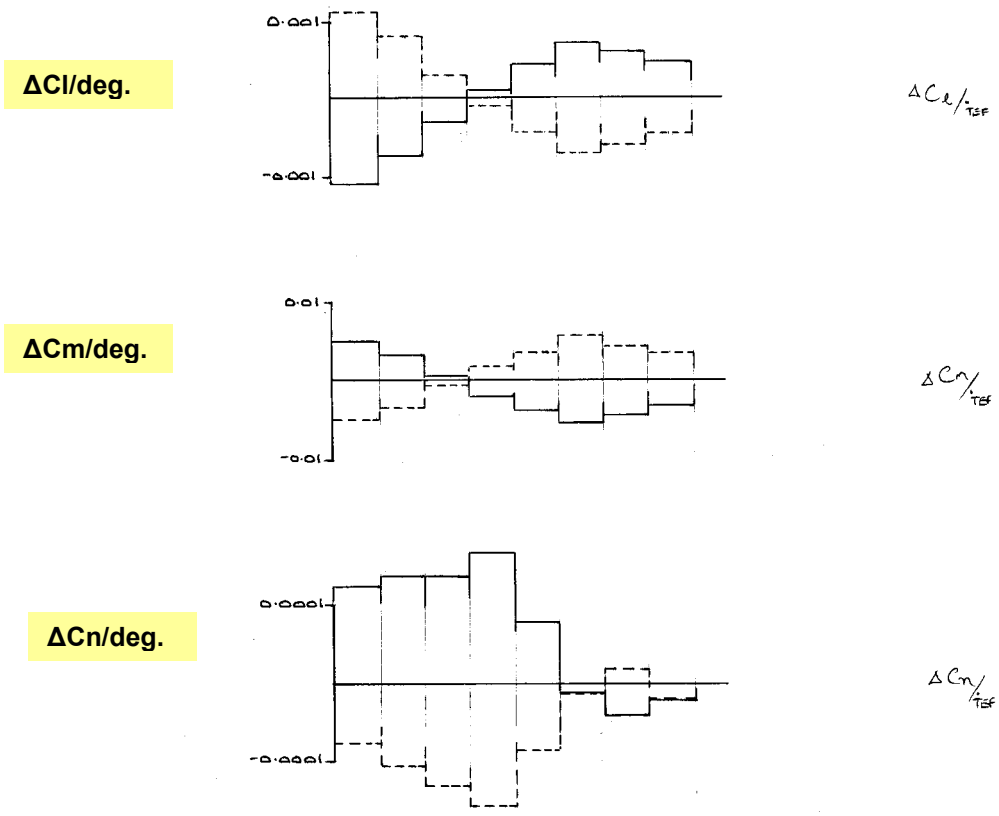


**FIG. 7.3.2 EFFECT OF TEF FLAP DEFLECTION ON $C_l$, $C_m$ and $C_n$**

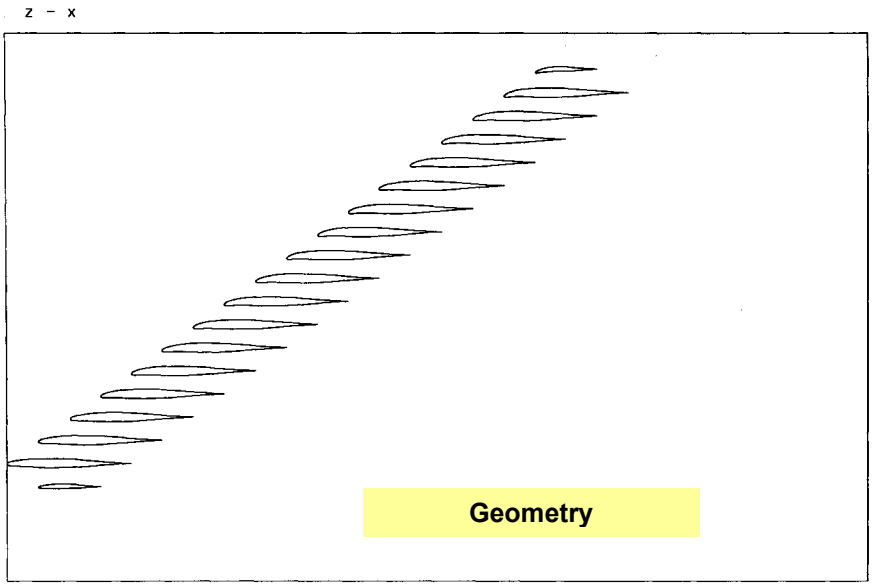


**FIG.8.1.1 DESIGNED WING-1, 21 SPANWISE STATIONS**

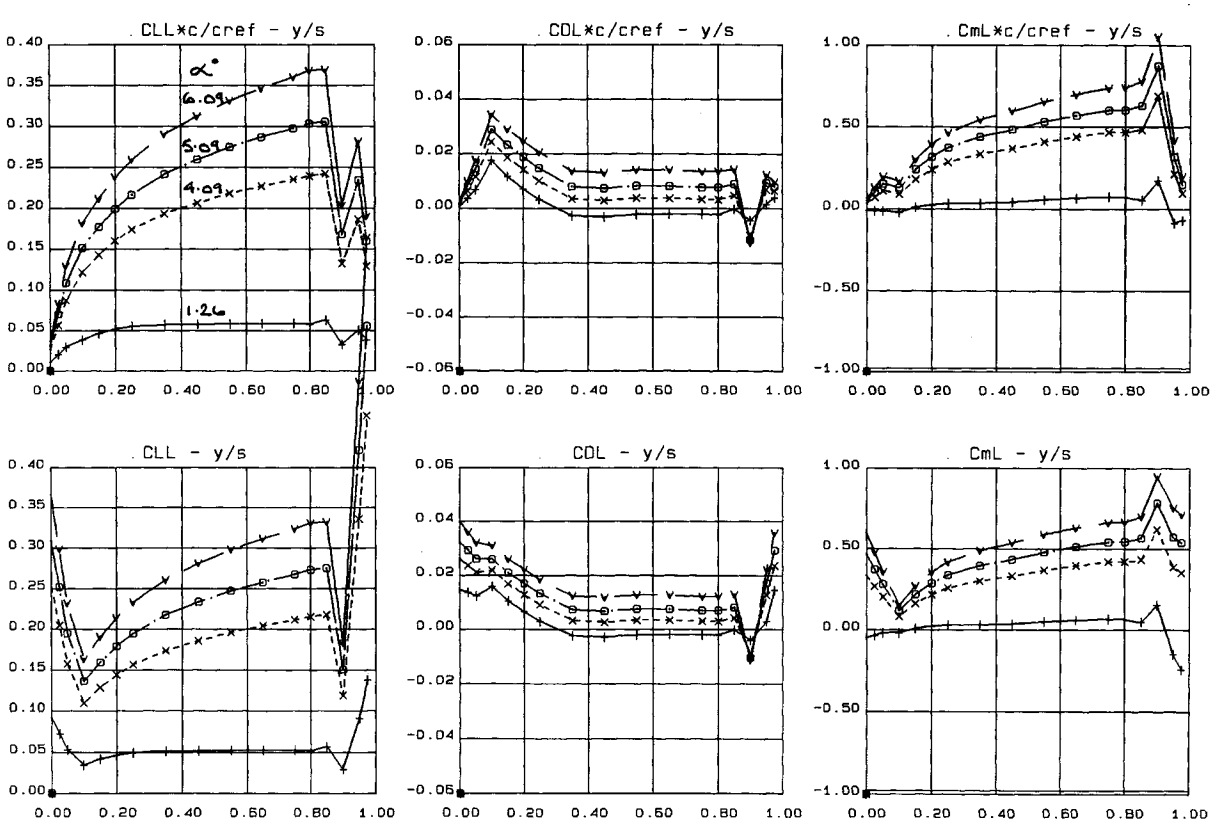


**FIG.8.1.2 DESIGNED WING-1, 21 stns, SPANWISE LOAD DISTRIBUTIONS**

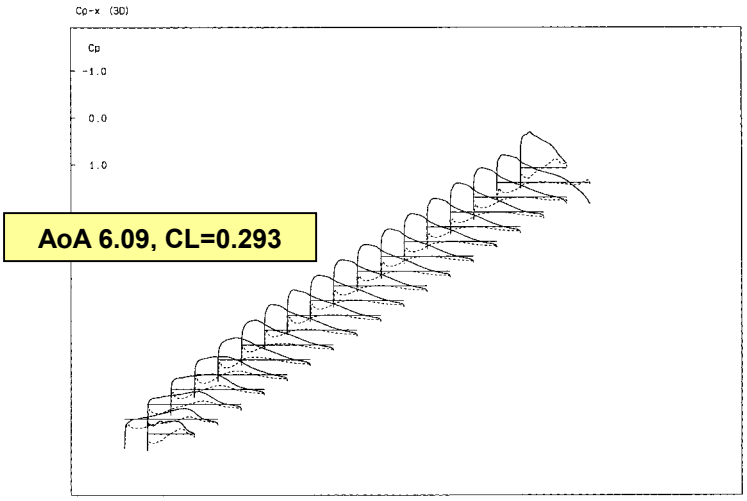


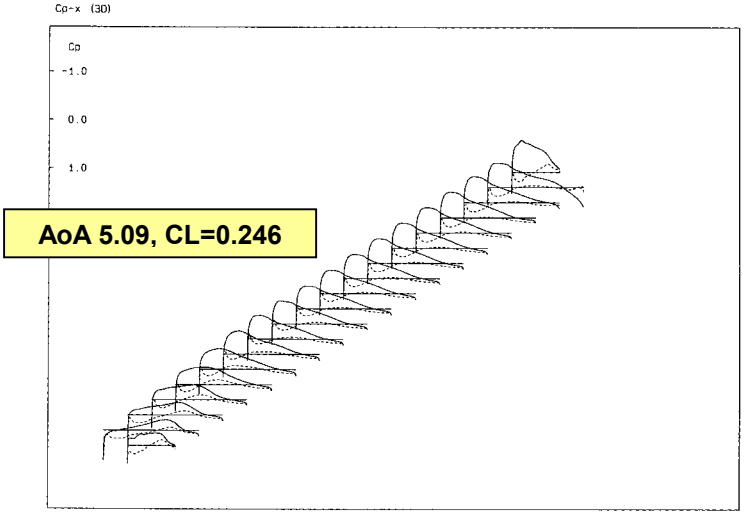


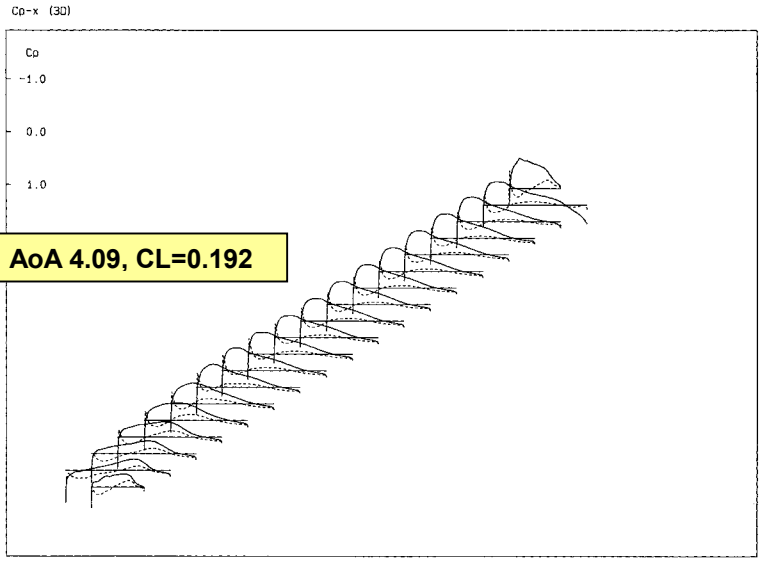


**FIG.8.1.3 DESIGNED WING-1, 21 stns, $C_P$ DISTRIBUTIONS**

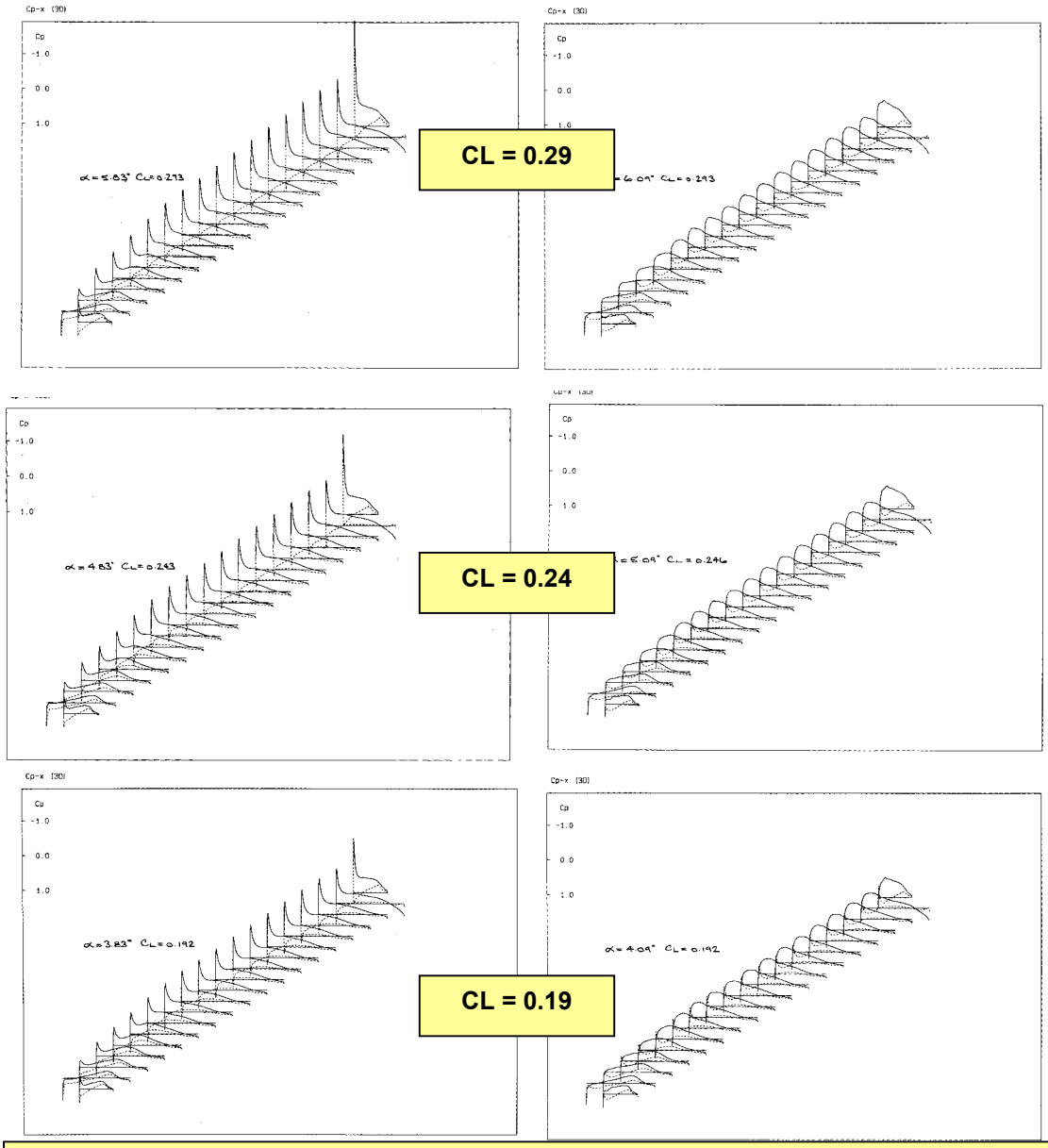


**FIG. 8.1.4 $C_P$ – x, COMPARE UNCAMBERED and DESIGNED WING-1, 21 Stations**

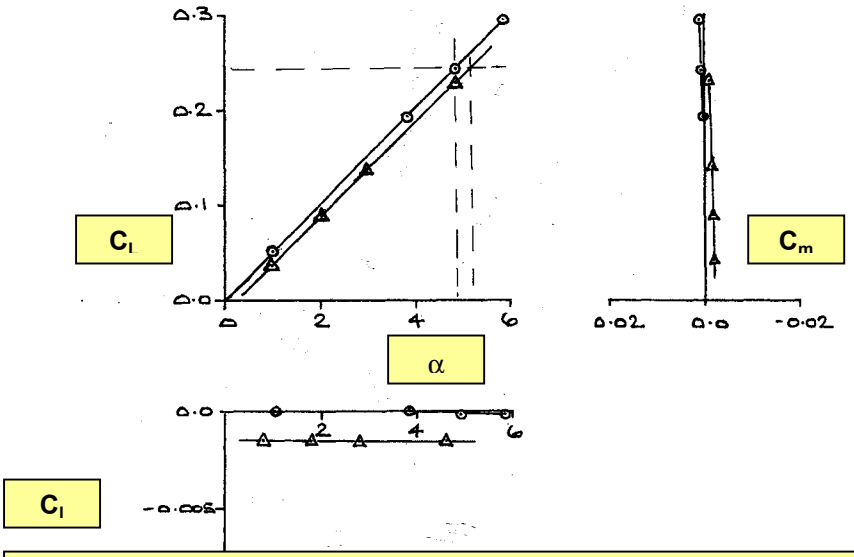


**FIG. 8.1.5 DESIGNED WING-1 and UNCAMBERED WING,
Total Loads ($C_L$ – α, $C_m$ – $C_L$, $C_l$ – α), Mach 1.4**

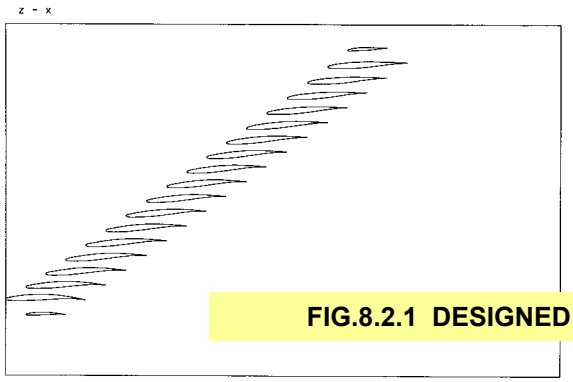


FIG.8.2.1 DESIGNED WING-2 ycg at 0.5b, 21 Stations

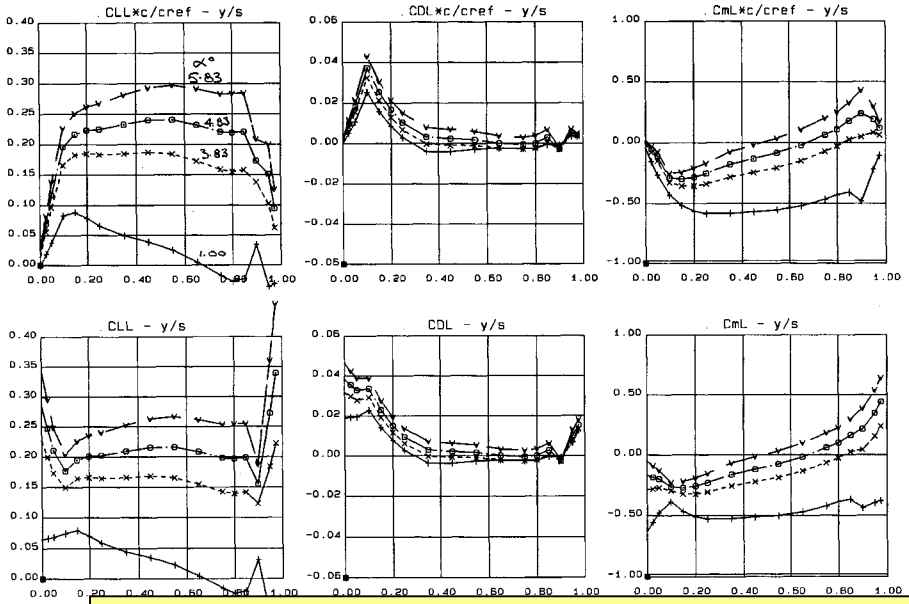


FIG. 8.2.2 DESIGNED WING-2, SPANWISE LOADINGS, 21 STATIONS

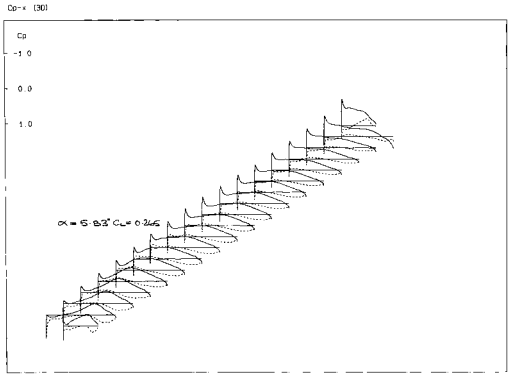

AoA 5.83, CL=0.265

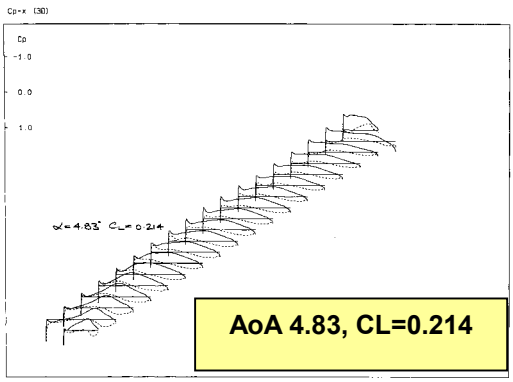

AoA 4.83, CL=0.214

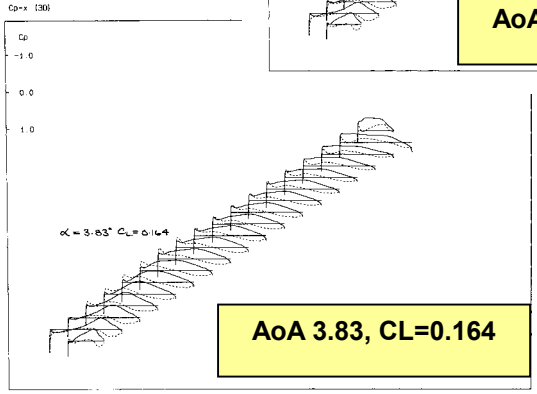

AoA 3.83, CL=0.164

FIG.8.2.3 DESIGNED WING-2, $C_P$ DISTRIBUTIONS, 21 STATIONS

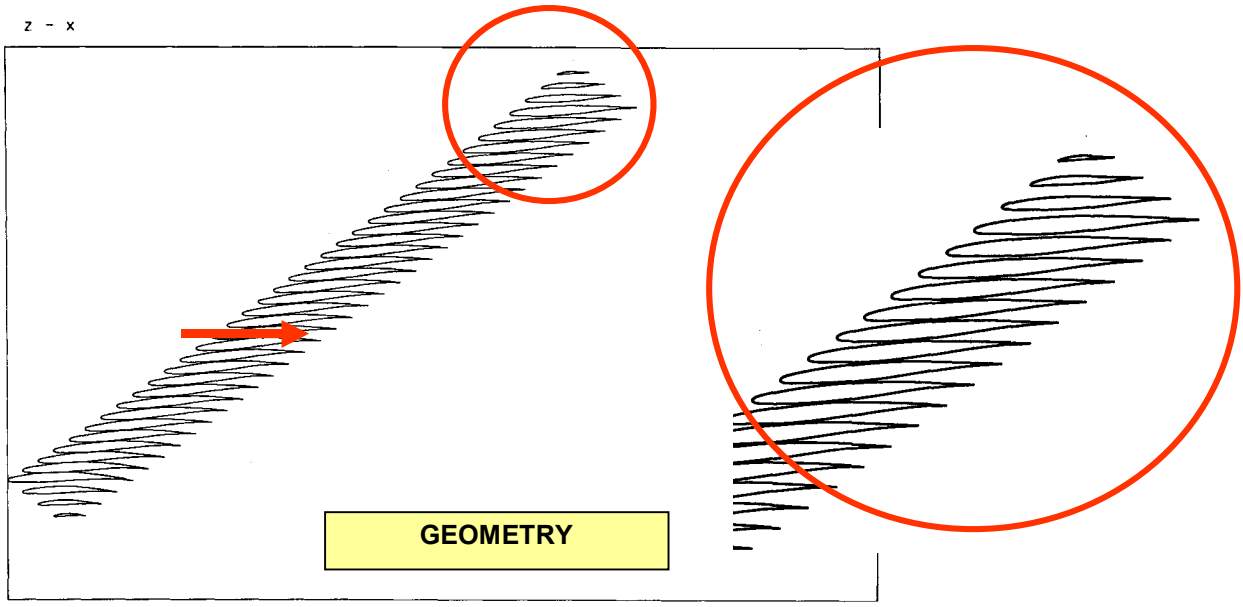


GEOMETRY

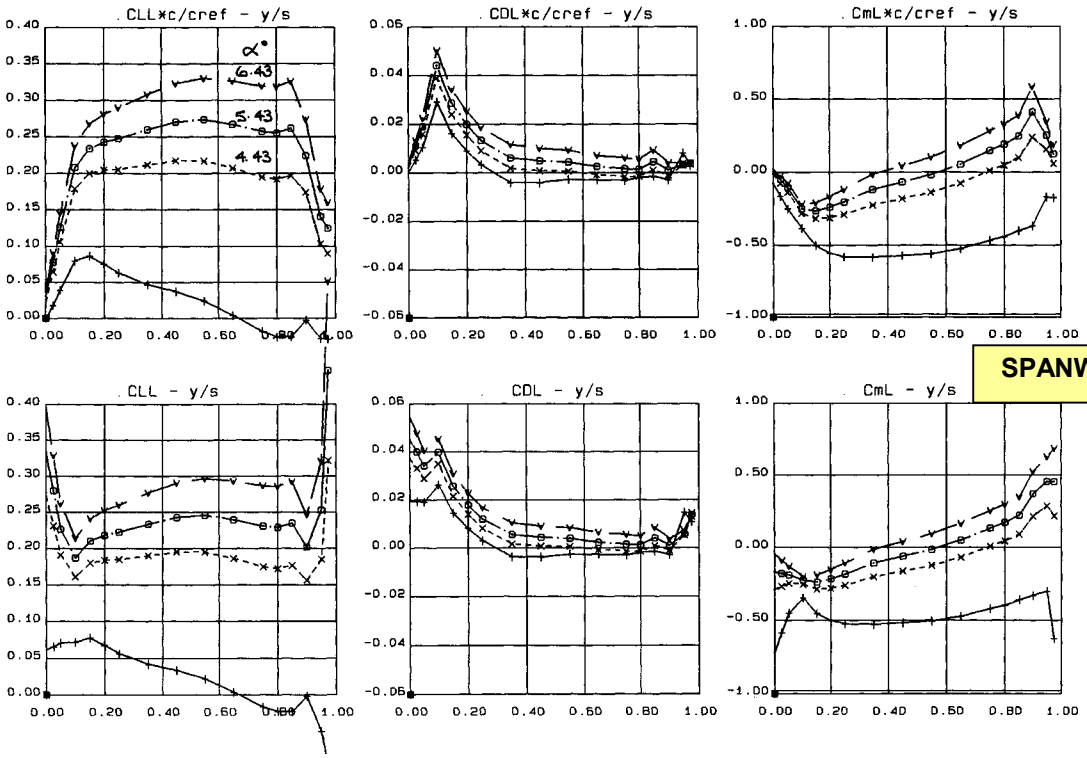


SPANWISE LOADINGS

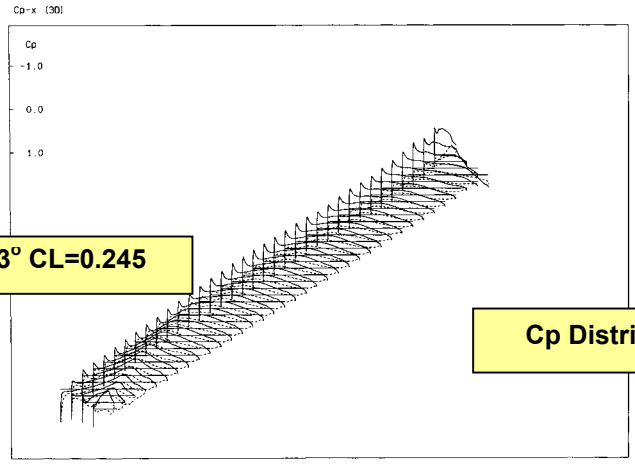


AOA 5.43° CL=0.245

Cp Distributions

**8.2.4 DESIGNED WING-2, 41 stns GEOMETRY, SPANWISE LOADINGS and CP DISTRIBUTIONS**

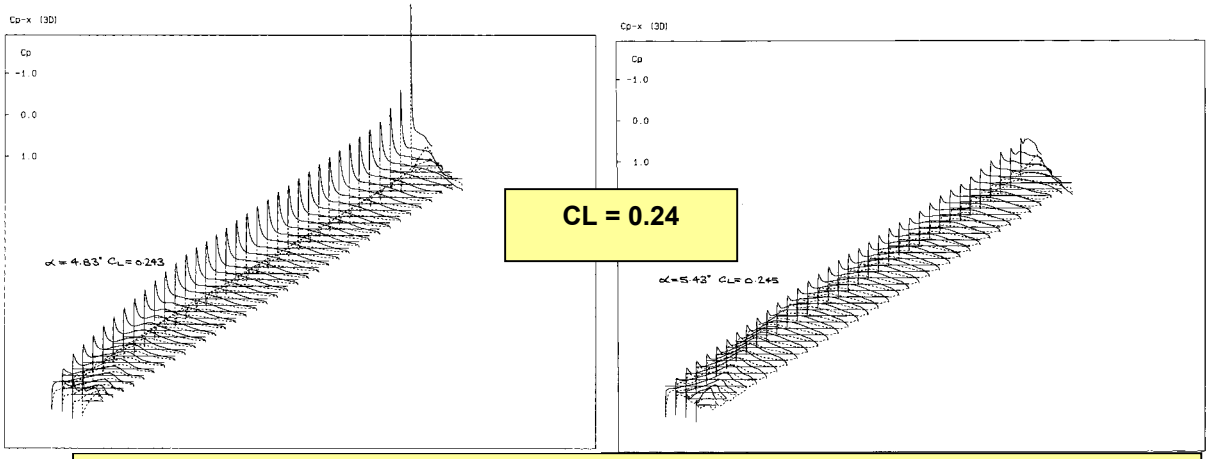


**FIG.8.2.5 $C_P$ – x, COMPARE UNCAMBERED and DESIGNED WING-2, 41 Stations**

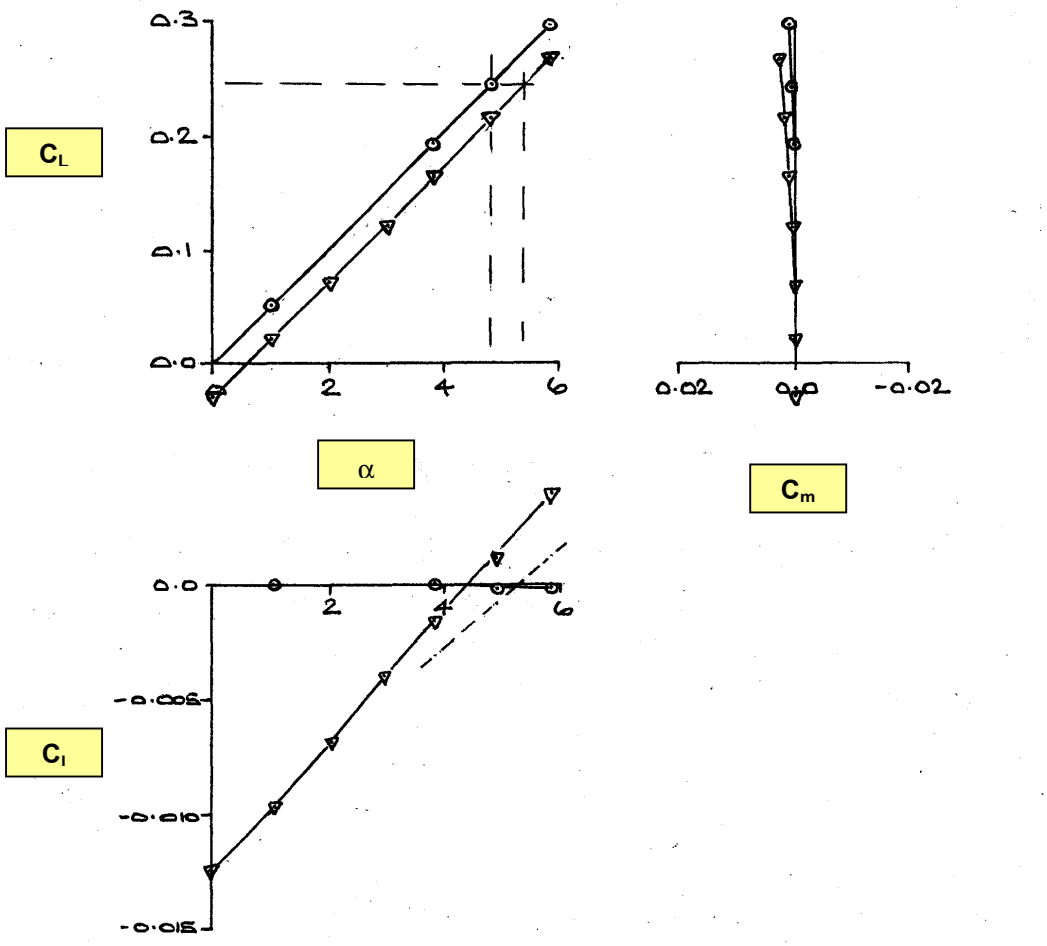


**FIG.8.2.6 DESIGNED WING-2, DESIGNED WING-1 and UNCAMBERED WING, Total Loads ($C_L$ – α, $C_m$ – $C_L$, $C_l$ – α), Mach 1.4**

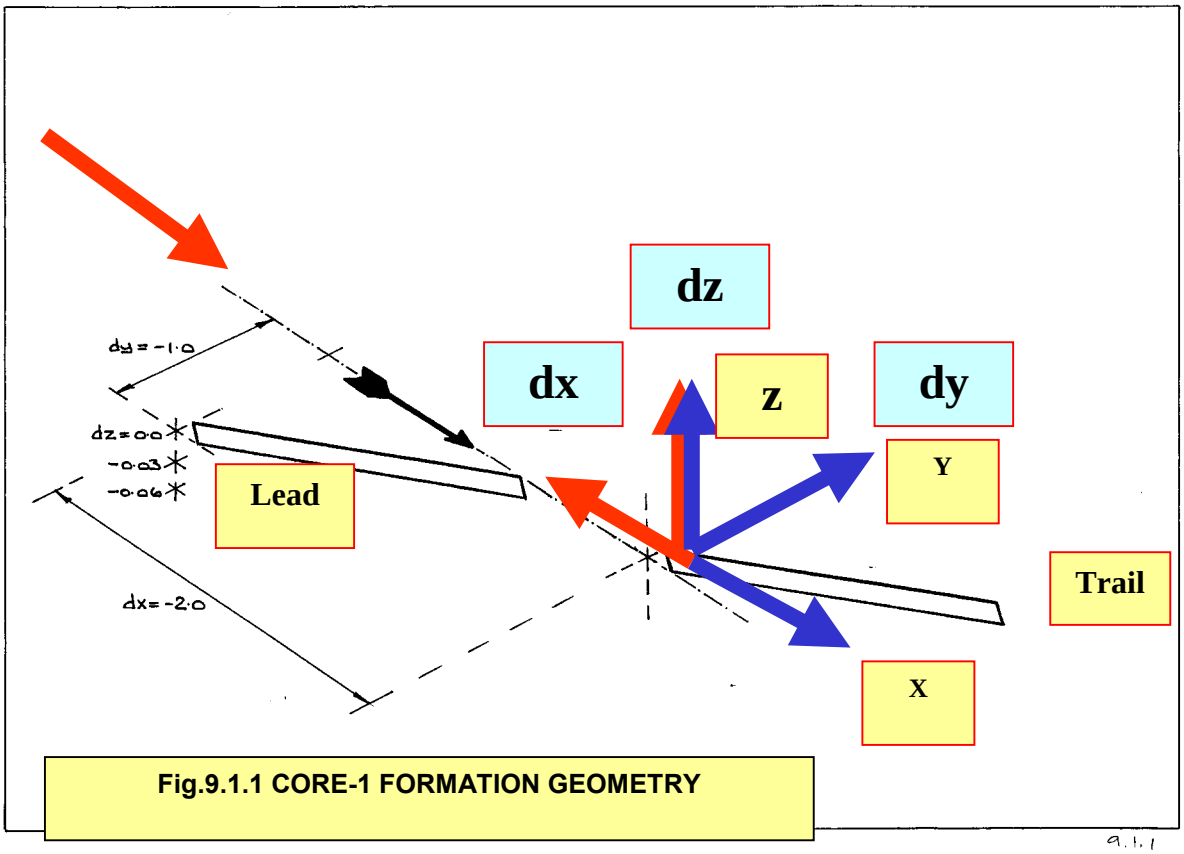


**Fig.9.1.1 CORE-1 FORMATION GEOMETRY**

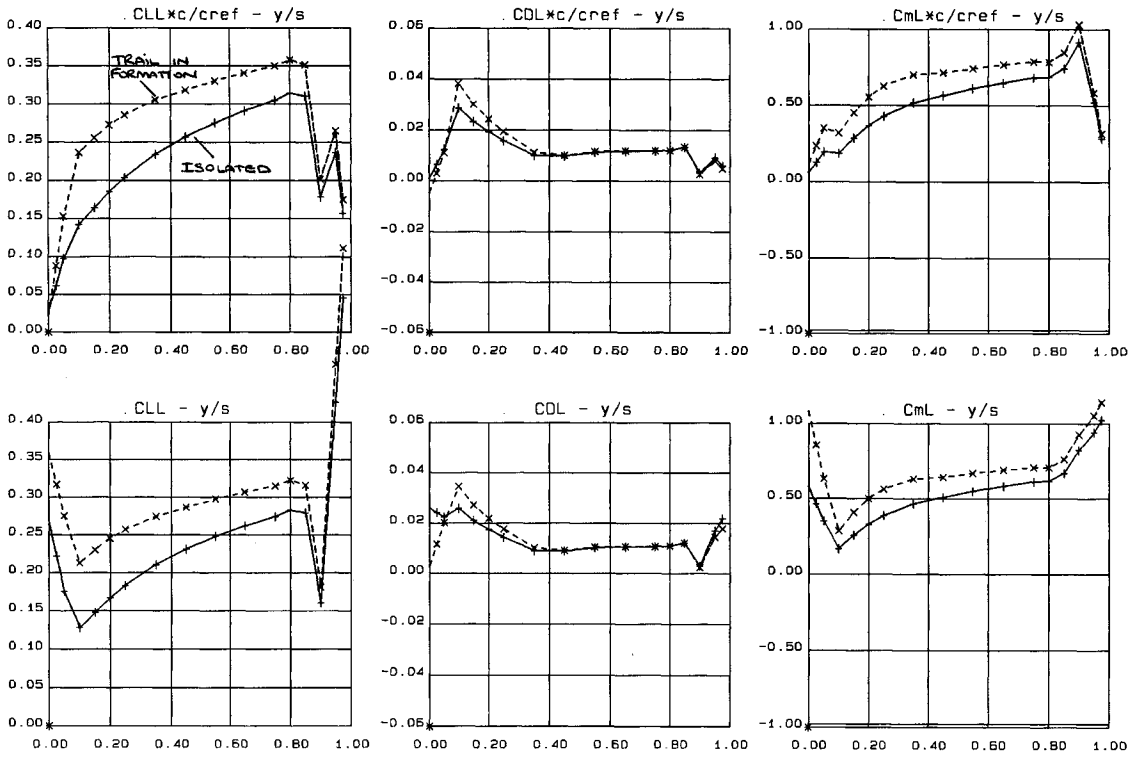


**FIG. 9.1.2 TWO UNCAMBERED WINGS IN FORMATION**
**dx=-2, dy=-1.0, dz= +0.03,**

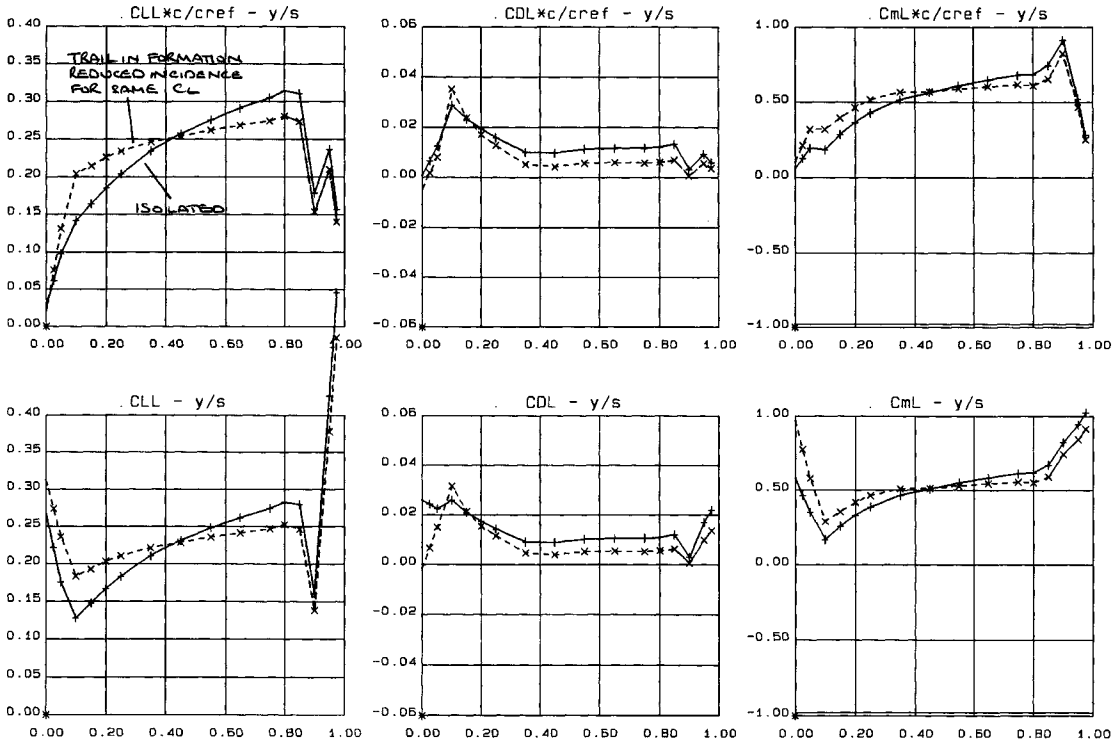


**FIG.9.1.3 TWO UNCAMBERED WINGS IN FORMATION, SAME CL**
**dx=-2, dy=-1.0, dz= +0.03,**

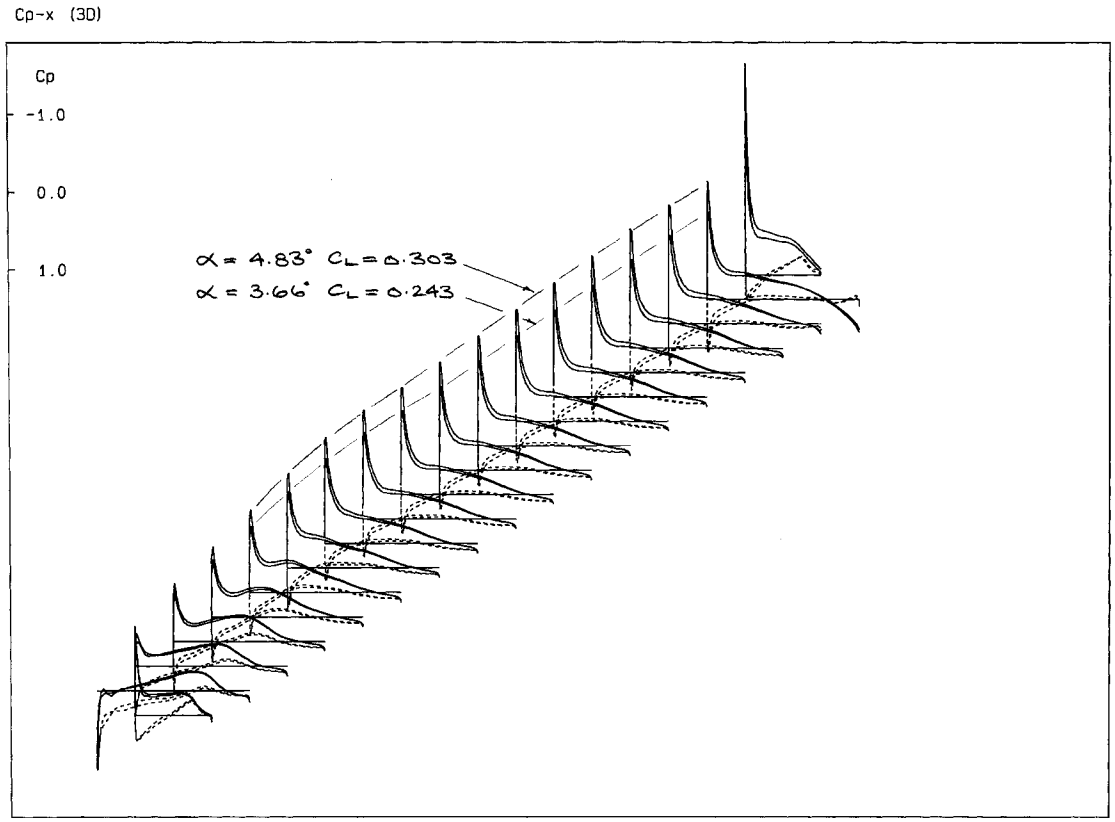


**FIG.9.1.4 Cp – x, Trail Wing in Formation dx=-2, dy=-1.0, dz= +0.03,**
**Uncambered Wings,**
**Results at Same AoA as Lead wing and also at reduced AoA to give same CL**

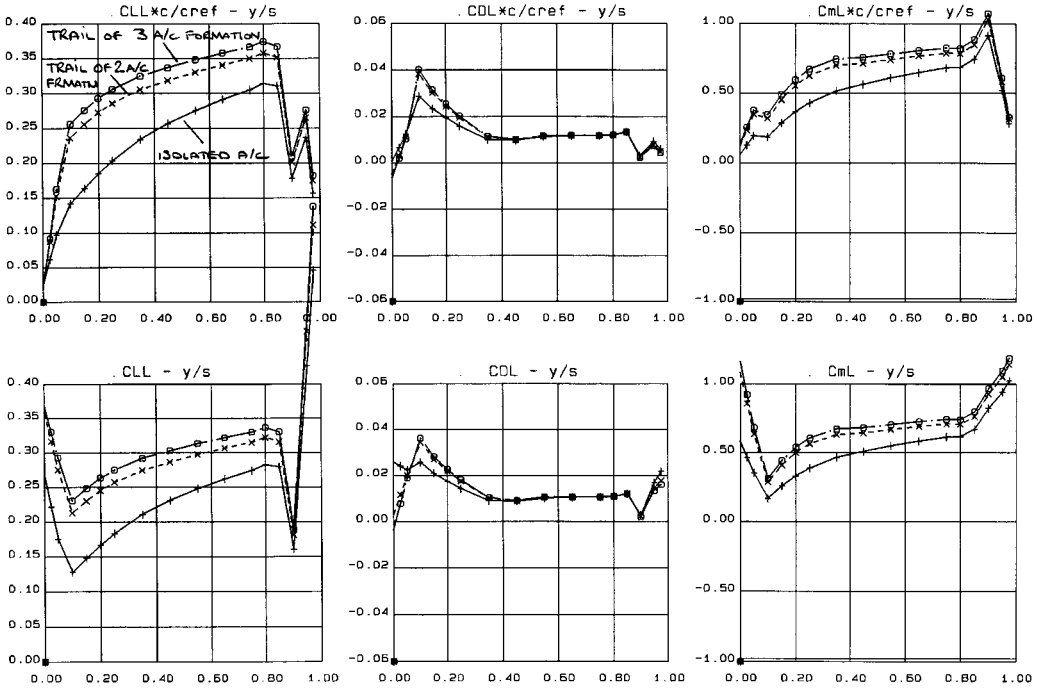


**FIG. 9.1.5 THREE UNCAMBERED WINGS IN FORMATION**
**dx=-2, dy=-1.0, dz= +0.03, dx=-4, dy=-2.0, dz= +0.06,**

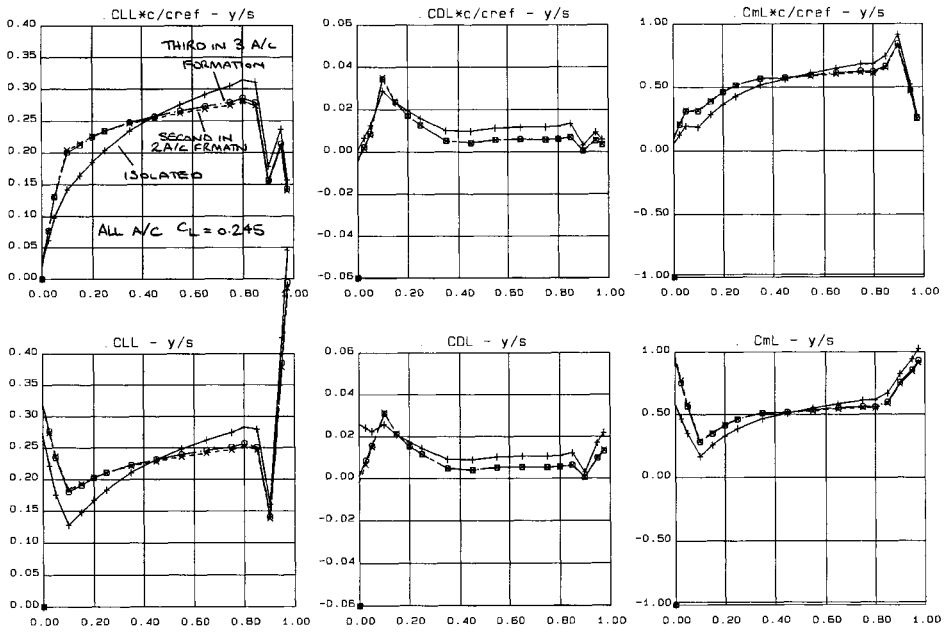


**FIG. 9.1.6 THREE UNCAMBERED WINGS IN FORMATION, ALL AT SAME CL**
**dx=-2, dy=-1.0, dz= +0.03, dx=-4, dy=-2.0, dz= +0.06,**

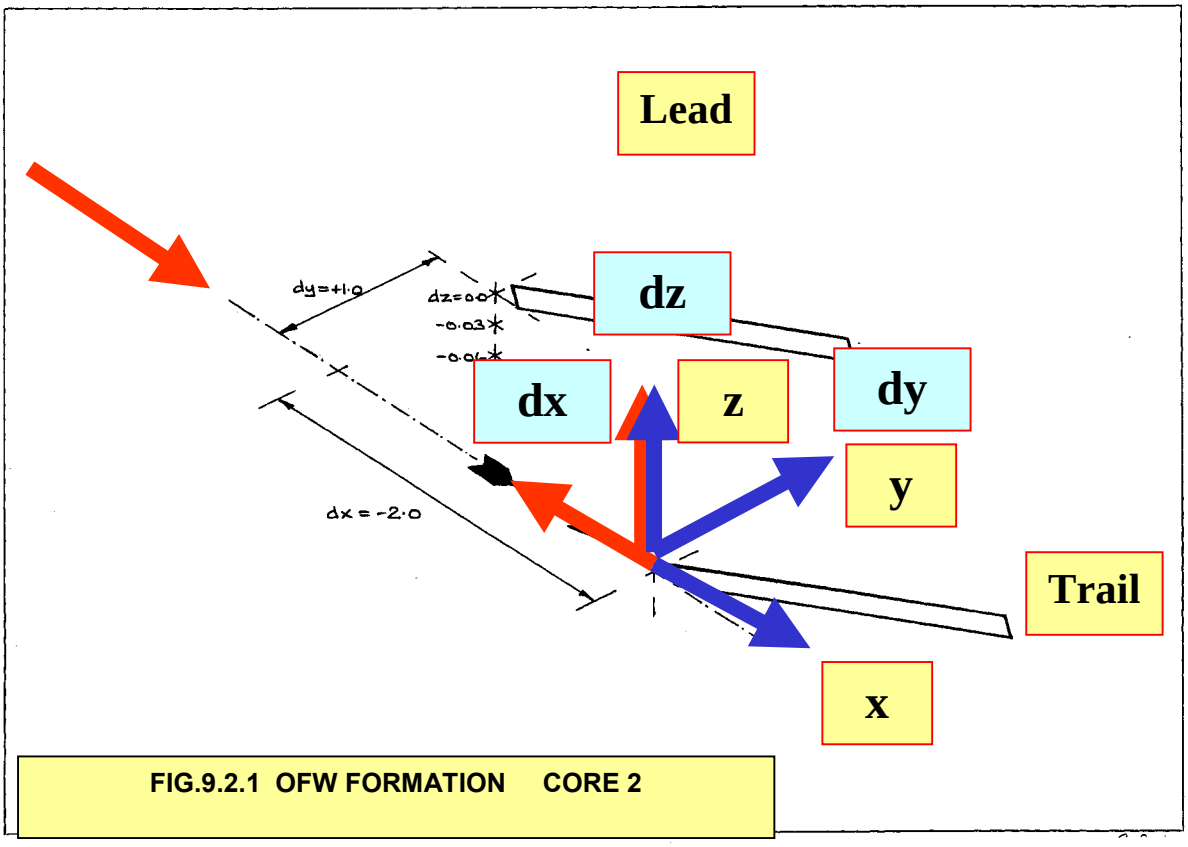


FIG.9.2.1 OFW FORMATION CORE 2

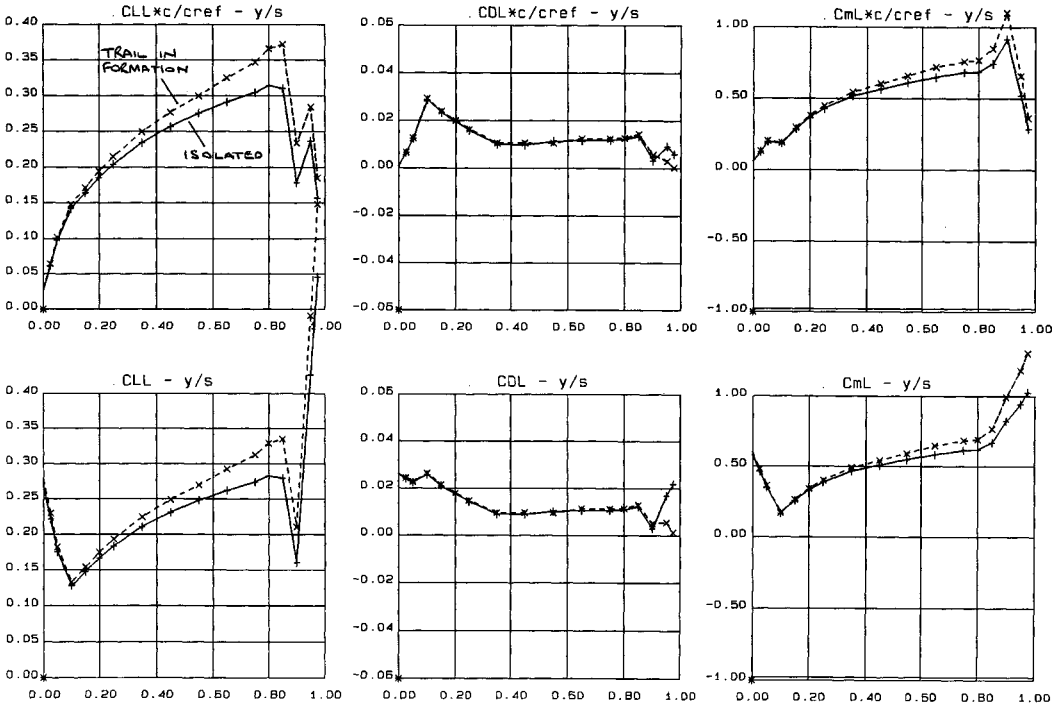


**FIG. 9.2.2 TWO UNCAMBERED WINGS IN FORMATION,**
**dx=-2, dy=+1.0, dz= +0.03,**

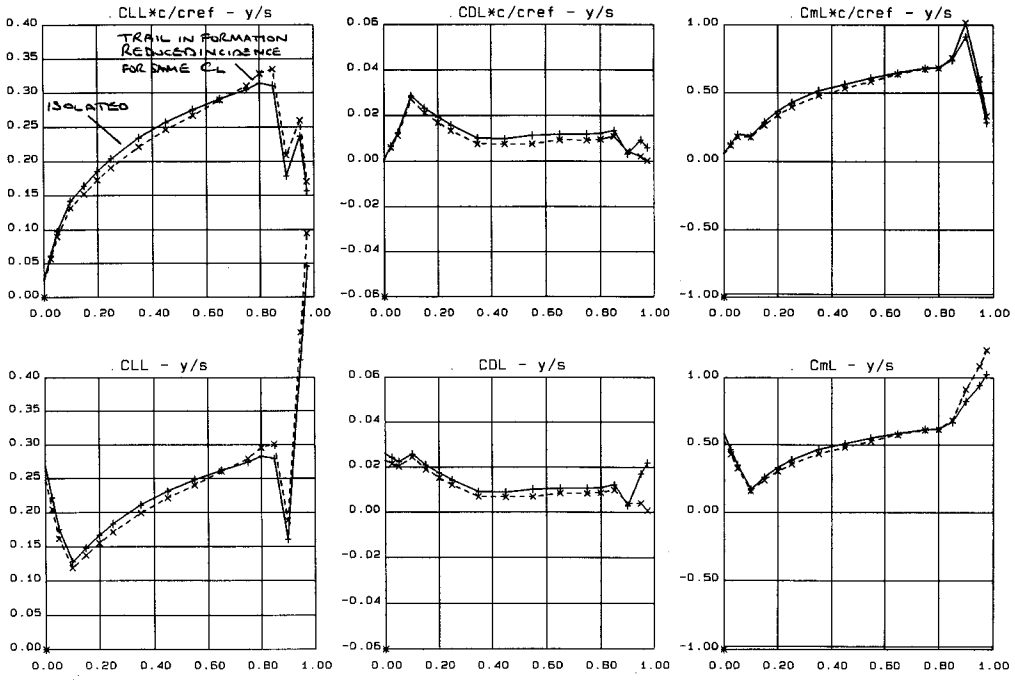


**FIG.9.2.3 TWO UNCAMBERED WINGS IN FORMATION, SAME CL**
**dx=-2, dy=+1.0, dz= +0.03,**

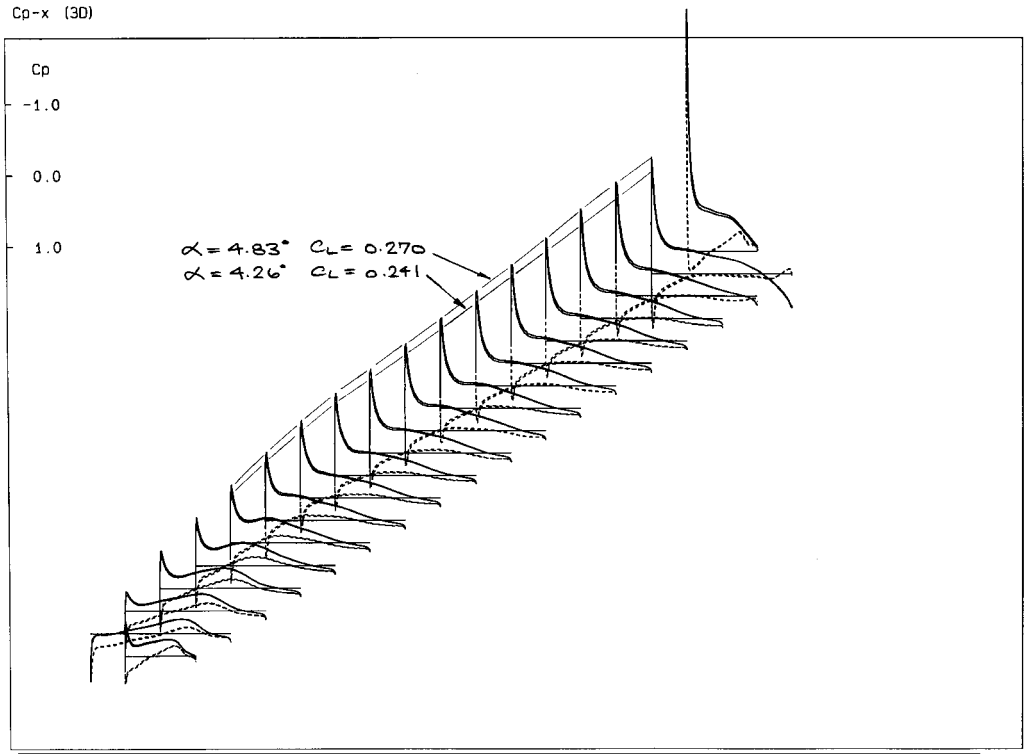


**FIG.9.2.4 Cp – x, Trail Wing in Formation dx=-2, dy=+1.0, dz= +0.03, Uncambered Wings, Same AoA as Lead wing and reduced AoA to give same CL**

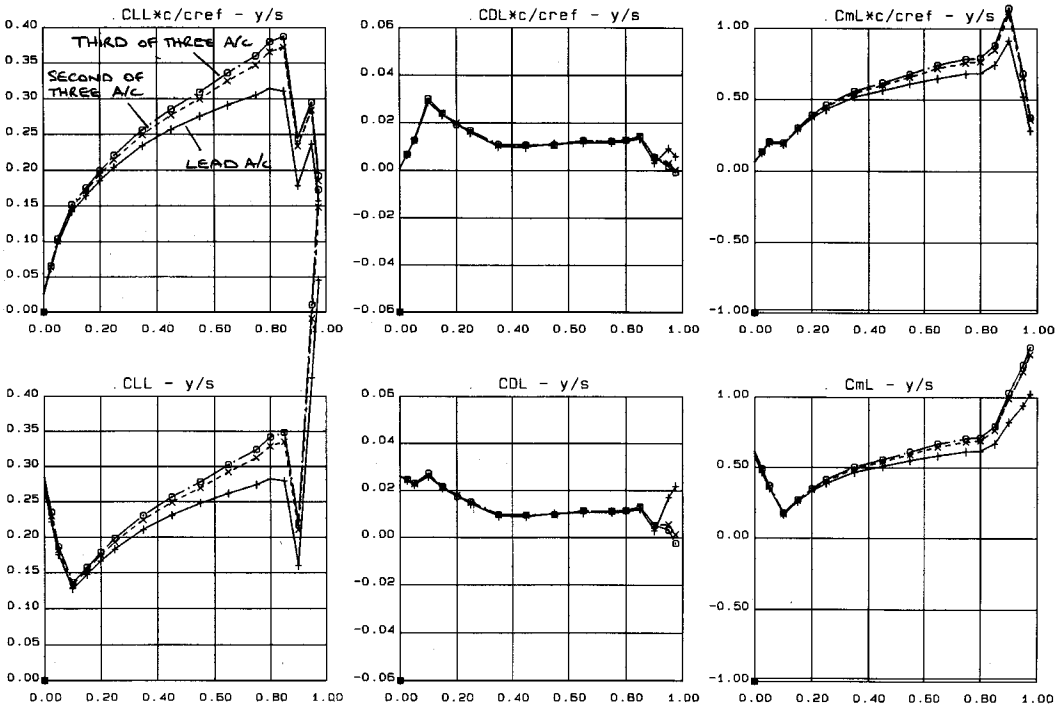


**FIG. 9.2.5 THREE UNCAMBERED WINGS IN FORMATION, dx=-2, dy=+1.0, dz= +0.03, dx=-4, dy=+2.0, dz= +0.06,**

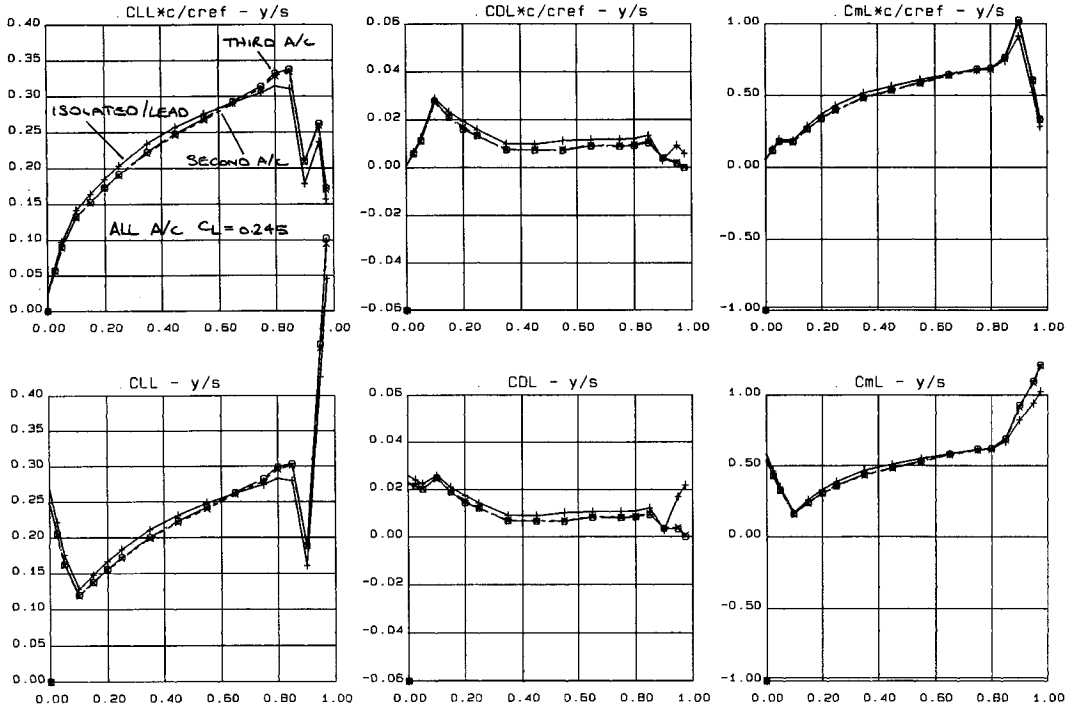


**FIG.9.2.6 THREE UNCAMBERED WINGS IN FORMATION, ALL AT SAME CL**
**dx=-2, dy=+1.0, dz= +0.03, dx=-4, dy=+2.0, dz= +0.06,**

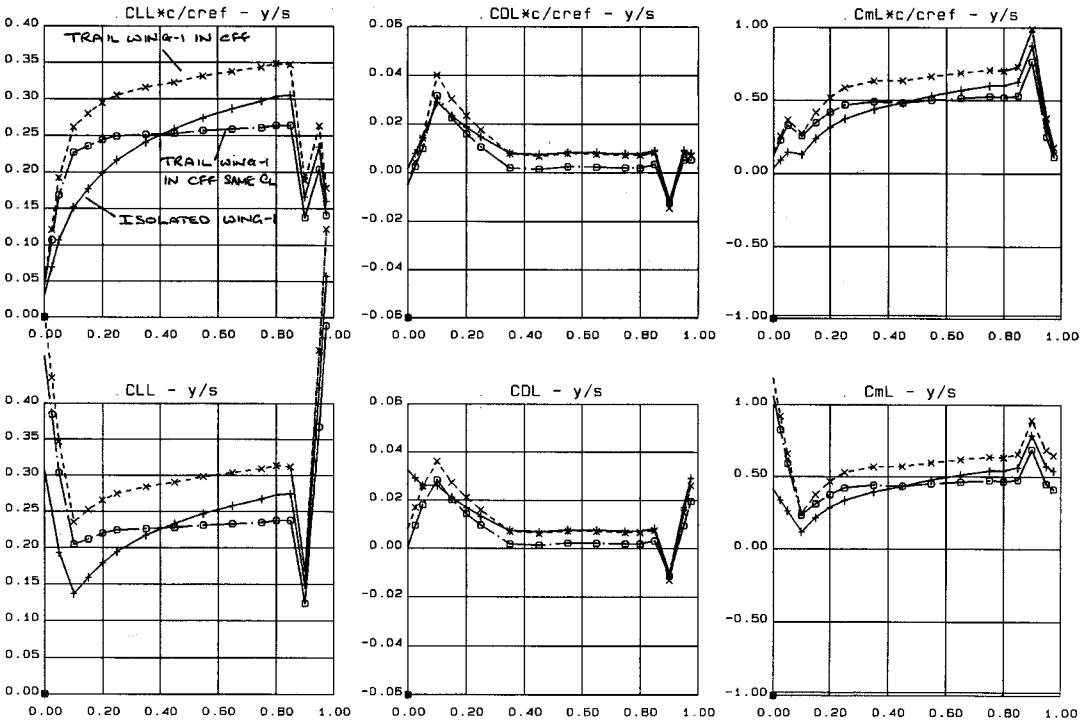


**FIG. 10.1.1**
**TWO DESIGNED WINGS IN FORMATION, WING-1,**
**dx=-2, dy=-1.1, dz= +0.01,**
**TRAIL WING UNTRIMMED AND TRIMMED FOR SAME CL**

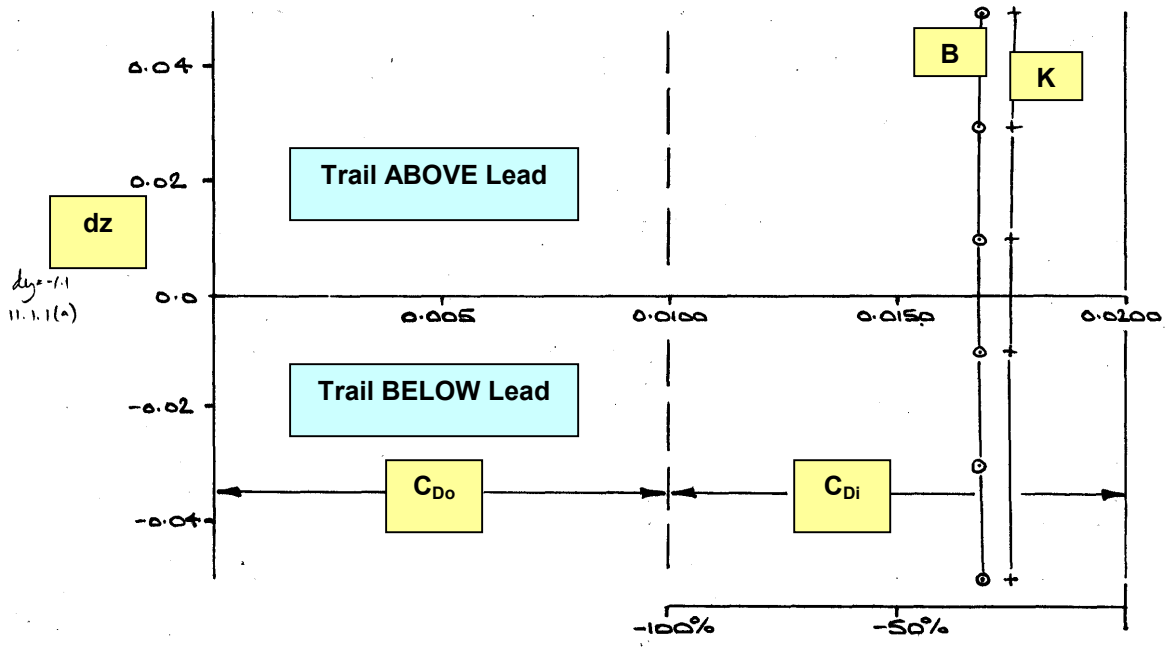


**FIG.11.1.1(a) EFFECT OF VERTICAL DISPLACEMENT ON DRAG BREAKDOWN OF PLANAR TRAIL OFW IN TWO AIRCRAFT FORMATION, BOTH AT SAME $C_L$ CORE 1, dx = -2, dy = -1.1,**

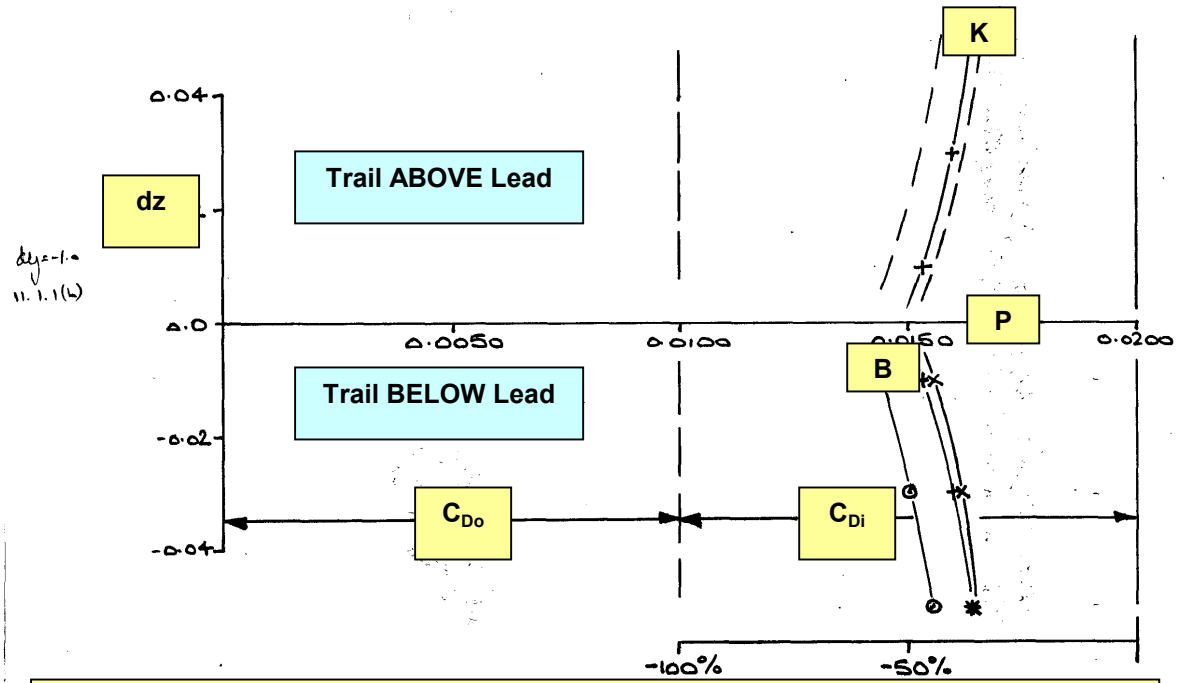


**FIG.11.1.1(b) EFFECT OF VERTICAL DISPLACEMENT ON DRAG BREAKDOWN OF PLANAR TRAIL OFW IN TWO AIRCRAFT FORMATION, BOTH AT SAME $C_L$ CORE 1, dx=-2, dy=-1.0,**

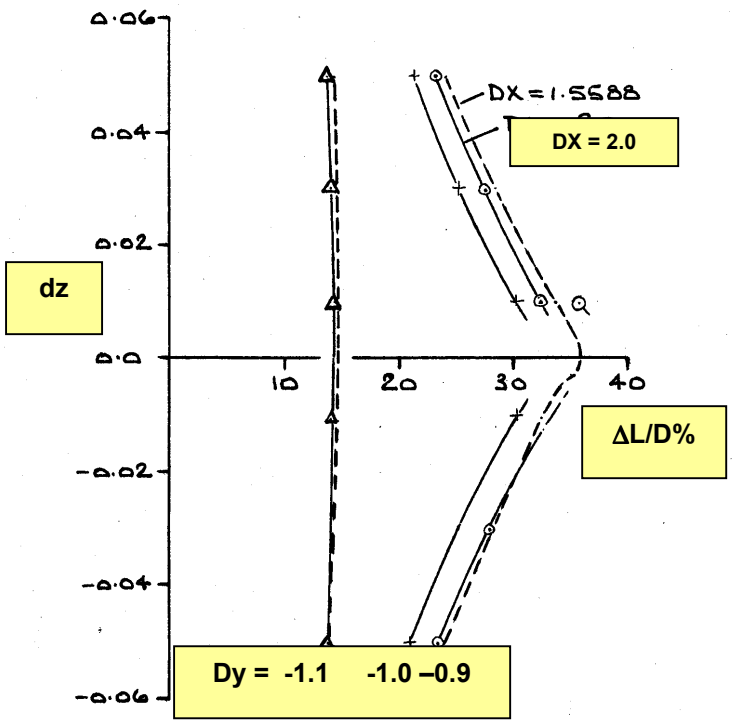


**FIG.11.1.2 EFFECT OF VERTICAL AND LATERAL DISPLACEMENT ON ΔL/D% OF PLANAR TRAIL OFW IN TWO AIRCRAFT FORMATION, BOTH AT SAME $C_L$ CORE 1, dx = -2**

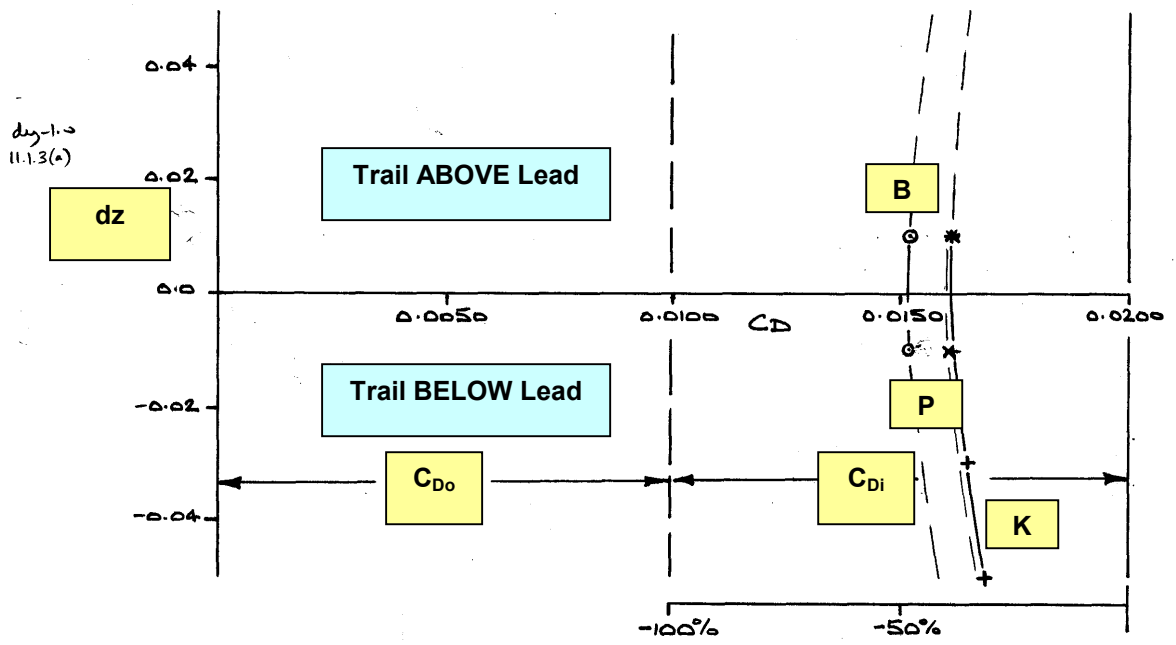


**FIG.11.1.3(a) EFFECT OF VERTICAL DISPLACEMENT ON DRAG BREAKDOWN OF DESIGN WING-2 TRAIL OFW IN TWO AIRCRAFT FORMATION, BOTH AT SAME $C_L$ CORE 1, dx=-2, dy=-1.0**

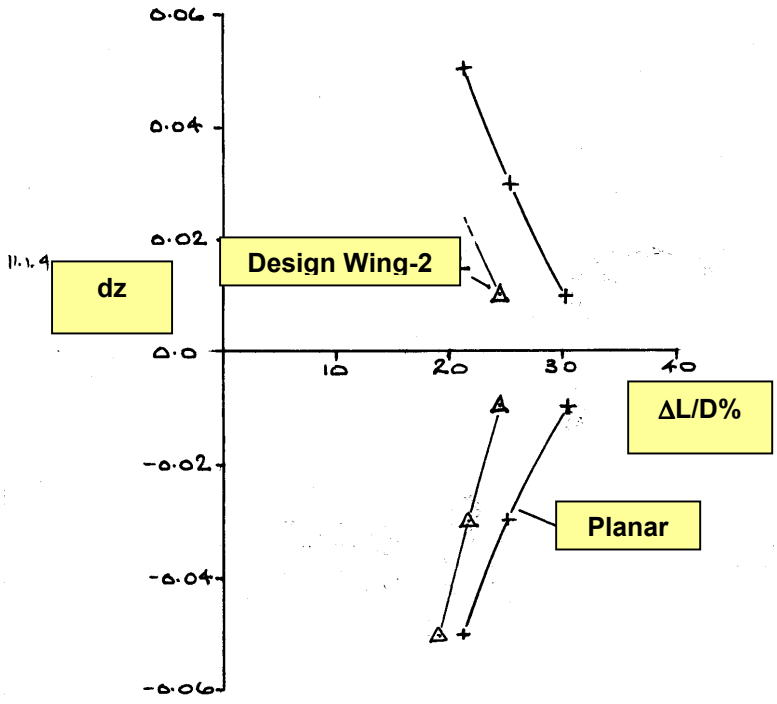


**FIG.11.1.4 EFFECT OF VERTICAL DISPLACEMENT ON ΔL/D% OF TRAIL OFW IN TWO AIRCRAFT FORMATION, BOTH AT SAME $C_L$ PLANAR AND DESIGN WING-2 COMPARED, CORE 1, dx=-2, dy=-1.0**

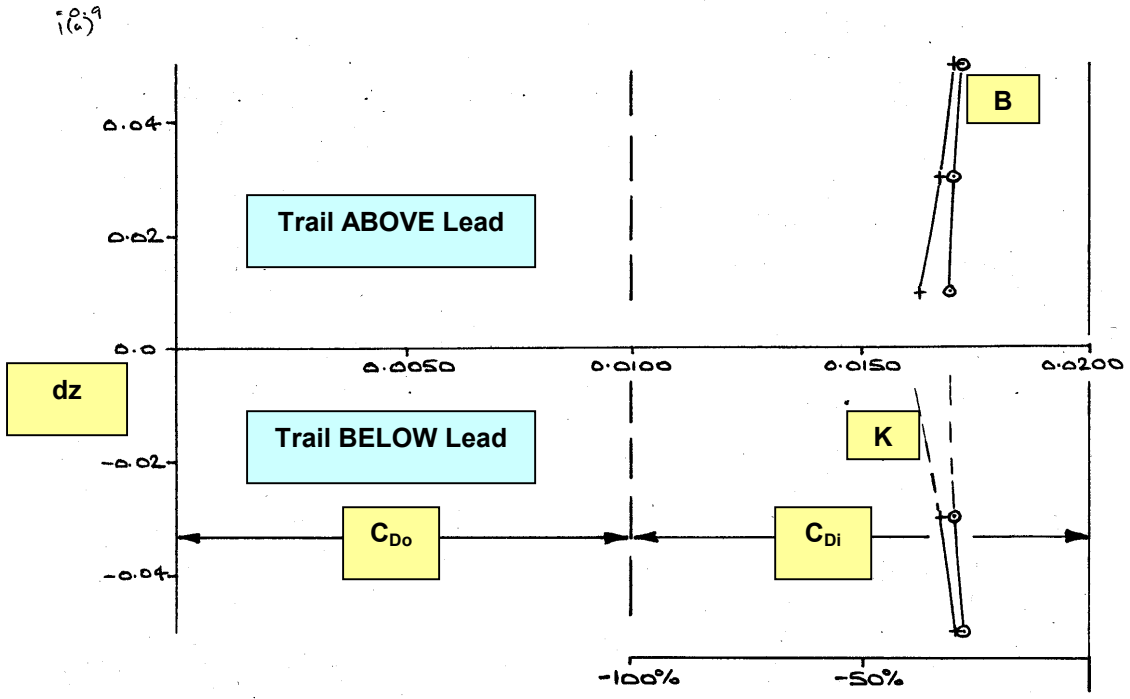


**FIG.11.2.1(a) EFFECT OF VERTICAL DISPLACEMENT ON DRAG BREAKDOWN OF PLANAR TRAIL OFW IN TWO AIRCRAFT FORMATION, BOTH AT SAME $C_L$ CORE 2, dx=-2, dy=+0.9,**

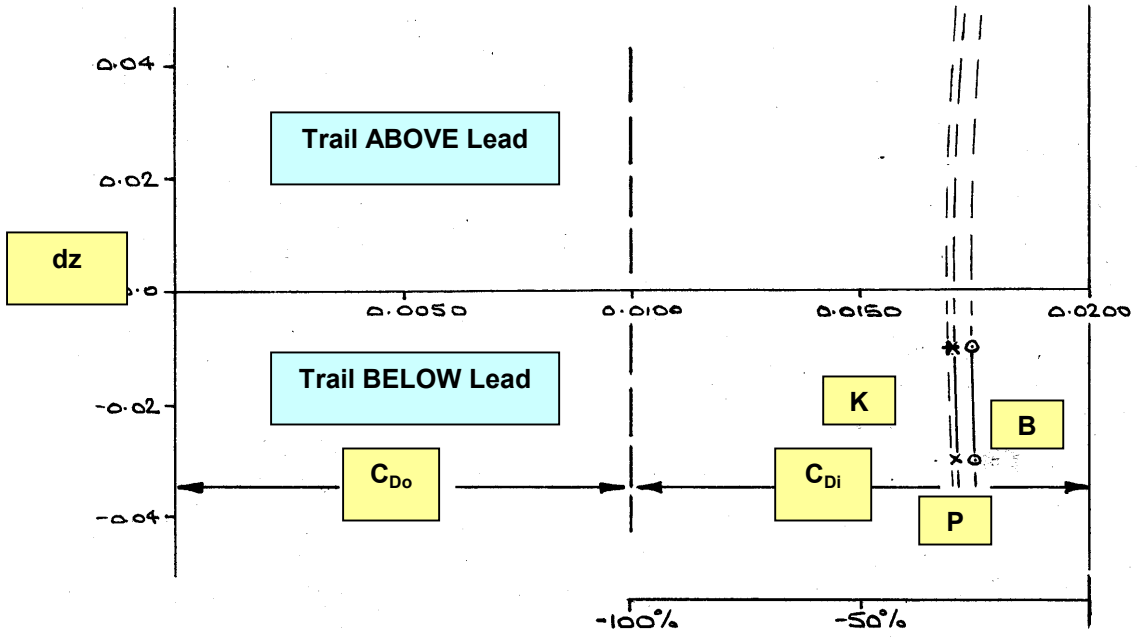


**FIG.11.2.1(b) EFFECT OF VERTICAL DISPLACEMENT ON DRAG BREAKDOWN OF PLANAR TRAIL OFW IN TWO AIRCRAFT FORMATION, BOTH AT SAME $C_L$ CORE 2, dx=-2, dy=+1.0,**

11.2.2

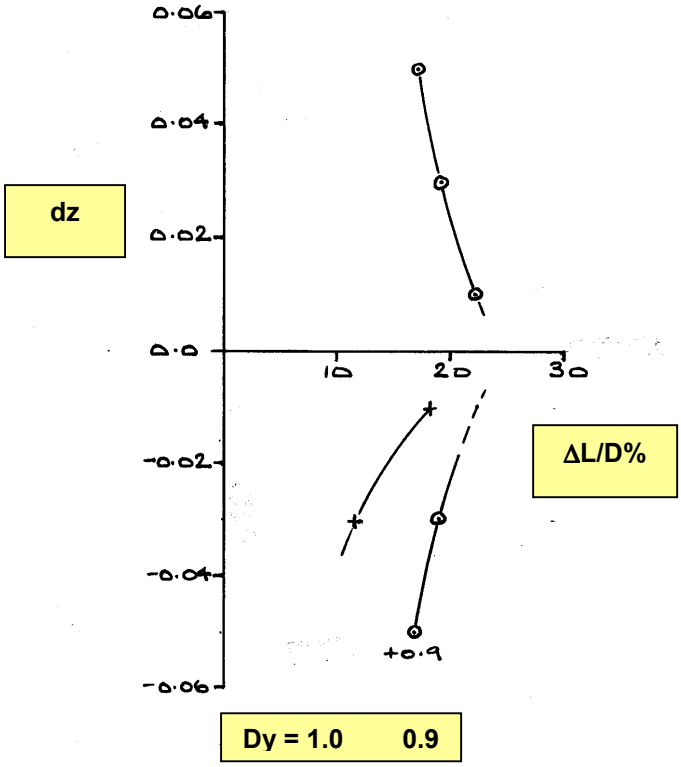


**FIG.11.2.2 EFFECT OF VERTICAL AND LATERAL DISPLACEMENT ON ΔL/D% OF PLANAR TRAIL OFW IN TWO AIRCRAFT FORMATION, BOTH AT SAME $C_L$ CORE 2, dx = -2**

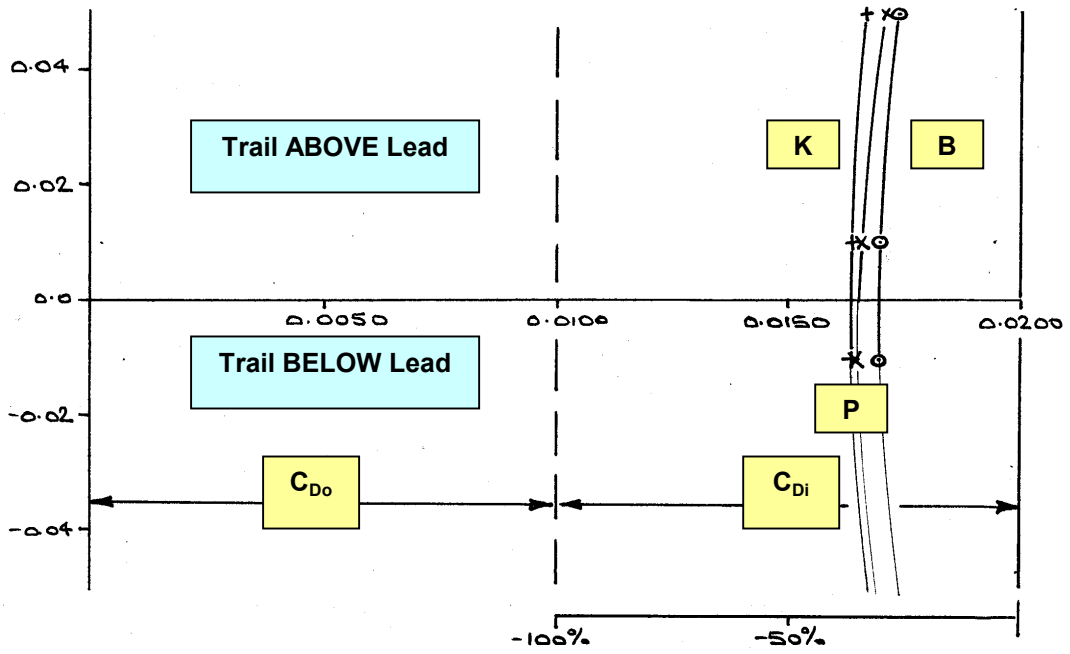


**FIG.11.2.3 EFFECT OF VERTICAL DISPLACEMENT ON DRAG BREAKDOWN OF DESIGN WING-2 TRAIL OFW IN TWO AIRCRAFT FORMATION, BOTH AT SAME $C_L$ CORE 2, dx = -2, dy = +1.0,**

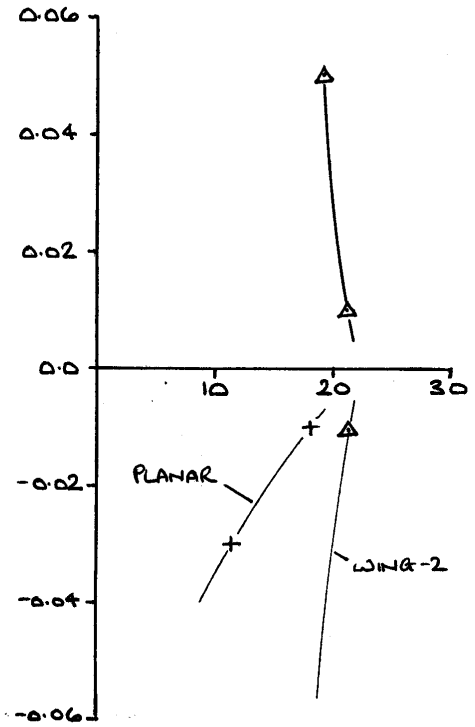


**FIG.11.2.4 EFFECT OF VERTICAL DISPLACEMENT ON ΔL/D%
OF TRAIL OFW IN TWO AIRCRAFT FORMATION, BOTH AT SAME $C_L$
PLANAR AND DESIGN WING-2 COMPARED, CORE 2, dx=-2, dy=-1.0**

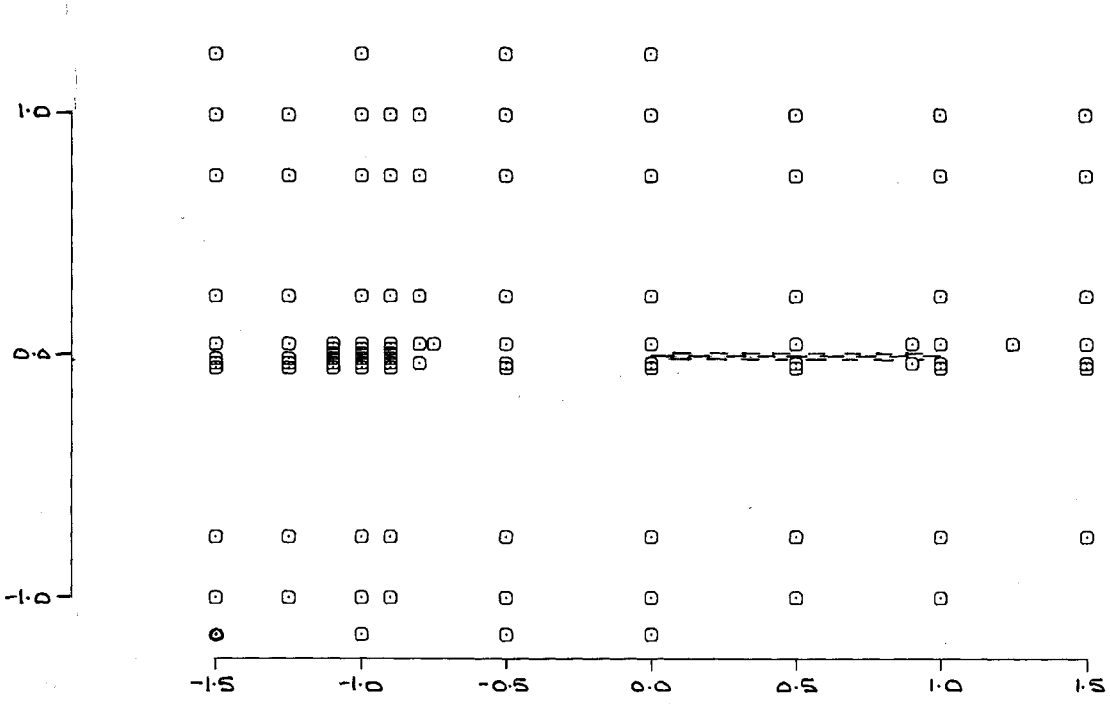


**FIG.11.4.1 UNCAMBERED WINGS, RELATIVE POSITIONS STUDIED AT dx=-2,**

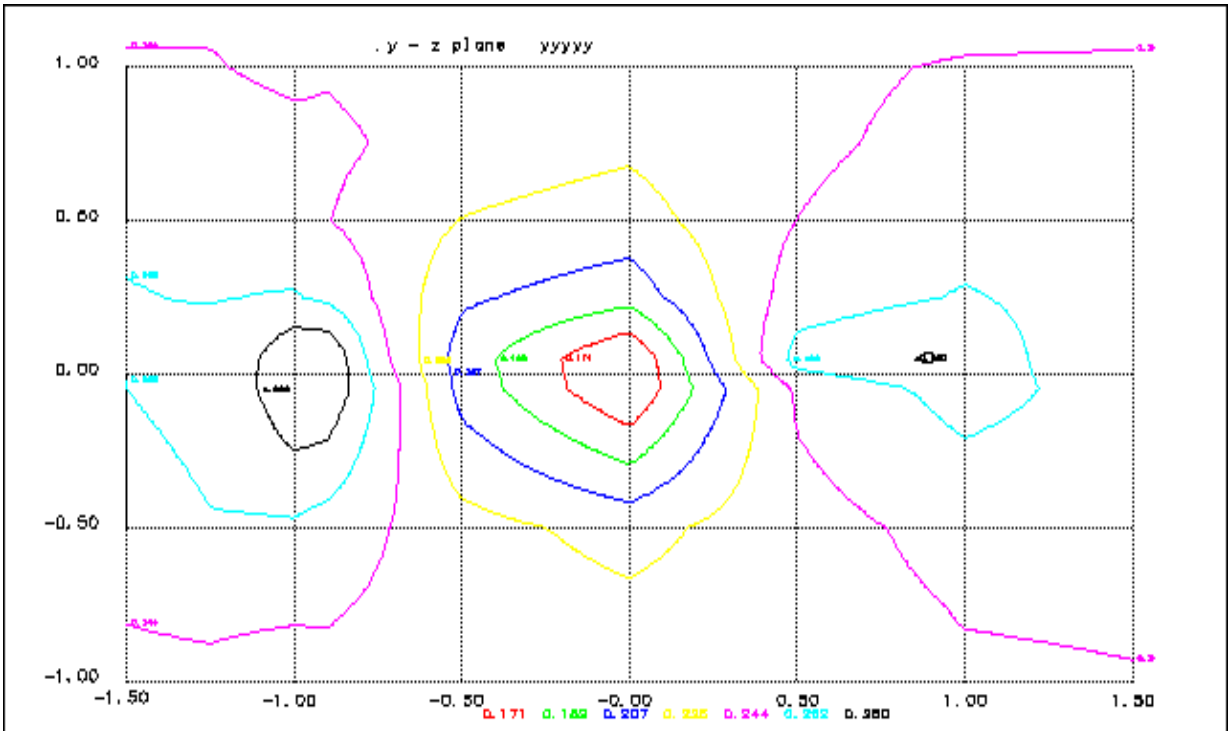


(a) CL arising

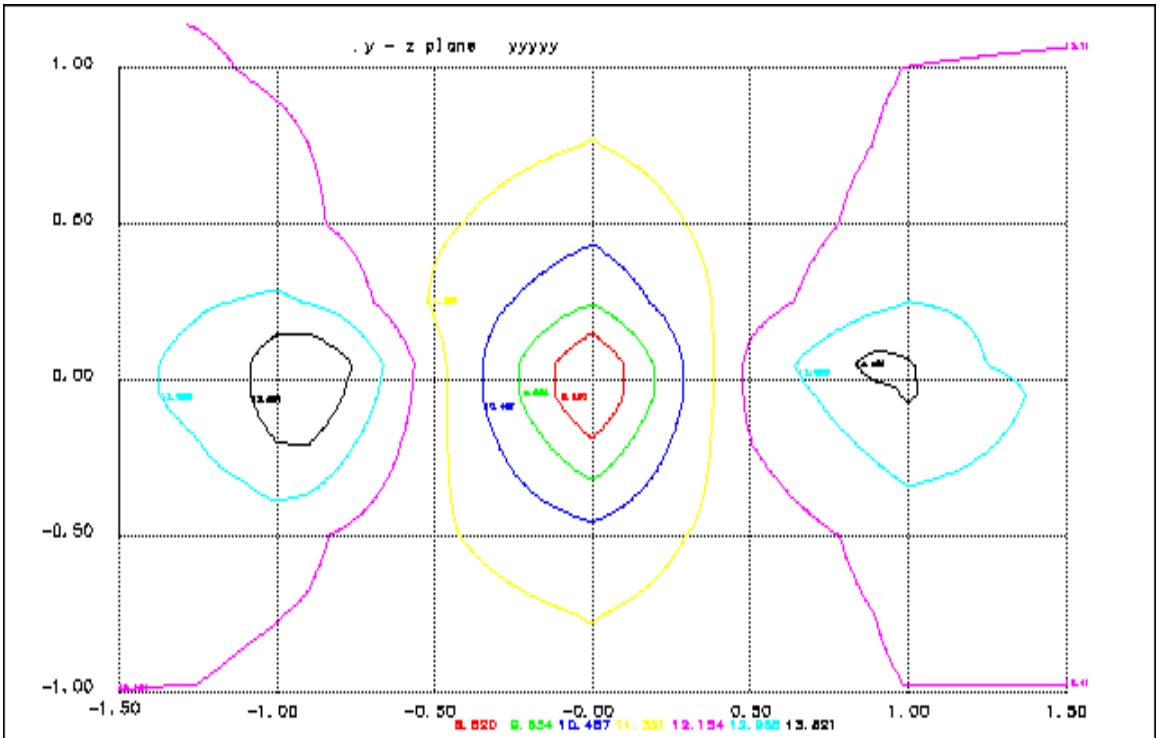


(b) CL/CD arising

**FIG.11.4.2 UNCAMBERED WINGS, NO AoA CORRECTION**
**dx=-2, delk=0.6**

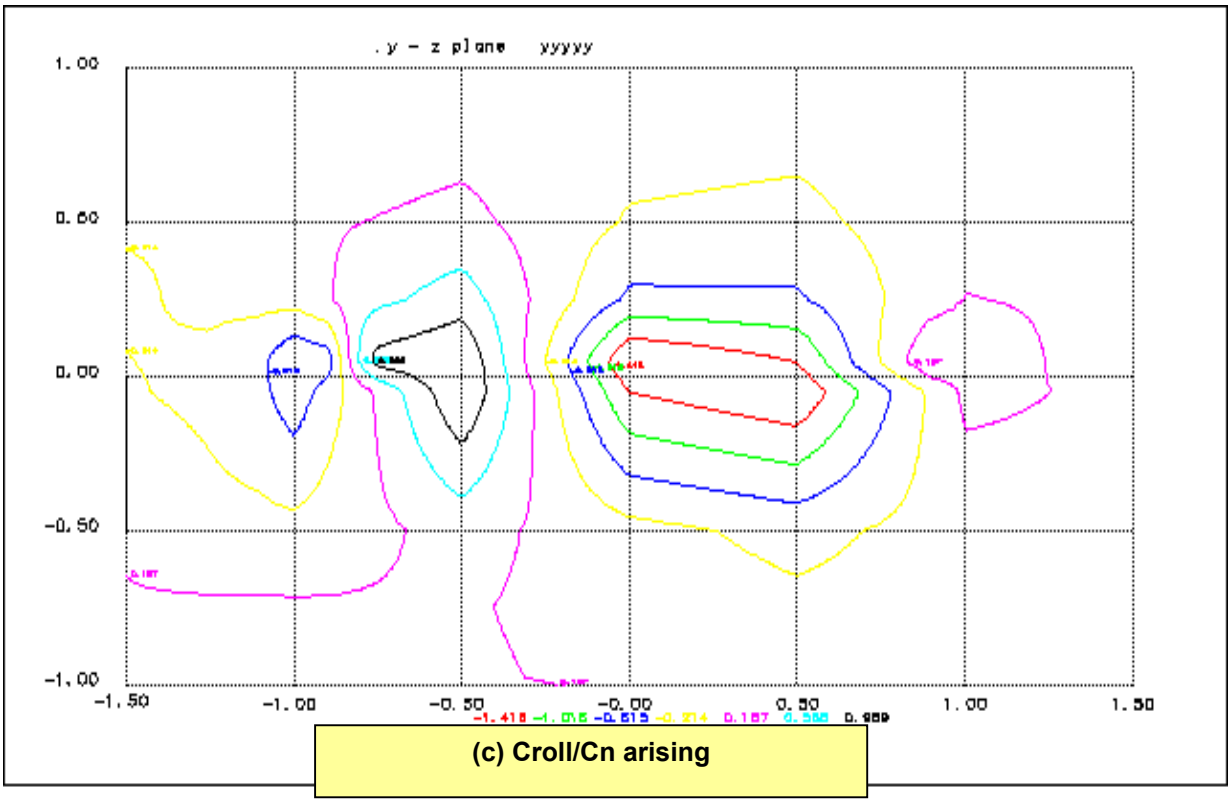


(c) Croll/Cn arising

FIG. 11.4.2 (Cont'd)

CL/CD arising

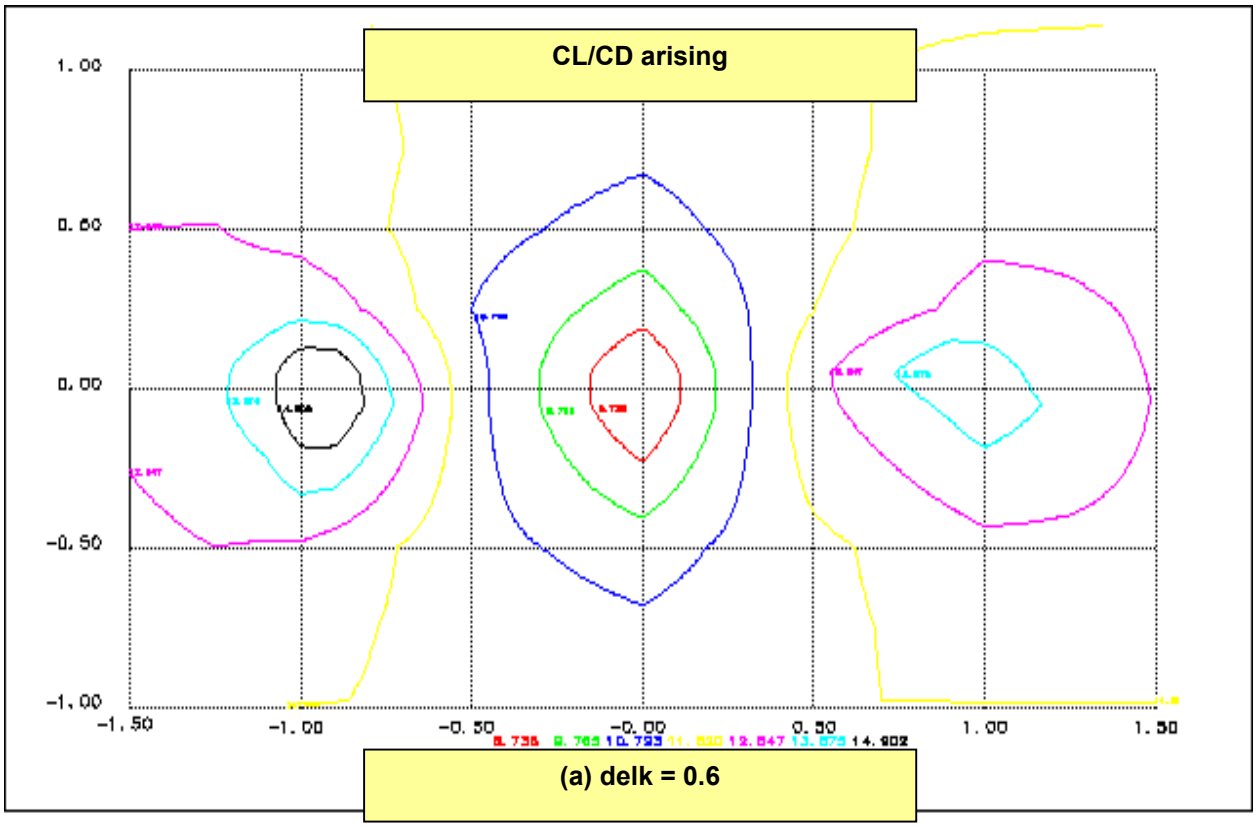


(a) delk = 0.6

FIG. 11.4.3 UNCAMBERED WINGS, WITH AoA CORRECTION
dx=-2, delk = 0.6 & 0.7

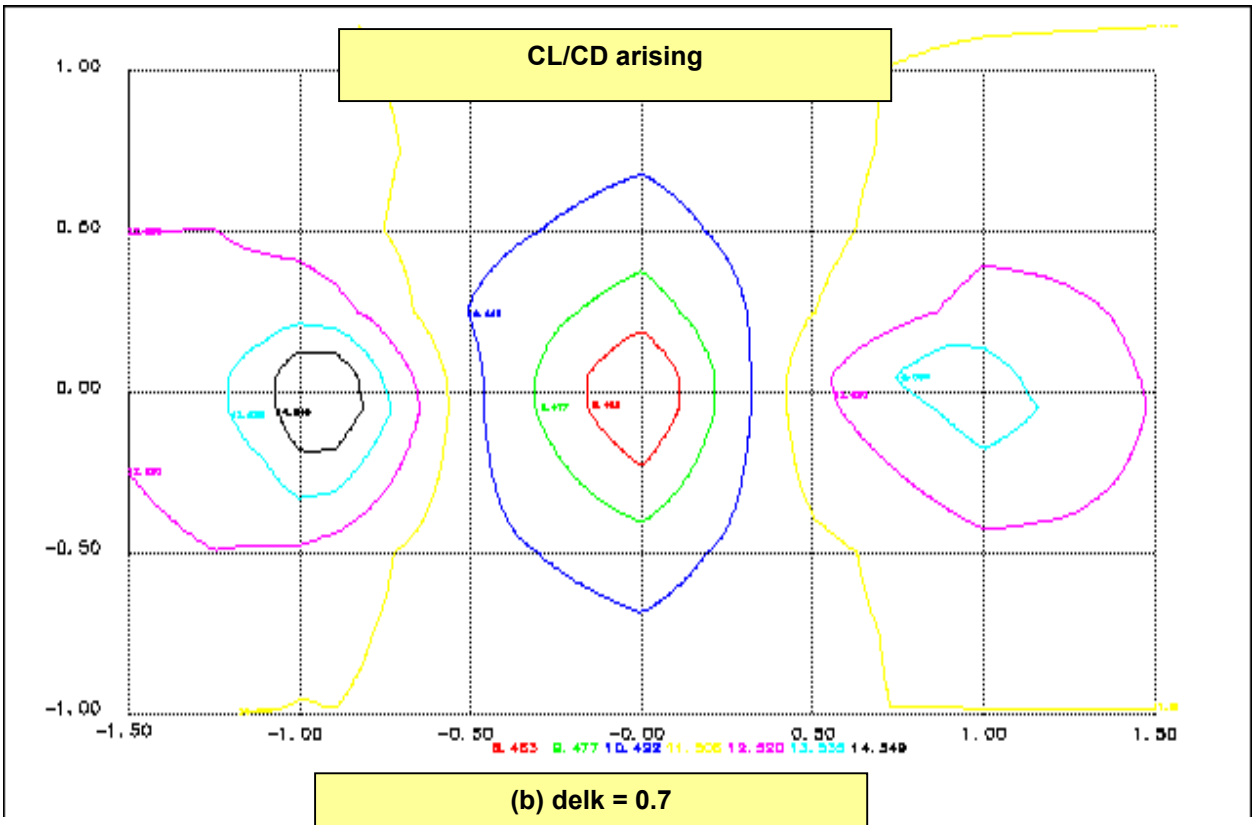


(b) delk = 0.7

FIG.11.4.3 (Cont'd)

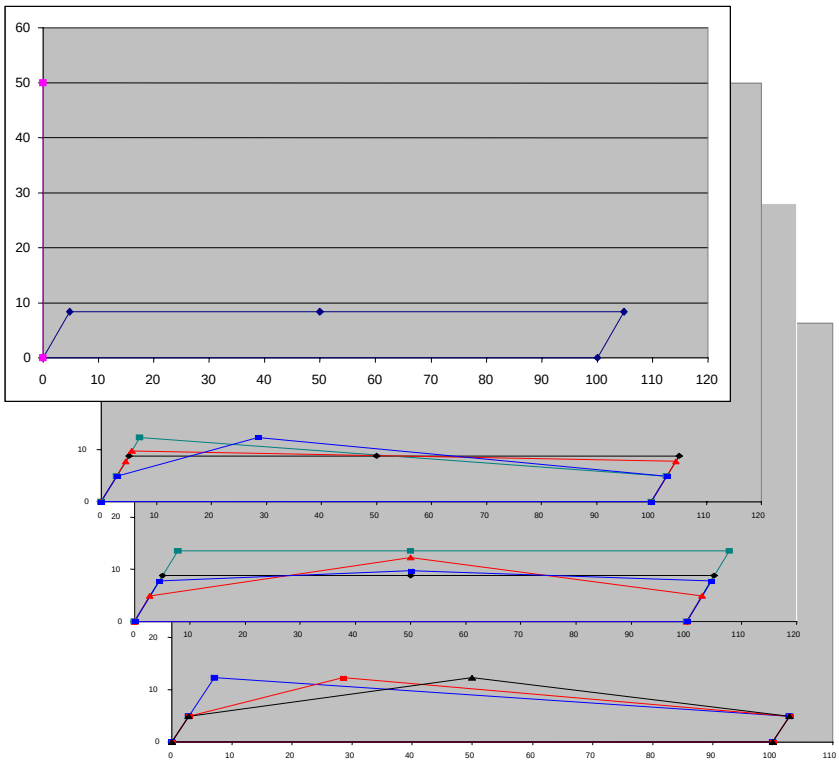


FIG.12.1 PLANNED WORK ON DIFFERENT OFW PLANFORMS in FLYING FORMATION

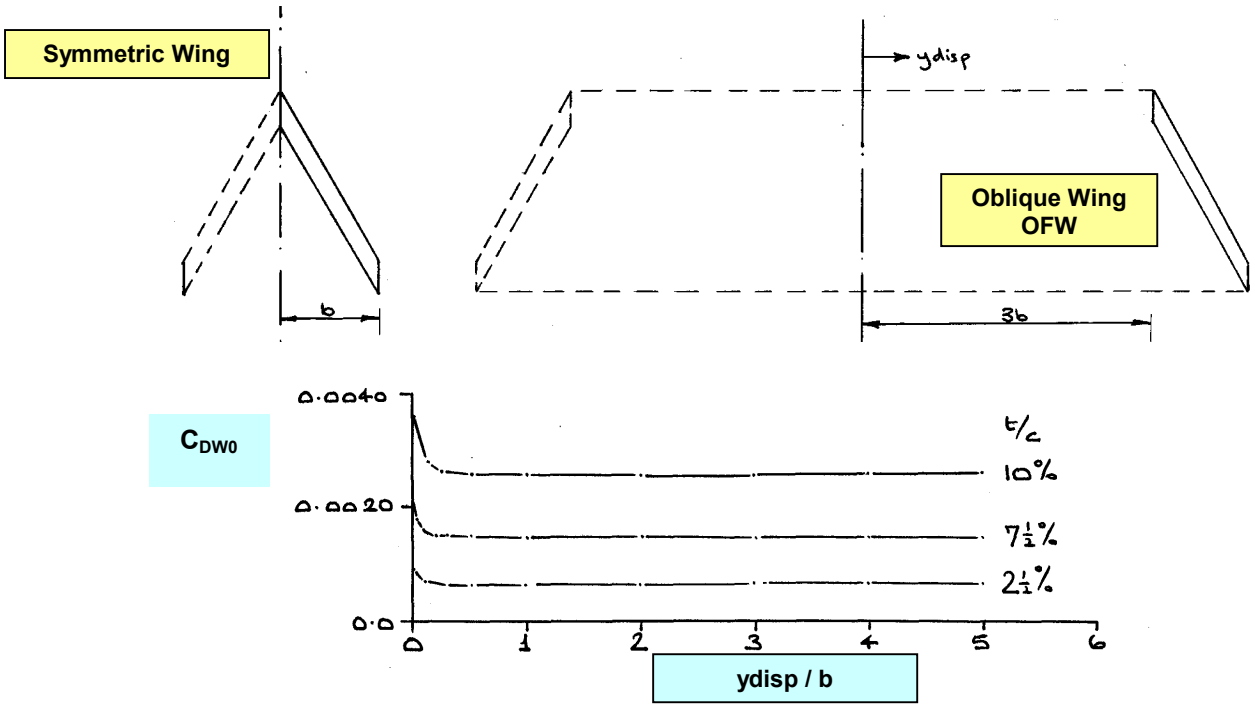


**FIG. A1.1 EFFECT on $C_{DW0}$ of BIFURCATING TWO HALVES OF AN UNTAPERED SWEPT WING OF LE SWEEP 60 deg., Mach 1.4, t/c varies from 2.5 to 10%**

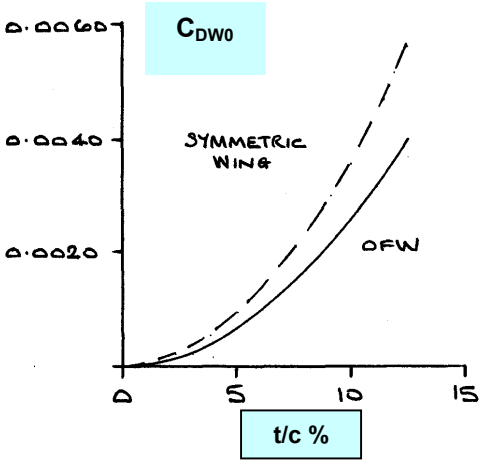


**FIG. A1.2 OFW, EFFECT on $C_{DW0}$ due to t/c, Mach 1.4**

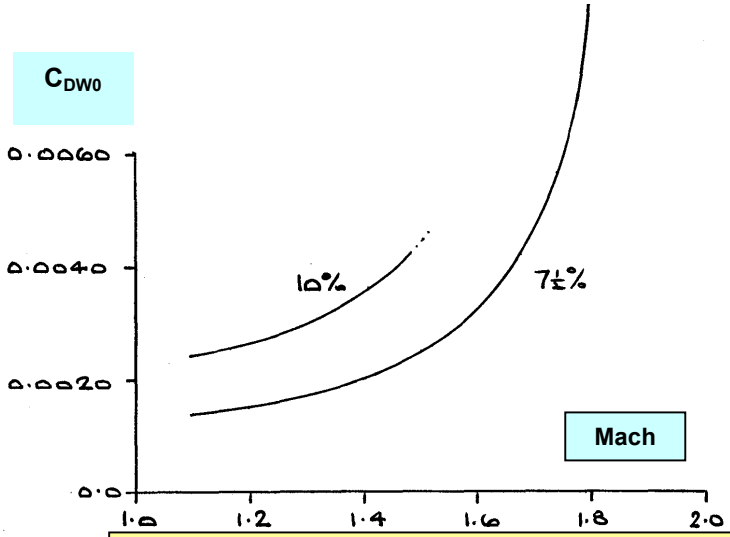


**FIG. A1.3 OFW, EFFECT on $C_{DW0}$ OF Mach No. for t/c = 7.5% & 10%**

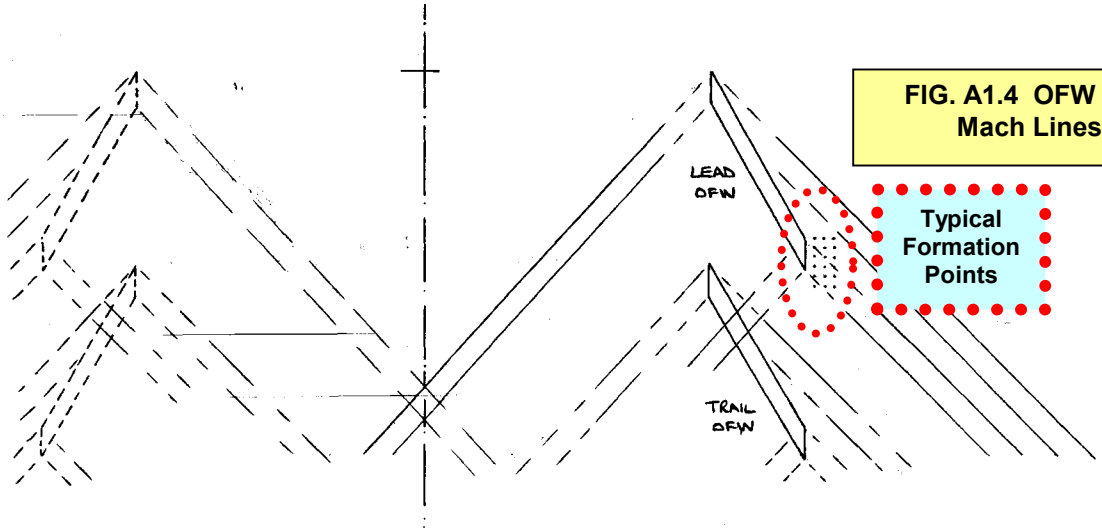


**FIG. A1.4 OFW IN FORMATION, Mach Lines at Mach 1.4**

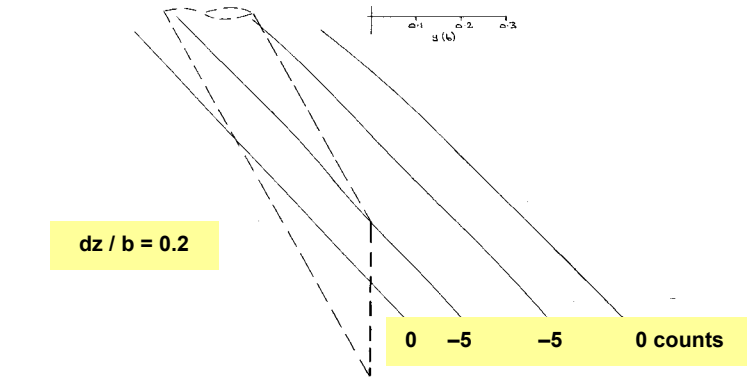


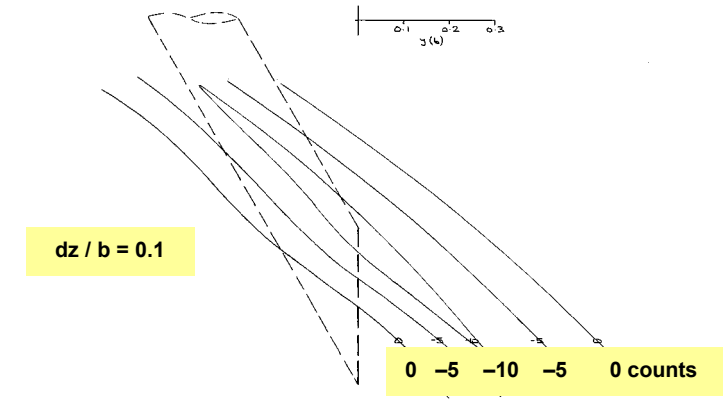


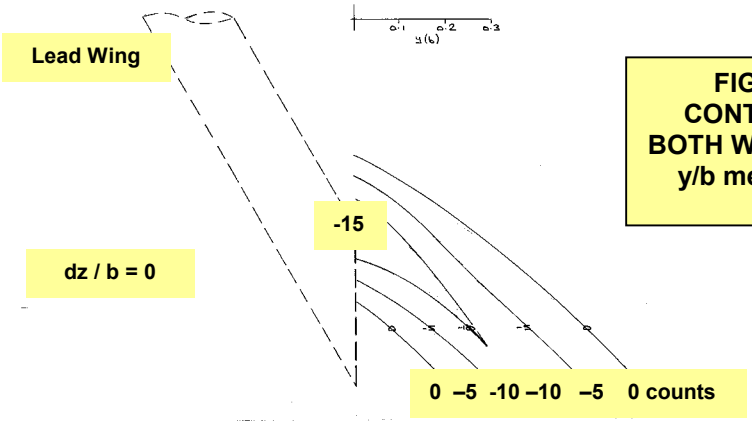


**FIG. A1.5 OFW FLYING FORMATION, CONTOURS OF REDUCTION IN $C_{DW0}$ FOR BOTH WINGS AT 3 HEIGHTS, t/c 7.5%, Mach 1.4 y/b measured wrt to TIP LE OF LEAD WING**

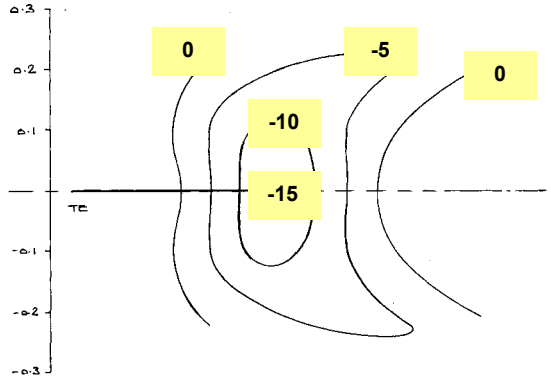


**FIG. A1.6 OFW FLYING FORMATION, CONTOURS OF REDUCTION IN $C_{DW0}$ FOR PLANE THROUGH LEAD WING TIP**

+